THE METABOLIC CONSEQUENCES OF MOUSE BETAINE HOMOCYSTEINE *S*-METHYLTRNASFERASE DEFICIENCY

Ya-Wen Teng

A dissertation submitted to the faculty of the University of North Carolina at Chapel Hill in partial fulfillment of the requirements for the degree of Doctor of Philosophy in the Department of Nutrition (Biochemistry) of School of Public Health.

Chapel Hill
2011

Approved by:

Steven H. Zeisel

Rosalind A. Coleman

Timothy A. Garrow

Nobuyo N. Maeda

Mihai D. Niculescu

ABSTRACT

YA-WEN TENG: The Metabolic Consequences of Mouse Betaine Homocysteine *S*-Methyltransferase Deficiency
(Under the direction of Steven H. Zeisel)

Betaine homocysteine *S*-methyltransferase (BHMT, EC 2.1.1.5) catalyzes the conversion of homocysteine to methionine. Homocysteine is a potentially harmful amino acid. Its elevation is often associated with cardiovascular disease, birth defect, renal insufficiency, and age-related cognitive impairment in humans. Humans have common single nucleotide polymorphisms (SNPs) in the *BHMT* gene that can alter its enzyme activity and function. Elucidation of the metabolic consequences of *BHMT* deficiency is critical to the understanding of the relationship between *BHMT* mutations and diseases. To directly investigate the role of BHMT *in vivo*, we generated and characterized the mice with the gene encoding *Bhmt* deleted ($Bhmt^{-/-}$). This dissertation describes two separate projects. The first project examines the roles of BHMT in one-carbon metabolism and the development of hepatic steatosis and hepatocellular carcinoma. The second project examines the role of BHMT in energy metabolism.

In the first project, we generated and characterized the $Bhmt^{-/-}$ mouse. We found that deletion of *Bhmt* resulted in elevated homocysteine concentrations, in reduced methylation potential, and in profound alterations of choline metabolites in various tissues. $Bhmt^{-/-}$ mice

developed fatty liver at five weeks of age due to reduced phosphatidylcholine concentration. Phosphatidylcholine is required for the synthesis of lipoproteins, which carry lipids from the liver to circulation. By one year of age, 64% of *Bhmt*$^{-/-}$ mice had visible hepatic tumors. Histopathological analysis revealed that *Bhmt*$^{-/-}$ mice developed hepatocellular carcinoma or carcinoma precursors.

We observed that *Bhmt*$^{-/-}$ mice had reduced body weight from five to nine weeks of age. This observation led us to investigate the potential role of BHMT in energy metabolism. We found that the reduced body weight in *Bhmt*$^{-/-}$ mice was due to reduced fat mass. *Bhmt*$^{-/-}$ mice had smaller adipocytes, better glucose tolerance, and enhanced insulin sensitivity. Several factors contributed to the reduced adiposity phenotype observed in *Bhmt*$^{-/-}$ mice; these included increased energy expenditure, reduced mobilization of lipid from the liver to adipose tissue, decreased lipid synthesis within adipocytes, and enhanced whole-body glucose oxidation. This dissertation provides novel findings that BHMT plays critical roles in hepatocellular carcinoma development and energy metabolism.

To my grandparents, my father Shuang-Kuei Teng, my mother Hsiu-Feng Tien, my siblings, and my husband Shane Chang.

.

ACKNOWLEDGEMENTS

I extend my deepest appreciation to my mentor, Dr. Steven Zeisel, for his guidance and support throughout my graduate career. I am extremely grateful to members of my dissertation committee: Dr. Rosalind Coleman, Dr. Timothy Garrow, Dr. Noboyo Maeda, and Dr. Mihai Niculescu, who have all taken time to provide thoughtful discussion pertaining to this work. I thank Zeisel laboratory members for their technical support, advice, and companionship. I thank Dr. Rosalind Coleman and her laboratory members for sharing their experimental expertise with me. I thank my family and my husband for all their love and encouragement.

TABLE OF CONTENTS

LIST OF TABLES

LIST OF FIGURES

LIST OF ABBREVIATIONS

BHMT	Betaine homocysteine *S*-methyltransferase
AdoHcy/SAH	Adenosylhomocysteine
AdoMet/SAM	Adenosylmethionine
ALT	Alanine transaminase
ASM	Acid soluble metabolites
BA	Bile acid
BADH	Betaine aldehyde dehydrogenase
BAT	Brown adipose tissue
Bet	Betaine
BSA	Bovine serum albumin
BUN	Blood urea nitrogen
CBHcy	S-(δ-carboxybutyl)-DL-homocysteine
CBS	Cystathionine ß-synthase
CCT	CTP-phosphocholine cytidylyltransferase
CHDH	Choline dehydrogenase
CHK	Choline kinase
Chol	Cholesterol
CHOP	C/EBP homologous protein
CK	Creatinine kinase
CL	CL316243
CMP	Cytidine monophosphate

CpG	Cytosine guanosine
CPT	CDP choline: diacylglycerol choline phosphotransferase
CTP	Cytidine triphosphate
CγL	Cystathionine γ-lase
CYP7A1	Cholesterol 7α hydroxylase
DAG	Diacylglycerol
DDH	Dimethylglycine dehydrogenase
DHF	Dihydrofolate
Dio2	Deiodinase 2
DMG	Dimethylglycine
dTMP	Deoxythymidine monophosphate
ER	Endoplasmic reticulum
ERK	Extracellular signal-regulated kinases
FA	Fatty acids
FFF-BSA	Fatty acid free bovine serum albumin
FGF21	Fibroblast growth factor 21
FLP	Flippase
FOXO1	Forkhead box protein O1
FRT	Flippase recognition target
G-6-P	Glucose-6-phosphate
GC/MS	Gas chromatography/mass spectrometry
gGT1	Gamma glutamyltransferase 1
GH	Growth hormone

Glu	Glucose
GLUT4	Glucose transporter 4
Gly	Glycine
GSK3ß	Glycogen synthase kinase 3ß
GNMT	Glycine *N*-methyltransferase
GPCho	Glycerophosphocholine
GRP78	Glucose regulated protein 78
GSH	Glutathione
GSSG	Glutathione disulfide
GWAT	Gonadal white adipose tissue
HCA	Hepatocellular adenoma
HCC	Hepatocellular carcinoma
Hcy	Homocysteine
HDL	High density lipoprotein
HHcy	Hyperhomocysteinemia
HPLC	High pressure liquid chromatography
IGF-1	Insulin-like growth factor 1
IRS	Insulin receptor substrate
Iso	Isoproterenol
IWAT	Inguinal white adipose tissue
KO	Knockout
LC/MS	Liquid chromatography/mass spectrometry
LDH	Lactate dehydrogenase

LDL	Low density lipoprotein
loxP	locus of X-over P1
LPL	Lipoprotein lipase
MAT	Methionine adenosyltransferase
MCDD	Methionine choline deficient diet
MCPT1	Muscle carnitine palmitoyl transferase 1
Met	Methionine
MRI	Magnetic resonance image
MTA	Methylthioadenosine
MTHF/methyleneTHF	Methylenetetrahydrofolate
mTHF/methylTHF	5-methyltetrahydrofolate
MTR/MS	Methionine synthase
NAFLD	Nonalcoholic fatty liver disease
NASH	Nonalcoholic steatohepatitis
NEFA	Non esterified fatty acid
Neo	Neomycin
PCho	Phosphocholine
PEMT	Phosphatidylethanolamine N-methyltransferase
PEPCK	Phosphoenolpyruvate carboxykinase
PGC1α	Pparγ coactivator 1α
PKB/Akt	Protein kinase B
PKC	Protein kinase C
PPAR	Peroxisome proliferator activated receptor

PtdCho/PC	Phosphatidylcholine
PtdCho/PE	Phosphatidylethanolamine
PtdIns	Phosphatidylinositol
PtdSer	Phosphatidylserine
RER	Respiratory exchange ratio
ROSs	Reactive oxygen species
SAHH	S-Adenosylhomocysteine hydrolase
Sarc	Sarcosine
SDH	Sarcosine dehydrogenase
Ser	Serine
SHMT	Serine hydroxymethyltransferase
SM	Sphingomyelin
SMM	*S* methylmethionine
SNPs	Single nucleotide polymorphisms
SREBP1C	Sterol response element binding protein 1C
T3	Triiodothyronine
T4	Thyroxine
TAG	Triacylglycerol
TH	Thyroid hormone
THF	Tetrahydrofolate
TLC	Thin layer chromatography
TNF-α	Tumor necrosis factor-α
TR	Thyroid hormone receptor

UCP1	Uncoupling protein 1
VLDL	Very low density lipoprotein
WAT	White adipose tissue
WT	Wildtype

CHAPTER I

INTRODUCTION

One-carbon metabolism is a network of interrelated biological reactions that donate, accept, and regenerate the one-carbon moieties (-CH_3, methyl group) needed for numerous cellular processes. Over the past few years, one-carbon metabolism has received increasing attention due to its involvement in epigenetic modification and cancer risk. One-carbon metabolism includes both the choline and the homocysteine pathways. Betaine homocysteine *S*-methyltransferase (BHMT) is the enzyme that integrates these pathways. BHMT uses a methyl group from the choline-metabolite betaine to methylate homocysteine. Homocysteine becomes methionine, the precursor of *S*-adenosylmethionine that is the universal methyl donor for most cellular methylation processes. **While the importance of one-carbon metabolism in human diseases is being gradually elucidated, we have very limited information on BHMT, a key enzyme in one-carbon metabolism.**

Humans have common single nucleotide polymorphisms (SNPs) in the *BHMT* gene that can alter its enzyme activity and function. SNPs are identified in several epidemiological studies in humans as bring associated with the altered risks of various diseases. The epidemiological evidence regarding the functional effects of *BHMT* SNPs, however, remains controversial. **The goal of this dissertation is to elucidate the metabolic consequences of**

***BHMT* deficiency in order to understand the relationship between *BHMT* mutations and diseases.**

To achieve this goal, we generated the mouse model with the gene encoding *Bhmt* deleted (*Bhmt*$^{-/-}$). We found that *Bhmt* deficiency resulted in one-carbon metabolism distortion with elevated homocysteine concentrations, altered choline metabolites, and reduced methylation potential. *Bhmt* deficiency disturbed hepatic health as these mice developed fatty liver at five weeks of age and hepatocellular carcinoma at one year of age. *Bhmt* deficiency also affected growth. Compared to the controls, *Bhmt*$^{-/-}$ mice had reduced body weight, which was due to decreased fat mass. *Bhmt* deficiency reduced adiposity by increasing energy expenditure, reducing lipid mobilization from the liver to adipose tissue, limiting lipid synthesis within adipocytes, and enhancing whole body glucose metabolism.

This dissertation affirms the critical role of BHMT in one-carbon metabolism. It also provides novel and convincing data that BHMT is involved in hepatocellular carcinogenesis and energy metabolism. Liver cancer is among one of the most lethal cancers. Fatty liver and obesity are highly prevalent in the United States. This work has identified a new mechanism potentially involved in these diseases.

Specific Aims:

1. **Generate the mouse with the gene encoding *Bhmt* deleted globally.**
2. **Determine the role of *Bhmt* deficiency in one-carbon metabolism and in hepatic health.**
3. **Determine the role of *Bhmt* deficiency in energy metabolism.**

CHAPTER II

BACKGROUND

2.1 General Aspects of Betaine Homocysteine *S*-Methyltransferase (BHMT)

Betaine homocysteine *S*-methyltransferase (BHMT, EC 2.1.1.5) is a zinc-dependent cytosolic enzyme found in the choline oxidation pathway. BHMT catalyzes the transfer of a methyl group (-CH_3) from betaine (also known as *N,N,N*-trimethylglycine or glycine betaine) to homocysteine (Hcy). The products of this reaction are dimethylglycine and methionine (**Figure 2.1**). This reaction follows an ordered Bi-Bi mechanism with Hcy being the first substrate to bind and methionine being the final product off [1, 2].

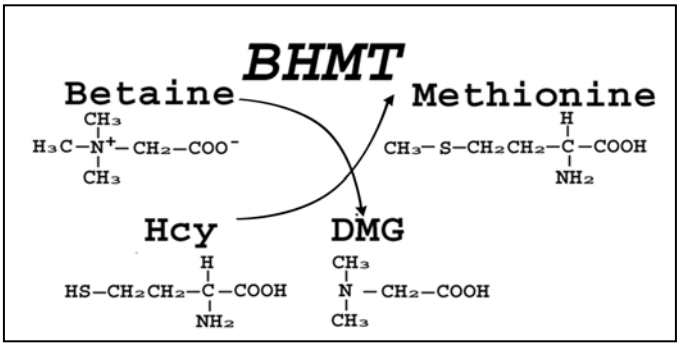

Figure 2.1 Action of BHMT. BHMT converts betaine and homocysteine to dimethylglycine and methionine respectively. BHMT, betaine homocysteine *S*-methyltransferase; Hcy, homocysteine; DMG, dimethylglycine. Figure from Teng Y. *J. Biol. Chem.* 2011; 286(42):36258-67.

In mammals, BHMT protein is detected as early as day 10 of gestation [11, 12], and is present in adults [13]. BHMT is found in liver, kidney, brain and lenses of humans, and in liver and kidney of rodents [14]. It is one of the most abundant proteins in mammalian liver; BHMT is estimated to account for 0.6-1.6% of the total protein in the liver [14]. On the other hand, its activity is low in the human kidney and extremely low in the rodent kidney (**Table 2.1**) [13, 15]. *BHMT* gene expression and BHMT activity increase when dietary choline and betaine are abundant, and when methionine is limited [3, 16, 17]. BHMT activity is subject to feedback inhibition, as it is strongly inhibited by dimethylglycine and weakly inhibited by methionine [2].

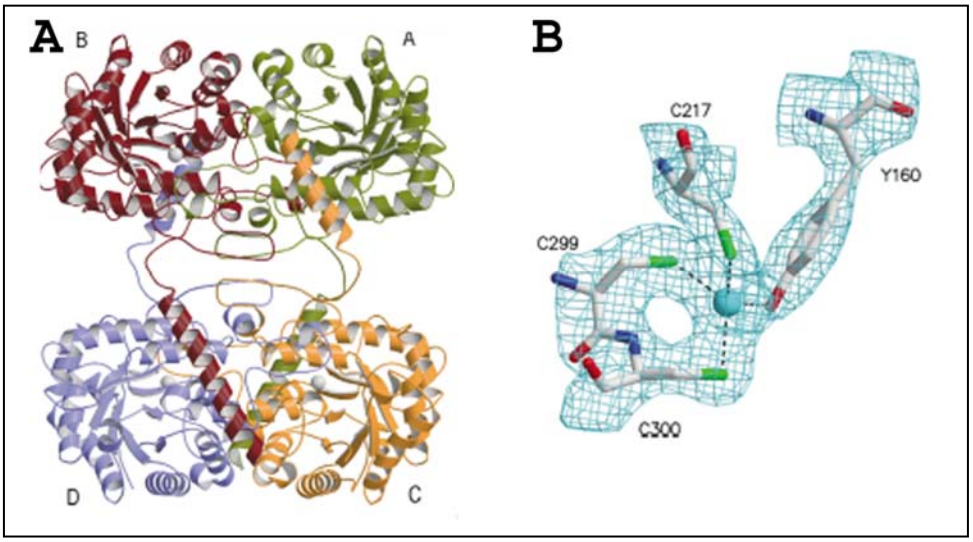

Figure 2.2 Structure of BHMT. (a) Structure of the rat liver BHMT tetramer. The asymmetric unit contains four molecules. Zinc atoms are represented as grey spheres at each active-site. (b) Electron density map showing the three essential cysteine residues coordinated to the zinc atom. Figures from Evans J. *Structure.* 2002; 10(9), 1159-71. Gozalez B. *J. Mol. Biol.* 2004; 338, 771-782.

Recently, betaine homocysteine methyltransferase 2 (BHMT2, EC 2.1.1.5) has been identified to also methylate Hcy to methionine [18, 19]. The human *BHMT2* gene is located 22.3 kb 5' of *BHMT* and encodes a protein that is 73% identical to that of BHMT. Unlike BHMT, BHMT2 cannot use betaine but uses *S*-methylmethionine (SMM) as the methyl donor [18, 20]. BHMT2 protein degrades rapidly unless it is bound to BHMT and stabilized by Hcy [18, 20]. In mouse liver, BHMT2 activity is very low, with activity less than 5% of that of BHMT (**Table 2.1**) [18]. As with BHMT, there have been low amounts of BHMT2 activity detected in mouse kidney [18]. No BHMT2 activity has been detected in the heart, skeletal muscle, spleen, brain, small intestine, or lung [18]. The role and the significance of BHMT2 remain to be determined.

BHMT and BHMT-2 activities in mouse liver and kidney

Assays (500 μl) contained 2.5 mM DL-Hcy and 250 μM methyl donor (0.5 μCi).

Protein	Activity	BHMT/BHMT-2 ratio[a]
Liver BHMT	79	
Liver BHMT-2	3.8	20.8
Kidney BHMT	0.41	
Kidney BHMT-2	0.32	1.3

[a] BHMT-2 assays were done in the presence of 62.5 μM CBHcy. Activities are reported as nanomole of Met formed per hour per mg of protein with an $n = 5$ for each organ.

Table 2.1 BHMT and BHMT2 activities in mouse liver and kidney. Table from Szegedi S. *J. Biol. Chem.* 2008; 283 (14), 8939-45.

2.2 Interactions of BHMT

2.2.1 BHMT and Choline Metabolism

Betaine, the methyl donor for BHMT, was first isolated from sugar beets (*Beta vulgaris*) by Scheibler, a German Chemist, in the 1860s [21, 22]. Scheibler named it "Betaine," and showed that it has the structure of a trimethylglycine (**Figure 2.1**). Aside from sugar beets high levels of betaine can be found in foods such as wheat germ, shrimp, and spinach [23]. Betaine is rapidly absorbed in the ileum via transporters, and its bioavailability is assumed to be close to 100% [24]. The estimated dietary intake of betaine ranges from 100-300 mg/day [25]. However, a recommended daily intake of betaine has not been established since betaine can also be produced endogenously from an essential nutrient, choline. Choline dehydrogenase (CHDH, EC 1.1.99.1) oxidizes choline to betaine aldehyde in the inner mitochondrial membrane (**Figure 2.3**). Betaine aldehyde dehydrogenase (BADH, EC 1.2.1.8) then transforms betaine aldehyde to betaine in the mitochondrial matrix [26, 27]. Betaine moves from mitochondria to cytosol, where BHMT is active. This movement is believed to be accomplished by passive diffusion as no active transport process has been identified. The liver and the kidney cortex are the principal sites for choline oxidation. Since betaine cannot be reduced back to choline, this oxidation pathway commits choline to be used for methylation.

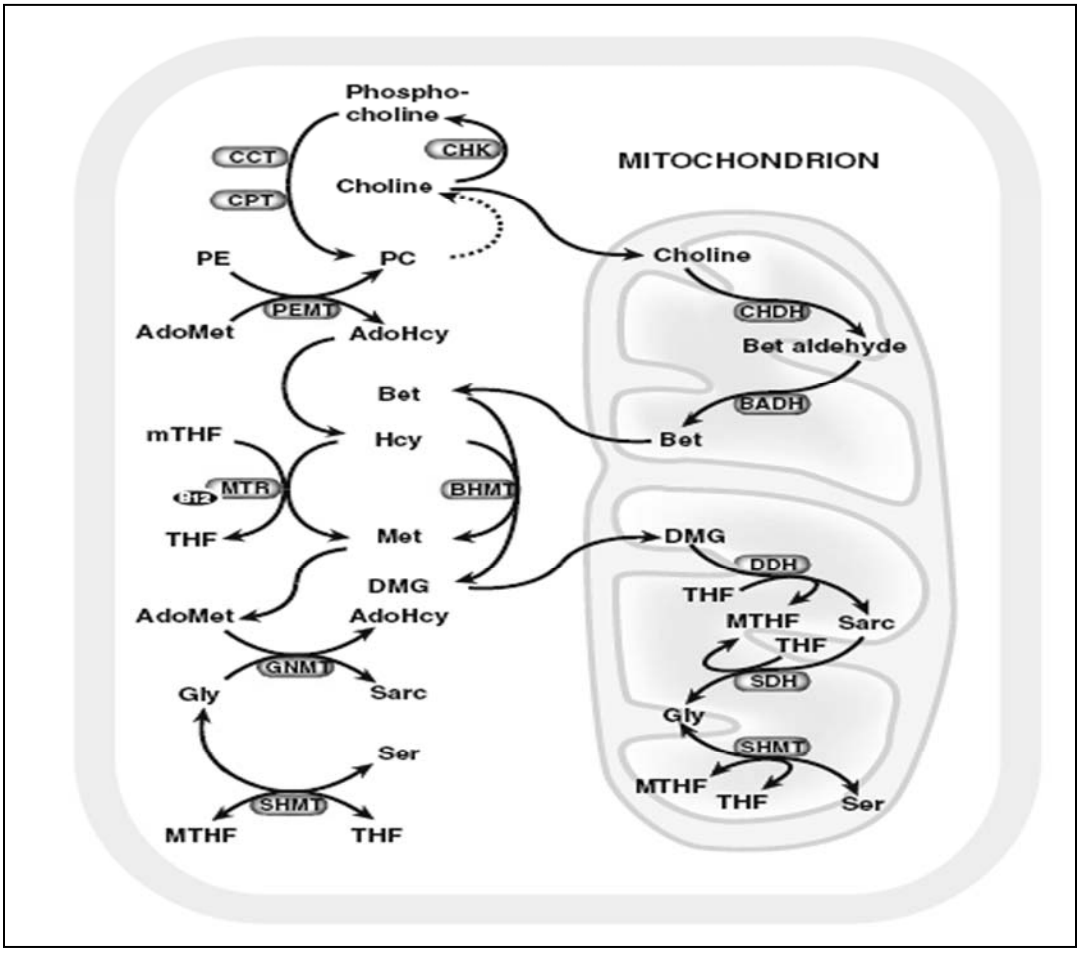

Figure 2.3 Metabolism of choline and betaine and its relationship to one-carbon metabolism. AdoHcy, *S*-adenosylhomocysteine; AdoMet, *S*-adenosylmethionine; BADH, betaine aldehyde dehydrogenase; Bet, betaine; BHMT, betaine homocysteine *S*-methyltransferase; CCT, CTP-phosphocholine cytidylyltransferase; CHK, choline kinase; CHDH, choline dehydrogenase; CPT, cytidine 5-diphosphate (CDP) choline: diacylglycerol choline phosphotransferase; DDH, dimethylglycine dehydrogenase; DMG, dimethylglycine; Gly, glycine; GNMT, glycine *N*-methyltransferase; Hcy, homocysteine; Met, methionine; mTHF, 5-methyltetrahydrofolate; MTHF, methylenetetrahydrofolate; MTR, methionine synthase; PC, phosphatidylcholine; PE, phosphatidylethanolamine; PEMT, phosphatidylethanolamine *N*-methyltransferase; Sarc, sarcosine (monomethylglycine); SDH, sarcosine dehydrogenase; Ser, serine; SHMT, serine hydroxymethyltransferase; THF, tetrahydrofolate. Figure from Ueland P. *J. Inherit. Metab. Dis.* 2011; 34, 3-15.

Choline, the precursor of betaine, comes from the diet or *de novo* synthesis in tissues. Excellent sources of dietary choline are foods that contain membranes, such as eggs and liver. The recommended daily intake for choline is 550 mg/day for men and 425 mg/day for women [28]. Choline exists in foods as free choline or choline esters, from which choline is freed by pancreatic enzymes. These choline esters include phosphocholine, glycerophosphocholine, phosphatidylcholine (PtdCho), and sphingomyelin [26]. Choline is absorbed in the small intestine. Free choline enters the portal circulation and is mostly taken up by the liver [29], whereas lipid-soluble PtdCho and sphingomyelin enter via lymph and bypass the liver. Therefore, different forms of choline may have different bioavailability [30]. In addition, choline can be formed endogenously (mainly in the liver) by the enzyme phosphatidylethanolamine-*N*-methyltransferase (PEMT, EC 2.1.1.17). PEMT catalyzes the conversion of phosphatidylethanolamine (PtdEtn) to PtdCho using three *S*-adenosylmethionine (AdoMet) molecules. PtdCho is either incorporated into cell membranes or degraded to regenerate choline through phospholipase D (EC 3.1.4.4) [31]. PtdCho serves as the reservoir for choline, accounting for 95% of the total choline pool in mammalian tissues. The remaining 5% includes choline species such as choline, phosphocholine, glycerophosphocholine, cytidine 5-diphosphocholine, and acetylcholine [27, 32].

Choline is a water-soluble nutrient that is often grouped with the Vitamin B complex. However, because it is not catalytic in function and is used as a substrate, it is not truly a vitamin. Choline is crucial for the normal function of all cells [26]. As mentioned above, choline can be converted to betaine, the carrier of methyl groups. Choline is used to form the neurotransmitter acetylcholine, the main mediator of the parasympathetic nervous system.

Choline is needed for membrane phospholipid formation. Choline enters the CDP-choline (Kennedy) pathway, forming phosphocholine and ultimately PtdCho (**Figure 2.3 & 2.4**), which accounts for over 50% of the phospholipids in mammalian membranes. Thereby, choline ensures the structural integrity and the signaling function of cell membranes [26, 33]. PtdCho is involved in the assembly and the secretion of the very low density lipoproteins (VLDLs), which export fat from the liver to circulation [26]. Choline deficient humans develop fatty liver [27] due to the lack of PtdCho to export triacylglycerol from the liver [34]. Choline deficiency in humans is also associated with liver damage [27], muscle damage [35], lymphocyte DNA damage and apoptosis [36] and elevated plasma Hcy after a methionine load [37].

As mentioned before, PtdCho can also be formed by the action of PEMT from PtdEtn in three steps using AdoMet molecules as the methyl donors [38]. The PEMT pathway generates approximately 30% of the PtdCho in the liver, while the CDP-choline pathway generates the other 70% [39]. Mice that lack the *Pemt* gene develop fatty liver and severe liver damage, and die after 3 days when fed a choline-deficient diet; choline supplementation prevents this [40]. *Pemt*$^{-/-}$ mice have lower choline pools in the liver despite being fed sufficient or supplemental choline, suggesting that choline production by PEMT in the liver is a significant source of choline relative to dietary choline [41]. AdoMet, the methyl donor required for PEMT action, is a product of BHMT (as discussed below). BHMT could potentially affect PtdCho synthesis via both CDP-Choline and PEMT pathways.

2.2.2 BHMT and Homocysteine and One-Carbon Metabolism

Homocysteine is a thiol-containing amino acid that is potentially harmful. Humans who have plasma total homocysteine (tHcy) of 10 to 100 μmol/L are considered to be moderately hyperhomocysteinemic, while tHcy >100 μmol/L is considered to be severe hyperhomocysteinemic [42]. Elevation of tHcy is associated with cardiovascular disease, neural tube defects, renal insufficiency, Alzheimer's, and cognitive impairment in the elderly [43]. Moderate hyperhomocysteinemia (HHcy) is common in humans. It is detected in 10-20% of the general population as a result of genetic or non-genetic factors (such as diet, drugs, and impaired renal function) [43]. It is detected in up to 20-40% of patients with cardiovascular complications [42].

Hcy is metabolized by both transsulfuration and transmethylation processes. In the transsulfuration pathway, Hcy forms cystathionine and then cysteine in reactions catalyzed by the enzymes cystathionine-β-synthase (CBS, EC 4.2.1.22) and cystathionine-γ-lyase (CγL, EC 4.4.1.1), respectively (**Figure 2.4**). Both enzymes require vitamin B_6. Cystathionine-β-synthase also requires AdoMet as the allosteric activator. Cysteine is the precursor to the osmolyte taurine and the antioxidant glutathione. In the transmethylation pathway, Hcy is remethylated to methionine by three reactions. BHMT and BHMT2 remethylate Hcy using betaine and *S*-methylmethionine as the methyl donor respectively. Methionine synthase (MS, EC 2.1.1.13) catalyzes the other reaction using methyl-tetrahydrofolate (MTHF) as the methyl donor. MTHF is supplied by methyl-tetrahydrofolate reductase (MTHFR, EC 1.5.1.20) [44]. Methionine synthase also requires vitamin B_{12} as a cofactor. BHMT processes an estimated 50% of the Hcy methylated capacity in an *in vitro* model of rat liver [45].

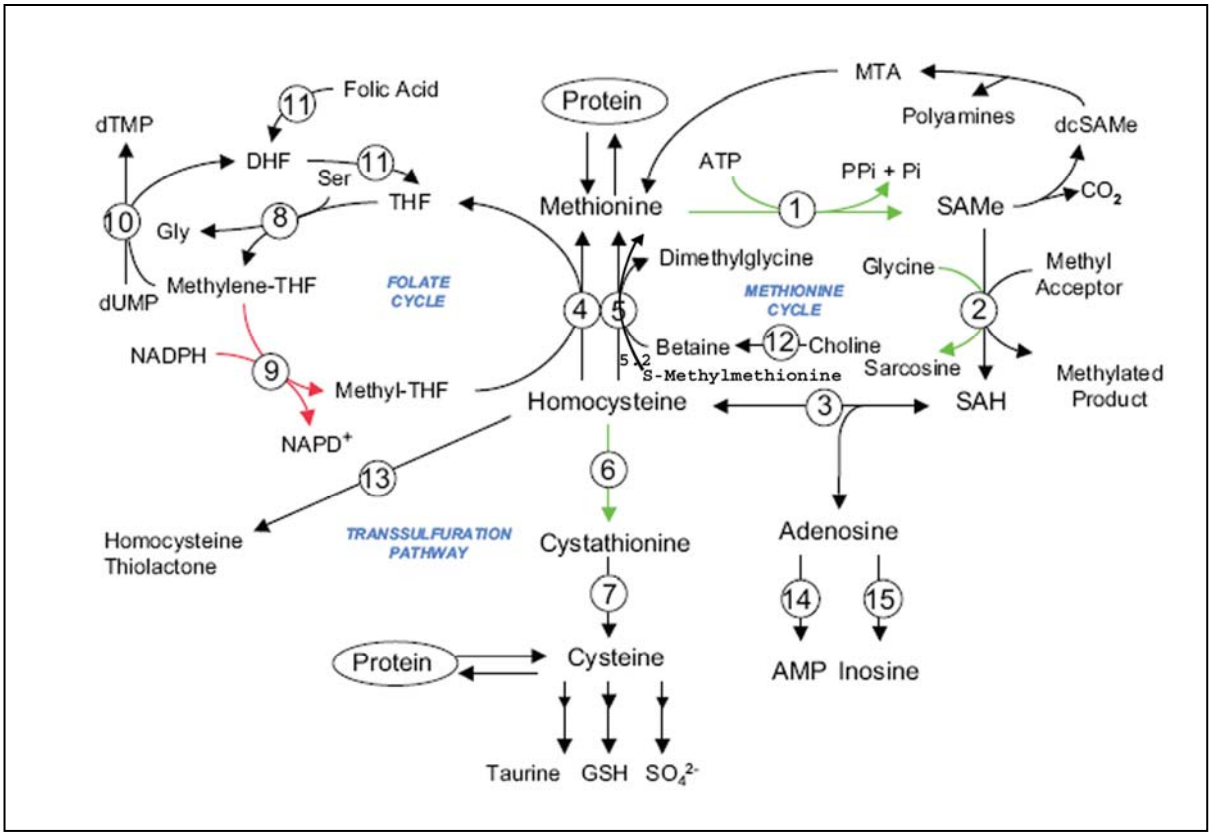

Figure 2.4 Homocysteine metabolism. Enzymes that catalyze the reactions: (1) methionine adenosyltransferase (MAT); (2) different methyltransferases, particularly glycine *N*-methyltransferase (GNMT); (3) SAH hydrolase (SAHH); (4) methionine synthase (MS); (5) betaine-homocysteine methyltransferase (BHMT); (5.2) betaine-homocysteine methyltransferase 2 (BHMT2); (6) cystathionine β-synthase (CBS); (7) cystathionase; (8) methylene-THF synthase (methyl-THF); (9) methyl-THF reductase (MTHFR); (10) thymidine synthase; (12) choline dehydrogenase (CHDH) and betaine aldehyde dehydrogenase (BADH) ; (13) thiolactone synthase; (14) adenosine kinase. Abbreviations: SAMe, *S*-adenosylmethionine; MTA, methylthioadenosine; SAH, *S*-adenosylhomocysteine; GSH, glutathionine; THF, tetrahydrofolate; methylene-THF, 5,10-methylene-tetrahydrofolate; methyl-THF, 5-methyl-tetrahydrofolate; dTMP, deoxythymidine monophosphate; DHF, dihydrofolate. Figure from Mato, J. *Annu. Rev. Nutr.* 2008; 28, 273-293.

Methionine, coming from either diet or the actions of MS and BHMTs, is the precursor of AdoMet. AdoMet is the principal biological methyl donor required for various cellular events, including the methylation of DNA, histones, phospholipids, biogenic amines, and other proteins. AdoMet is required for the synthesis of methylglycine from glycine by glycine *N*-methyltransferase (GNMT); for the formation of PtdCho from PtdEtn by PEMT; for the synthesis of cysteine and ultimately glutathione by the transsulfuration pathway; and many other methylation reactions (**Figure 2.3 & 2.4**). *S*-adenosylhomocysteine (AdoHcy) is formed after AdoMet donates its methyl group to diverse biological acceptors. AdoHcy then is hydrolyzed to form Hcy and adenosine by a reaction catalyzed by *S*-adenosylhomocysteine hydrolase (SAHH, EC 3.3.1.1) [46]. This reaction is reversible, but it favors the synthesis of AdoHcy, a potent inhibitor of many methylation reactions [46]. The ratio between AdoMet and AdoHcy (AdoMet:AdoHcy) estimates the methylation potential, as AdoMet is the universal methyl donor, while AdoHcy is an inhibitor for many known methyltransferases.

Several pathways are evolutionarily conserved to maintain a normal level of Hcy and an adequate supply of AdoMet, suggesting the significance of these compounds. Animal models of HHcy have been produced either through dietary modifications (by limiting dietary choline, vitamin B_6, vitamin B_{12}, or methyl-folate) or through genetic approaches (*Cbs*$^{-/-}$, *Mthfr*$^{-/-}$, *Ms*$^{-/-}$ mouse models) [42]. Perturbations of these pathways have resulted in elevated plasma tHcy levels [47], in reduced methylation potential (AdoMet:AdoHcy) [48], and in compensatory changes of other Hcy pathways [49, 50]. During choline and betaine deprivation, more 5-methyltetrahydrofolate is used for Hcy remethylation. Conversely, during folate deficiency, methyl groups from choline and betaine are used for Hcy

remethylation, thereby increasing choline and betaine requirements. BHMT interrelates with the transsulfuration and methylfolate pathways at the removal of Hcy. The *Bhmt*$^{-/-}$ mouse model was not created until this work was done. The lack of attention to BHMT's role in Hcy removal is probably due to the assumption that the alternative pathways could replace BHMT.

2.3 Physiological Implications of Betaine and BHMT – Human Studies

Reduced choline or methylation potential levels are associated with increased risk of cancer (as discussed below), while elevated Hcy levels are associated with increased risks of cardiovascular disease and neural tube defects. BHMT is the enzyme that integrates these pathways. Thus, epidemiological studies have focused on investigating the associations of human *BHMT* mutations with these diseases. Common single nucleotide polymorphisms (SNPs) in the *BHMT* gene in humans have been identified. These SNPs can alter BHMT protein level and enzyme activity [12]. The *BHMT* SNP rs3733890 (c.716G>A) is common; 41% of the NC population have 1 variant allele, and 8% have 2 alleles [51]. This SNP has been associated with increased risk [52], decreased risk [53], and no change in risk [54] of having babies with neural tube defects. Humans with the *BHMT* SNP rs3733890 have reduced risk [55], or no change in risk [56, 57] of developing cardiovascular disease. The Long Island Breast Cancer Study Project (LIBSP) finds that patients with this SNP have no change in risk of breast cancer [58], but have reduced breast cancer-specific mortality [59]. The epidemiological evidence regarding the functional effects of *BHMT* SNPs remains controversial.

While some epidemiological studies focus on genetic interactions in the etiology of diseases, others focus on the nutrients in diets. Many studies examine the effect of dietary betaine in reducing plasma tHcy that could potentially contribute to vascular complications. Fifty percent of patients with classical genetic homocystinuria have an adverse vascular event before they reach 30 years of age [60]. A study with 15 patients who are supplemented with 6-9 g betaine per day (average betaine intakes range from 100-30 mg/day) shows a 74% reduction in plasma tHcy levels and no vascular events over the course of a total of 258 studied patient years [61]. Other studies using patients with inborn errors of Hcy metabolism, particularly errors in *CBS* and *MTHFR*, have reaffirmed this beneficial effect of betaine supplementation [62-65]. It is pertinent to note that betaine therapy could result in hypermethioninemia, causing cerebral edema in some patients [66, 67]. Aside from treating patients with genetic homocystinuria, betaine also reduces plasma tHcy in the general population with mild hyperhomocysteinemia. One study demonstrates that a dose of 6g betaine per day reduces plasma tHcy level by approximately 20% in normal adults [68]. Another study demonstrates that 95% of patients with premature peripheral or cerebral occlusive arterial disease respond to betaine (6g/day) with a normal level of tHcy [69]. While many studies have shown the effectiveness of betaine in reducing plasma tHcy levels [68, 70-72], it remains a question whether betaine supplementation can serve as a preventative regimen for vascular dysfunction. Short or long-term betaine supplementation do not improve endothelial function in healthy subjects despite the reduced tHcy levels [72, 73]. A study on 3,000 healthy Greek men and women demonstrates that individuals with high intake of choline and betaine have low plasma levels of inflammatory markers, such as C reactive protein, interleukin-6, and tumor necrosis factor-α, suggesting a protective effect of choline

and betaine against cardiovascular disease [74]. However, two large prospective studies, Dutch PROSPECT-EPIC cohort and Atherosclerosis Risk in Communities (ARIC) study, find no association between the intake of choline and betaine and cardiovascular disease [75, 76]. The protective role of betaine against vascular dysfunction requires future study.

In addition to regulating Hcy levels, betaine appears to modify plasma lipid profiles, which further contributes to its potential role in altering cardiovascular risk. Recently, two independent cross-sectional studies reveal that increased plasma betaine is correlated with reduced plasma triacylglycerol and non-high density lipoprotein (non-HDL) cholesterol, which are the preferred plasma lipid profiles [77, 78]. In addition, in both studies, increased plasma betaine is associated with lower BMI in the study populations, suggesting a potential role of betaine in altering adiposity (as discussed below). In contrast, some studies argue that betaine supplementation increases plasma low density lipoprotein (LDL) cholesterol and triacylglycerol concentrations [70, 72, 79], effects that may counterbalance its Hcy lowering effects. However, the rise in LDL concentration may be an artifact of betaine increasing VLDL and triacylglycerol excretion from fatty liver to plasma, which is not an adverse outcome [80].

Nonalcoholic fatty liver disease (NAFLD) is the most common liver disease and is associated with components of the metabolic syndrome [81]. Betaine treatment of NAFLD has been evaluated in three human studies. When treated with betaine, patients with nonalcoholic steatohepatitis have improved liver function, including reduced hepatic steatosis and attenuated hepatic or plasma aminotransferases [82-84]. Information on the relationship

of dietary betaine and cancer risk in humans is scarce, because food composition data have not been available until recently. The Long Island Breast Cancer Study Project finds that high choline consumption reduces breast cancer risk [58], and high choline and betaine consumption reduces breast cancer mortality [59]. However, two later reports find no association between betaine and choline intake and cancer, either breast cancer [85] or ovarian cancer [86]. There are no data on the effect of betaine supplementation on cancer risk.

The evidence from human studies regarding the functional effects of *BHMT* mutations and dietary betaine intake in diseases remains controversial and warrants more studies. Nevertheless, these data suggest the importance of betaine/BHMT in the etiology and as a potential treatment of these diseases.

2.4 Physiological Implications of Betaine and BHMT – Animal Studies

Betaine is known for ameliorating the adverse effects of both nonalcoholic and alcoholic induced fatty liver. Fatty liver may progress to severe liver damage such as fibrosis and cirrhosis [87]. Alcoholic fatty liver is induced by excessive alcohol intake and is often associated with disturbed Hcy metabolism [88-90]. Betaine supplementation mitigates the adverse effects of alcoholic fatty liver, including reducing steatosis and maintaining Hcy and AdoMet levels [91-94]. Transgenic mice overexpressing human *BHMT* are resistant to alcohol-induced hepatic hyperhomocysteinemia and steatosis [95]. On the other hand, nonalcoholic fatty liver is commonly associated with obesity [96], insulin resistance, and diabetes [97]. Mice fed a high fat diet develop nonalcoholic fatty liver and insulin resistance, while betaine supplementation ameliorates these outcomes [98, 99].

The mechanisms by which betaine/BHMT improves hepatic steatosis are not thoroughly understood. Several mechanisms have been proposed. Betaine supplementation and its consequent BHMT induction generate AdoMet. AdoMet supplies the methyl groups needed for the synthesis of PtdCho from PtdEtn by PEMT. PtdCho enables the generation of VLDL, needed for secreting fat from the liver, thus ameliorating hepatic steatosis [100]. In addition, cultured hepatocytes overexpressing *Bhmt*, and rat livers following an *in vivo* induction of *Bhmt*, have increased apolipoprotein B expression [101-103]. These data suggest that betaine/BHMT might have multiple beneficial effects in lipoprotein synthesis. Others propose a role of betaine in reducing cellular stress [93, 104]. The antioxidant glutathione comes from cysteine, the generation of which requires AdoMet (**Figure 2.4**). Glutathione scavenges free radicals and is particularly important in mitochondria. The mitochondria are the primary intracellular site of oxygen consumption and the major source of reactive oxygen species (ROS) [105]. Glutathione maintains the redox balance and protects cells from oxidative stress [105]. One proposed mechanism is that betaine/BHMT restores AdoMet and glutathione concentrations, attenuates oxidative stress, and prevents further liver damage [104, 106, 107]. A growing body of evidence demonstrates that high Hcy induces ER stress [93, 95, 101, 108]. ER is an essential organelle, which provides a specialized environment for the production and post-translational modifications of secretory and membrane proteins. One proposed mechanism suggests that Hcy can be wrongly incorporated to proteins, causing protein misfolding and unfolding in the ER [93, 95, 101, 108]. An accumulation of these wrongly folded proteins then induces ER stress. ER stress activates *Srebp1c* (sterol regulatory element binding protein 1c), an ER bound transcription factor that induces lipid

synthesis. Activation of *Srebp1c* further contributes to the development of fatty liver [108]. Betaine/BHMT system may protect liver through reducing HHcy induced ER stress. Hepatocytes overexpressing *Bhmt* and transgenic mice expressing human *BHMT* were resistant to HHcy induced ER stress and cell death [95, 101].

In addition to reducing hepatic steatosis and preventing further liver damage, betaine/BHMT has a potential role in enhancing insulin sensitivity. Betaine supplementation alleviates insulin resistance and reduces hepatic steatosis in a high-fat-fed mouse model [99]. When supplemented with betaine, epidermal fat pad and adipocytes isolated from high-fat-fed mice have increased activation (phosphorylation) of protein kinase B (PKB/Akt) and extracellular signal-regulated kinases (ERK) that are normally suppressed by high-fat-diet [99]. PKB/Akt and ERK are two principal downstream kinases in the insulin-signaling pathway. This finding suggests that betaine could ameliorate fatty liver by improving insulin function in adipose tissue. Another study demonstrates that betaine treatment reverses the inhibition of hepatic insulin signaling in high-fat-fed mice and insulin-resistant HepG2 cells [98]. Betaine supplementation increases the activation of insulin receptor substrate 1 (IRS1), leading to enhanced glycogen synthesis and reduced gluconeogenesis. Taken together, these studies suggest roles for betaine/BHMT in alleviating fatty liver, fatty liver related cellular injury and insulin resistance.

An alternative way to study gene function is by studying the engineered knockout (deletion) mouse models. A *Bhmt* knockout mouse model was not available until now. Previously, a potent inhibitor of BHMT, S-(δ-carboxybutyl)-*DL*-homocysteine (CBHcy), was

administered intraperitoneally to mice [109] or fed to rats [110] to study the physiological implications of BHMT deficiency. Administration of CBHcy causes an elevation of plasma tHcy concentration and a reduction in hepatic AdoMet:AdoHcy ratio, reaffirming the role of BHMT in regulating Hcy and methyl donors. In these studies, inhibition of *Bhmt* does not affect markers of hepatic health such as fatty liver and plasma alanine transaminase. The lack of effects is probably due to a short term or an incomplete inhibition of BHMT.

2.5 One-Carbon Metabolism and Cancer

In 2008, the American Cancer Society (www.cancer.org) projected that about 780,300 people worldwide would have new liver cancer cases, and about 695,500 people would die from liver cancer. In 2011, an estimated 26,190 new cases of liver cancer and 19,590 liver cancer deaths are expected in the United States alone. Hepatocellular carcinoma (HCC) accounts for >80% of liver cancer cases. Liver cancer is among the most lethal cancers (five-year survival rates under 14%), making it the fifth most frequent cause of cancer death in American men and the ninth in American women [111]. The incidence rates are highest among Asian Americans/Pacific Islanders and Hispanics [111].

Mouse models for HCC are used to understand the molecular mechanisms underlying the pathogenesis of HCC. These mouse models are often genetically modified or cancers are induced by agents such as diethylnitrosamine, aflatoxin, and phenobarbital. Choline is the only nutritional deficiency that causes liver cancer without any known carcinogen [112]. In rodents, choline deficiency results in a higher incidence of spontaneous HCC [112]. Cancer

initiates with DNA damage within cells. Cancer ensues when these cells fail to repair and to recognize the DNA damage, and fail to die by apoptosis. Several mechanisms have been suggested for choline deficiency's carcinogenic effects. One proposed mechanism is based on the observation that rats fed a choline-deficient diet have increased lipid peroxidation in the liver [113]. Lipid peroxidation refers to the oxidative degradation of lipids, producing free radicals that can modify DNA in the nucleus and induce carcinogenesis. Another proposed mechanism is that choline deficiency perturbs signaling transduction. Large amounts of PtdCho are synthesized from choline and diacylglycerol (DAG) in cells. In cased of choline deficiency, PtdCho synthesis is diminished and DAG accumulates. DAG activates protein kinase C signaling cascades, resulting in altered cell proliferation signals and cell apoptosis and finally in carcinogenesis [114].

Methyl deficiency may also mediate the mechanisms that underlie the etiology of cancers. As discussed previously, AdoMet is required for the synthesis of the antioxidant glutathione, which attenuates oxidative stress by scavenging free radicals, protecting cells from DNA damage. Methyl deficiency may also affect DNA via epigenetic modification, such as DNA and histone methylation. DNA methylation predominantly involves the covalent addition of a methyl group to the 5' position of cytosine that precedes a guanosine (CpG) in the DNA sequence. This is referred to as an epigenetic modification since it does not change the coding sequence of the DNA. When DNA methylation occurs in the promoter regions, the expression of the associated gene is altered [115, 116]. Methylated CpG prevents the binding of the transcription factors, while unmethylated CpG allows the binding of the transcription factors to the gene [115, 116]. These actions alter gene expression based on the

roles of the transcription factors. For example, if the binding of the transcription factor is associated with inducing gene expression, then DNA methylation will result in gene silencing, and vice versa. Although there are exceptions, increased DNA methylation is usually associated with gene silencing, while decreased methylation usually associates with increased gene expression [117]. AdoMet is required for DNA methylation, while AdoHcy inhibits the methyltransferases. Methyl deficiency may alter epigenetic machinery by hypomethylating and paradoxically hypermethylating specific genes (e.g. tumor suppressor genes). Consequently, the expression of tumor suppressor genes responsible for DNA repair (*BRCA1, hMLH1*), cell cycle regulation (*p15, p16*), carcinogenesis metabolism (*GSTP1*), hormonal response (*RARβ2*), apoptosis (*DAPK, APAF-1*), cell adherence (*CDH1, CDH3*) [118-120] are silenced, leading to tumor development. Two mouse models with disturbed methyl group metabolism demonstrate the importance of methyl groups in cancer etiology. Methionine adenosyltranferase 1A knockout mouse model (cannot make AdoMet from methionine) has a persistent decrease in AdoMet concentration in the liver, leading to the development of HCC [121]. Glycine *N*-methyltransferase (GNMT) catabolizes AdoMet to AdoHcy, hence regulates the ratio of AdoMet/AdoHcy. The GNMT knockout mouse model has liver AdoHcy concentration 71 times higher than that of controls. These mice have steatosis and liver fibrosis after 3 months [122], and develope multifocal HCC at 8 months [123]. Together, these data demonstrate the importance of DNA methylation in cancer etiology.

2.6 Energy Metabolism and Insulin Sensitivity

The pathogenesis of obesity is complex, involving multiple organs and endocrine systems. Liver, white adipose tissue and brown adipose tissue are the key regulators of energy homeostasis. During glucose abundance (feeding), both adipose and liver can utilize glucose to synthesize lipid in the form of triacylglycerol [124]. Glucose provides glycerol phosphate, the backbone for triacylglycerol synthesis [124]. Excess glucose also forms acetyl CoA for *de novo* fatty acid synthesis [124]. Liver does not usually store lipid. Therefore, the synthesized TAG is packaged into VLDL and transported from the liver to circulation, where FA are taken up and stored in adipose tissue [87]. Liver can also store glucose as glycogen. White adipose tissue serves as an energy reservoir [125, 126]. It stores fuel in the form of triacylglycerol during energy excess and breaks down triacylglycerol and releases glycerol and fatty acids during energy deprivation [125, 126]. Glycerol and fatty acids from lipolysis then serve as fuels for organs. Fatty acids can be catabolized by β oxidation in the mitochondria, a step in which carnitine is required. White adipose tissue also acts as an endocrine organ; it may regulate glucose balance by secreting glucose regulating factors such as leptin, adiponectin, and tumor necrosis factor-α (TNF-α) [125, 126]. Brown adipose tissue functions to regulate thermogenesis, providing heat to mammals during cold exposure to maintain body temperature. Different from white adipose tissue, brown adipose tissue contains multi-locular lipid droplets, a high abundance of mitochondria, and a large amount of uncoupling protein 1 (UCP1) [127]. UCP1 allows the hydrogen ions to pump through the electron transport chain and release as heat instead of ATP [127]. Finally, the brain can sense nutrient availability and respond by altering food intake and stimulating the release of factors that regulate energy metabolism [128]. Taken together, homeostasis of energy stores is

regulated by mechanisms including modulation of metabolic rate and thermogenesis, regulation of metabolite fluxes among various organs, and modulation of fuel synthesis and usage within adipose tissue.

Alteration in fat stores in organs is associated with altered insulin sensitivity and glucose balance [126]. Insulin is a peptide hormone that is secreted by pancreatic β cells in response to elevated glucose levels after feeding [124, 129]. Insulin regulates blood glucose concentration via increasing glucose uptake by adipose tissue and muscle and inhibiting hepatic glucose production [124, 129]. Insulin also promotes the storage of glucose as glycogen in liver, and as triacylglycerol in adipose tissue. Insulin binds to the insulin receptor on cells. The receptor's tyrosine kinase activity autophosphorylates and activates the receptor, leading to recruitment and activation of insulin receptor substrate proteins (IRS) [124, 129]. IRS proteins initiate signaling cascades that mediate a variety of cellular processes, including glycogen synthesis and gluconeogenesis. IRS activates PKB/Akt (protein kinase B) via phosphorylation. PKB/Akt then inactivates (phosphorylates) GSK3β (glycogen synthase kinase 3β), which functions to inhibit glycogen synthase activity [124, 129]. Therefore, insulin's inhibition of GSK3β leads to enhanced glycogen synthesis [124, 129]. PKB/Akt also inactivates (phosphorylates) FoxO1 (Forkhead box protein O1), which normally induces *Pepck* (phosphoenolpyruvate carboxykinase), a gene involved in gluconeogenesis [124, 129]. Insulin reverses this induction, leading to suppressed gluconeogenesis [124, 129]. In adipose tissue, insulin enhances glucose uptake by stimulating glucose transporter 4 (GLUT4) and induces the expression of several lipogenic enzymes, leading to increased fatty acid and triacylglycerol synthesis [124, 129]. Insulin also inhibits lipolysis in adipocytes through the

inhibition of hormone sensitive lipase [124, 129]. Alterations in insulin receptor concentrations, IRS proteins concentrations, the translocation of glucose transporters, and the activities of various kinases and intracellular enzymes all contribute to insulin sensitivity and adiposity.

Several hormones and growth factors have been identified as important regulators of energy homeostasis and glucose metabolism. In this dissertation, we observed changes in the thyroid hormone, bile acids and fibroblast growth factor 21 (FGF21), all of which are associated with increased energy expenditure. The thyroid hormone has long been accepted to have a major impact on the basal metabolic rate [130]. The thyroid gland secretes two forms of thyroid hormone - the predominant but inactive form, thyroxine (T4), and the active form, triiodothyronine (T3). Thyroid hormone binds to its receptors. There are two forms of thyroid hormone receptor (TR) – TRα1 is typically found in adipose tissue, muscle, brain and heart tissues, while TRß is in liver and kidney tissues [131]. Within the cell, the inactive prohormone T4 is converted to T3 by the enzyme deiodinase II, which is induced by bile acid [132, 133]. In adipose tissue, thyroid hormone functions to stimulate thermogenesis, lipolysis and lipogenesis simultaneously [134]. With these processes, thyroid hormone results in increased oxygen consumption and metabolic rate. Thyroid hormone also regulates glucose metabolism via enhancing glucose transporter GLUT4 expression [135]. In the liver, thyroid hormone induces HMG-CoA reductase, the rate-limiting enzyme for *de novo* cholesterol synthesis [130]. This results in an enhanced synthesis of cholesterol in hyperthyroidism. However, there is an inverse relationship between thyroid hormone and serum cholesterol [136] because thyroid hormone may simultaneously affect the synthesis and degradation of

LDL cholesterol [137]. Thyroid hormone also induces cholesterol 7α hydroxylase (CYP7A1), the rate-limiting enzyme in bile-acid synthesis from cholesterol [138, 139]. This results in an enhanced synthesis of bile acids from cholesterol in hyperthyroidism. Taken together, thyroid hormone induces cholesterol turnover and bile acids synthesis.

A novel concept indicating a signaling role of bile acids (BAs) in the control of energy metabolism has emerged [132, 133]. CYP7A1 catalyzes the conversion of cholesterol to 7α hydroxycholesterol, which is subsequently converted to bile acids. Cholic acid and chenodeoxycholic acid are the primary bile acids and often conjugate with taurine (as taurocholate or taurochenodeoxycholate) or glycine (as glycocholate or glycochenodeoxycholate) forming bile salts. Mice fed a cholic acid supplemented diet have increased energy expenditure, and are protected from diet-induced obesity and insulin resistance [133]. On the contrary, mice that have reduced bile acids have decreased energy expenditure and increased body fat [132]. Although debatable, it is suggested that bile acids increase energy expenditure via inducing deiodinase 2, the enzyme that converts T4 to T3 within cells. It is interesting to note the interactions between thyroid hormone and bile acids. Thyroid hormone induces the synthesis of bile acids from cholesterol in the liver [138, 139]. In return, bile acids induce energy metabolism, perhaps through the activation of thyroid hormone [132, 133].

Fibroblast growth factor 21 (FGF21) is a member of the FGF superfamily that is synthesized predominantly in the liver and released into circulation [140]. FGF21 plays a critical role in energy metabolism. In mice, hepatic *Fgf21* expression is induced by fasting

and is regulated by *Pparα* (peroxisome proliferator activated receptor α), *Pparγ*, and *ChREBP* (carbohydrate response element binding protein) [141-143]. FGF21 increases glucose uptake [142, 144] and decreases intracellular TAG content in adipocytes [144]; it lowers plasma glucose and TAG when administered to diabetic mice [142]; and it increases energy expenditure and improves insulin sensitivity in diet-induced obese mice [145, 146]. Like bile acids, FGF21 appears to interact with thyroid hormone. Thyroid hormone treatment induces hepatic *Fgf21* expression in a *Pparα* dependent manner [147]. FGF21 also appears to interact with bile acids. The evidence comes from recent studies carried out in patients with nonalcoholic steatohepatitis (NASH). These studies demonstrate that plasma bile acids and FGF21 concentrations are elevated in patients with NASH [148, 149]. The authors suggest that bile acids induce hepatic *Pparα*, which activates *Fgf21*, resulting in increased hepatic fatty acid oxidation in NASH patients [148, 149]. FGF21, bile acids and thyroid hormone all induce similar metabolic changes such as energy expenditure and glucose uptake. All of these molecules are altered in the *Bhmt*$^{-/-}$ mice. The interactions between these molecules and *Bhmt* deficiency remain to be elucidated.

2.7 One-Carbon Metabolism, Energy Metabolism, and Adiposity

There has been no direct evidence that BHMT is involved in energy metabolism. However, there is accumulating data that BHMT's substrate betaine and betaine's precursor choline may be involved in energy metabolism. Diets deficient in choline alone, or both choline and methionine, have been used to investigate aspects of metabolic syndrome, particularly non-alcoholic fatty liver and insulin resistance. Mice fed a methionine and choline deficient (MCDD) diet develop hepatic steatosis due to impaired PtdCho

biosynthesis. Compared to controls, MCDD-fed mice have a 37% increase in metabolic rate, leading to a 26% loss of body weight [150]. Peripheral insulin action has been reported to be normal [151] or improved [152, 153] in MCDD-fed rodents. Mice fed a high fat diet without choline (but with methionine) have better insulin sensitivity and improved glucose tolerance compared to high-fat-choline-fed mice [154]. Mice with the *Pemt* (making PtdCho from PtdEtn) gene deleted have normal metabolic parameters on a regular chow diet compared to wildtype controls [155]. However, when fed a high fat diet, they have increased energy expenditure, accumulate less body fat, and have increased glucose sensitivity [155]. The lack of weight gain in $Pemt^{-/-}$ mice disappears when mice are fed a diet supplemented with choline. These observations suggest a potential role of choline deficiency in modulating energy metabolism and insulin sensitivity.

Betaine is widely discussed as a "carcass modifier" due to its lipotropic and growth-promoting effects, generating leaner meat [156]. Betaine was originally introduced to the feed industry as a substitute for methionine and choline in diets for livestock. This was done based on economic interest and the possibility that betaine may enhance methionine and choline availability. Numerous investigations have been carried out to evaluate the effectiveness of dietary betaine supplementation on livestock (**Table 2.2**) [156-181]. In poultry, betaine supplementation resultes in reduced abdominal fat [156-181]. In pigs, betaine supplementation reduces carcass fat by 10-18% and increases lean mass by 4-8% [156-181]. The reduction of total carcass fat content is reflected by reduction in backfat thickness in pigs [156-181].

Information on the mechanisms of how betaine reduces the fat content of animals is scarce, though some mechanisms have been proposed. Betaine supplementation may increase the availability of methionine, perhaps explaining the increased protein production [156]. Betaine may enhance the synthesis of carnitine (a methylated compound formed from methionine and lysine), which is required for transporting long-chain fatty acids into mitochondria, where fatty acid oxidation takes place. Carnitine in liver and muscle increases from 9% to 53% in betaine supplemented poultry and pigs [156, 175]. However, there is no evidence that increased carnitine concentration translates into increased fatty acid oxidation. One study shows that betaine has no significant impact on β-oxidation in either *in vivo* or *in vitro* system in pigs [182]. Other studies suggest that betaine supplementation reduces body fat via reducing lipid synthesis and/or enhancing lipid breakdown. Betaine supplementation decreases the activities and the gene expressions of fatty acid synthesis, acetyl-CoA carboxylase, and malic enzyme (enzymes involved in lipogenesis) in the subcutaneous adipose tissue in pigs [183, 184]. In addition, betaine supplementation increases hormone sensitive lipase activity (enzyme involved in lipolysis) in broilers [185] and pigs [183]. In the agouti mouse model, the transgenerational amplification of obesity is prevented when mice are fed a diet high in betaine and choline, suggesting that epigenetic methylation is involved [186]. Most studies show interactions of betaine with growth-regulating and metabolic factors (**Table 2.3**) [172, 175, 179, 181, 187-191]. Betaine supplementation elevates the plasma growth hormone (GH) level between 46 to 102%, and the insulin-like growth factor 1 (IGF-1) level between 39 to 75 % in pigs and poultry [156]. The dietary supplementation of betaine also increases serum levels of triiodothyronine (T3) and thyroxine (T4) in pigs and poultry [156]. The direct interactions of betaine with these

hormones are not fully understood. However, there is evidence that betaine is linked to thyroid hormone (T3 and T4) secretion, since thyroidectomy induces an increase in the activity of BHMT [192].

Betaine supplementation has been advertised to humans due to its potential role in reducing obesity. However, its lipotropic property has not been demonstrated in humans. A 12-week study of betaine supplementation finds no effect on body fat and resting energy expenditure in obese adult subjects [70]. Alternatively, in a population-based study, plasma betaine is inversely related to the components of metabolic syndrome (BMI, % body fat, waist circumference, glucose, non-HDL cholesterol) and positively related to HDL cholesterol [77, 193]. These data suggest that BHMT and its metabolites, such as choline and betaine, may have a role in the regulation of energy metabolism and adiposity.

Table 2.2 Effect of betaine on carcass composition in pigs and poultry

Animal	Betaine supplementation (%)	Betaine effects	Reference
Pigs			
Barrows, gilts; 83–116 kg	0·13	–	156
56–113 kg	0·11	–	155
24–111 kg	0·11	–	155
Barrows; 36–64 kg	0·13–0·5	↓ Carcass fat, 10 %	157
		↓ Fat depth, 26 %	
		↑ Total carcass protein, carcass protein:fat ratio, 23 %	
30–112 kg	0·2	–	158
Barrows; >45 kg	0·13	↑ Shoulder weight	159
Barrows; 83–116 kg	0·13	↓ Fat depth	160
Gilts; 83–116 kg		–	
Barrows, gilts; 60–115 kg	0·13–0·5	↑ Carcass length, fat-free lean, ham weight, ham fat-free lean, ham percentage lean	162
		↓ 10th Rib backfat thickness, percentage fat, total ham fat, percentage ham fat, butt-fat thickness	
Barrows; 50–110 kg	0·25	–	161
Grower–finisher pigs; >20 kg	1·5	–	163
Pigs; >30 kg	0·03–0·1	–	164
Grower–finisher pigs; >34 kg	0·1	–	166
Barrows, gilts; 60–104 kg	0·1	↑ Loin depth	165
Pigs	0·2	↓ Backfat thickness, 5·2 %*	167
Pigs	0·2	↓ Backfat thickness, 6·3 %	167
Barrows, gilts	0·2	–	168
30–112 kg	0·2	–	169
Barrows, gilts; 20–65 kg	0·15	↑ Dissected lean of the carcass: barrows, 3 %; gilts, 8·2 %	170
		↑ *Longissimus dorsi* area: gilts, 39·2 %	
		↓ Backfat thickness: barrows, 18·1 %; gilts, 10·8 %	
Pigs; >60 kg	0·1	↑ Intramuscular fat of *longissimus dorsi*, 17·7 %	171
		↓ Percentages of dissected fat, 18·3 %	
		↑ Percentages of dissected lean, 5·7 %	
Pigs; 83–118 kg	0·13	–	172
Weaned, grower, finisher pigs	0·08–0·18	↓ Percentages of dissected fat: weaned pigs, 13 %; grower pigs, 9·6 %; finisher pigs, 12·5 %	173
		↑ Percentages of dissected lean carcass: weaned pigs, 4·1 %; grower pigs, 7·2 %; finisher pigs, 3·3 %	
Poultry			
Broiler chick	0·5	↑ Carcass yield	174
Broiler chick; male	0·05	↑ Breast-meat yield	175
Broiler chick; male	0·04	↑ Trend breast-meat yield	176
Meat duck	0·03–0·1	↑ Percentage of breast muscle	178
Meat duck; male, female; >21 d	0·03–0·1	↓ Percentages of dissected abdominal fat	177
		↓ Subcutaneous fat depth	
		↓ Crude fat content of the liver	
		↑ Inter-muscular fat depth	
		↑ Crude fat content of the breast muscle	
Laying hen; >20 weeks	0·06	↓ Abdominal fat: week 50, 19·6 %; week 70, 22·4 %	179
		↓ Liver fat: week 50, 8·5 %; week 70, 16·3 %	

–, No effect; ↓, significant decrease relative to control (no betaine supplementation); ↑, significant increase relative to control (no betaine supplementation).
* Second half of fattening period.

Table from Eklund M. *Nutrition Research Reviews* 2005; 18, 31-48.

Table 2.3 Effect of betaine on hormone levels in pigs and poultry

Animal	Betaine supplementation (%)	Betaine effects	Reference
Pigs			
Barrows, gilts; 20–65 kg	0·15	↑ Serum GH: barrows, 62·5 %; gilts, 71 % ↑ Serum IGF-1: barrows, 74·3 %; gilts, 45 %	170
Finisher pigs	0·1	↑ Serum GH, 59·1 %	186
Grower pigs	0·1	↑ Serum GH, 101·8 % ↑ Serum IGF-1, 44·8 % ↑ Serum T_3, 26·5 % ↑ Serum T_4, 16·8 %	185
Piglets; male, female; >10 kg	0·08	↑ Serum GH, IGF-1	187
Weaned, grower, finisher pigs	0·08–0·18	↑ Serum GH: weaned pigs, 46·2 %; grower pigs, 102·1 %; finisher pigs, 58·3 % ↑ Serum IGF-1: weaned pigs, 38·7 %; grower pigs, 44·7 %; finisher pigs, 48 %	173
Poultry			
Meat duck; >21 d	0·03–0·1	↑ Serum GH	177
Laying hen; >20 weeks	0·06	↑ Serum T_3: week 50, 43·3 %; week 70, 44 %	179
Laying hen	0·08	↑ FSH and LH, serum and pituitary ↑ Serum T_3 ↑ Serum parathyroid hormone ↑ Serum oestradiol ↑ Serum progesterone	188
Laying hen	0·08	↑ Serum T_3 ↑ Serum T_4	189

↑, Significant increase relative to control (no betaine supplementation); GH, growth hormone; IGF, insulin-like growth factor; T_3, triiodothyronine; T_4, thyroxine; FSH, follicle-stimulating hormone; LH, luteinising hormon

Table from Eklund M. *Nutrition Research Reviews* 2005; 18, 31-48

CHAPTER III

THE ROLE OF BHMT IN ONE-CARBON METABOLISM AND LIVER HEALTH

DELETION OF BETAINE-HOMOCYSTEINE *S*-METHYLTRANSFERASE IN MICE PERTURBS CHOLINE AND 1-CARBON METABOLISM, RESULTING IN FATTY LIVER AND HEPATOCELLULAR CARCINOMA[1]

Ya-Wen Teng, Mihai G. Mehedint, Timothy A. Garrow, and Steven H. Zeisel

3.1 ABSTRACT

Betaine-homocysteine *S*-methyltransferase (BHMT) uses betaine to catalyze the conversion of homocysteine (Hcy) to methionine. There are common genetic polymorphisms in the *BHMT* gene in humans that can alter its enzymatic activity. We generated the first *Bhmt*$^{-/-}$ mouse to model the functional effects of mutations that result in reduced BHMT activity.

---

[1]Teng, Y., Mehedint, M.G., Garrow, T.A., and Zeisel, S.H. (2011). Deletion of Murine Betaine-Homocysteine S-Methyltransferase in Mice Perturbs Choline and 1-Carbon Metabolism, Resulting in Fatty Liver and Hepatocellular Carcinoma. *JBC.* 286(42):36258-67.

Deletion of *Bhmt* resulted in a 6-fold increase ($p<0.01$) in hepatic and an 8-fold increase ($p<0.01$) in plasma total Hcy concentrations. Deletion of *Bhmt* resulted in a 43% reduction in hepatic *S*-adenosylmethionine (AdoMet) ($p<0.01$) and a 3-fold increase in hepatic *S*-adenosylhomocysteine (AdoHcy) ($p<0.01$) concentrations, resulting in a 75% reduction in methylation potential (AdoMet:AdoHcy) ($p<0.01$). *Bhmt*$^{-/-}$ mice accumulated betaine in most tissues, including a 21-fold increase in the liver concentration compared to wildtype (WT) ($p<0.01$). These mice had lower concentrations of choline, phosphocholine, glycerophosphocholine, phosphatidylcholine and sphingomyelin in several tissues. At 5 weeks of age, *Bhmt*$^{-/-}$ mice had 36% lower total hepatic phospholipid concentrations and a 6-fold increase in hepatic triacyglycerol concentrations compared to WT ($p<0.01$), which was due to a decrease in the secretion of very low density lipoproteins. At 1 year of age, 64% of *Bhmt*$^{-/-}$ mice had visible hepatic tumors. Histopathological analysis revealed that *Bhmt*$^{-/-}$ mice developed hepatocellular carcinoma (HCC) or carcinoma precursors. These results indicate that BHMT has an important role in Hcy, choline and one-carbon homeostasis. A lack of *Bhmt* also affects susceptibility to fatty liver and HCC. We suggest that functional polymorphisms in *BHMT* that significantly reduce activity may have similar effects in humans.

3.2 INTRODUCTION

Betaine-homocysteine *S*-methyltransferase (BHMT) is a zinc dependent cytosolic enzyme that catalyzes the transfer of a methyl group from betaine to homocysteine (Hcy) forming dimethylglycine (DMG) and methionine (Met). Humans have common single nucleotide polymorphisms (SNPs) in the *BHMT* gene that alter BHMT enzyme activity and function [12]. A common *BHMT* SNP rs3733890 (41% of NC population has 1 variant allele, and 8% have 2 alleles [51]) was associated with increased risk for having babies with neural tube defects (NTDs) [53], decreased risk for developing cardiovascular disease [55] and reduced risk for breast cancer-specific mortality [59]. The epidemiological evidence suggests the importance of SNPs in the gene. However, the metabolic consequences of having null mutations of *BHMT* gene have not been thoroughly-investigated. To directly investigate the role of BHMT *in vivo*, we generated and characterized mice in which the gene encoding *Bhmt* was deleted (*Bhmt*$^{-/-}$).

BHMT activity is found at high levels in the liver and kidney, and low levels in the brain, lenses and other human tissues. In rodents, high levels of BHMT activity are only found in the liver [18]. Betaine, the methyl donor for BHMT, comes from either dietary sources or from oxidation of choline (an irreversible reaction) by choline dehydrogenase (CHDH). Alternatively, choline can be used to form the phospholipid phosphatidylcholine (PtdCho) or the neurotransmitter acetylcholine [194]. The product of BHMT, methionine, is the precursor for *S*-adenosylmethionine (AdoMet), the major methyl donor for most biological methylations, including DNA and histone methylation, the conversion of glycine

to methylglycine (catalyzed by glycine methyltransferase (GNMT)), and the methylation of phosphatidylethanolamine (PtdEtn) to form PtdCho (catalyzed by phosphatidylethanolamine-*N*-methyltransferase (PEMT)).

The other substrate for BHMT is Hcy, a thiol-containing amino acid, which, when elevated in plasma, is associated with cardiovascular diseases, pregnancy complications, renal insufficiency and cognitive impairment [43]. Hcy is converted to methionine by BHMT or by methionine synthase (MS), the latter of which uses methyltetrahydrofolate (methylTHF) as the methyl donor (supplied by methylenetetrahydrofolate reductase (MTHFR)) [195]. Alternatively, Hcy is removed by the trans-sulfuration pathway, forming cystathionine and cysteine catalyzed by the enzymes cystathionine-β-synthase (CBS) and cystathionine-γ-lyase (CγL), respectively [195]. Both enzymes require vitamin B_6; CBS also requires AdoMet as the allosteric activator [195]. All the above pathways might be perturbed with the deletion of *Bhmt.* Here, we report on the metabolic phenotype of the first *Bhmt* knockout mouse created.

3.3 EXPERIMENTAL PROCEDURES

Generation of *Bhmt*$^{-/-}$ mice - The gene targeting vector was designed to remove exons 6 and 7, the zinc binding domains of the gene (**Figure 3.1A**). The targeting vector was constructed by placing a MC1-neomycin (Neo) selectable marker flanked by 2 flippase (FLP) recognition target (FRT) sites and 1 locus of X-over P1 (loxP) site ~330 bp downstream of exon 7. A second loxP site was introduced ~240 bp upstream of exon 6. The vector was electroporated into E14Tg2A embryonic stem (ES) cells. Targeted cells were screened by PCR, confirmed by Southern-blot analysis, and injected into blastocysts derived from mouse strain C57Bl/6 to create *Bhmt* transmitting chimeras. Neo deleted mice were generated by crossing the transmitting chimeras with Flpe deleters (#003800, Jackson Laboratory, Bar Harbor, ME), which expressed Flpe recombinase that recognized FRT sites and deleted the Neo cassette. *Bhmt* knockout (KO) mice were generated by crossing the Neo deleted mice with Cre deleters (#003724, Jackson Laboratory), which expressed Cre recombinase that recognized loxP sites and deleted exons 6 and 7. *Bhmt* KO mice were continuously backcrossed to C57Bl/6 mice. Generations F1 to F4 were used in this study.

For all experiments, *Bhmt*$^{+/+}$, *Bhmt*$^{+/-}$, and *Bhmt*$^{-/-}$ littermates born of *Bhmt*$^{+/-}$ mating pairs were used to control the mixed genetic background. Mice were genotyped by PCR using TaKaRa Ex Taq DNA polymerase (TaKaRa Bio USA, Madison, WI) and the following primer sequences: *Bhmt*$^{+/+}$ forward 5'-GACTTTTAAAGAGTGGTGGTACATACCTTG-3', *Bhmt*$^{+/+}$ reverse 5'-TCTCTCTGCAGCCACATCTGAACTTGTCTG-3', *Bhmt*$^{-/-}$ forward 5'TTAACTCAACATCACAACAACAGATTTCAG-3', *Bhmt*$^{-/-}$ reverse 5'-TTGTCGACGGATCCATAACTTCGTATAAT-3'. PCR conditions were as follows: 94°C

for 2 min; 40 cycles of 94°C for 30 sec, 64°C for 2 min, and 72°C for 2 min; and 72°C for 6 min. *Bhmt*$^{+/+}$ PCR product was 1.6 kb in size, while *Bhmt*$^{-/-}$ was 545 bp (**Figure 3.1B**). The animals were kept in a temperature-controlled environment at 24°C and exposed to a 12h light and dark cycle. All animals received AIN-76A pelleted diet with 1.1 g/kg choline chloride (Dyets, Bethlehem, PA). The Institutional Animal Care and Use Committee of the University of North Carolina at Chapel Hill approved all experimental protocols.

Reproducibility, viability, body weight, body length, and life span - Pairs of *Bhmt*$^{+/+}$, *Bhmt*$^{+/-}$, and *Bhmt*$^{-/-}$ parents were bred to assess their reproductive potential. Sizes, genotype distribution, and gender distribution of litters were recorded. Body weights and lengths (nose to hip, nose to tail) of *Bhmt*$^{+/+}$, *Bhmt*$^{+/-}$, and *Bhmt*$^{-/-}$ mice were measured from age 3.5 to 20 weeks old using a scale and a ruler respectively. Eleven *Bhmt*$^{+/+}$, and fourteen *Bhmt*$^{-/-}$ mice were maintained over the course of a year to determine one-year survival rates.

Western blot and enzymatic assay - Mice were anesthetized by inhalation of isoflurane (Hospira, Lake Forest, IL). Tissues were harvested, weighted, snap frozen, pulverized under liquid nitrogen and stored at -80^{o}C until used. Western blot analysis of BHMT was performed in liver homogenate as previously described [196]. For all enzymatic assays, pulverized liver from 5-week-old mice were homogenized in buffer using a motorized tissue homogenizer (Talboys Engineering Corporation, Montrose, PA). BHMT activity was measured as the conversion of [^{14}C]betaine to [^{14}C]methionine and [^{14}C]dimethylglycine as previously described [14]. CHDH activity was measured as the conversion of [^{14}C]choline to [^{14}C]betaine as previously described [197] using high pressure liquid chromatography (HPLC)

on a Varian ProStar HPLC system (PS-210, Varian Inc., Palo Alto, CA) with a Pecosphere Silica column, 4.6mm x 83 mm (Perkin Elmer, Norwalk, CA) and a Berthold LB506 C-1 radiodetector (Oak Ridge, TN). GNMT activity was measured as the conversion of [^{3}H]AdoMet to [^{3}H]methylglycine using the charcoal absorption method as previously described [198]. PEMT activity was measured as the conversion of [^{3}H]AdoMet to [^{3}H]PtdCho as previously described [199, 200]. Protein concentrations were measured using the Bradford Assay [201].

Choline and homocysteine metabolites - Tissues from 5-week-old animals were harvested as described above. Blood was collected via cardiac puncture, and plasma isolated by centrifugation at 3000 rpm for 5 min at room temperature. The concentrations of choline metabolites were measured by liquid chromatography-electrospray ionization-isotope dilution mass spectrometry (LC–ESI–IDMS) as previously described [202]. The concentration of AdoMet and *S*-adenosylhomocysteine (AdoHcy) were measured using the Varian ProStar HPLC system as previously described [203, 204] with an Ultrasphere ODS 5µm C18 column, 4.6mm x 25cm (#235329, Fullerton, CA) and a UV/VIS detector (model 118, Gilson, Middleton, WI). Plasma total Hcy (tHcy) and cysteine were measured after derivatizing 50 µL of plasma with 7-fluorobenzofurazan-4-sulfonic acid. The derivatized products were measured as previously described [205] using the Varian ProStar HPLC system with a Microsorb-MV 5µm C18 column, 4.6mm x 25cm (Varian) and a Prostar model 360 fluorescence detector (Varian). Mercaptopropinylglycine (10 µM) was used as an internal standard. Hepatic tHcy, cystathionine, methionine, cysteine, methylglycine, dimethylglycine, and glycine were measured as previously described [206] using capillary

stable isotope dilution gas chromatography/mass spectrometry (Hewlett-Packard Co., Pal Alto, CA). Plasma total folate was measured using *Lactobacillus casei* assay as previously described [207].

Clinical analysis - Concentrations of plasma urea nitrogen (BUN) and creatinine as well as activities of lactate dehydrogenase (LDH), alanine transaminase (ALT), and creatinine kinase (CK) were measured using an automatic chemical analyzer (Johnson and Johnson VT250, Rochester, NY) at the Animal Clinical Chemistry and Gene Expression Facility, UNC-Chapel Hill. Urine specific gravity was measured using a refractometer (AO Instrument Company, Buffalo, NY) at the Department of Laboratory Animal Medicine Veterinary and Technical Services Facility, UNC- Chapel Hill. Plasma triacylglycerol (TAG), β-hydroxybutyrate (Stanbio, Boerme, TX), cholesterol, high density lipoprotein cholesterol (HDL-C), non-esterified fatty acids (NEFA), and glucose (Wako, Richmond, VA) were measured colorimetrically per manufacturers' instructions.

Triacylglycerol, phospholipids, and cholesterol - PtdCho, PtdEtn, phosphatidylserine (PtdSer) and phosphatidylinositol (PtdIns) were extracted from 5-week-old mouse liver using the Bligh and Dyer method [208], and isolated by thin layer chromatography (TLC) [209]. Concentrations were determined using a phosphate assay [210]. TAG was extracted from liver samples using the Folch method [211] and measured colorimetrically as described above.

***In vivo* VLDL secretion rate -** 5-week-old animals were fasted for 4 hours. 500 mg/kg BW of Triton WR1339 (as a 7.5% solution dissolved in in PBS) was injected retro-orbitally. Blood samples were taken using heparinized capillary tubes retro-orbitally at 2, 30, 60, and 120 min after Triton WR1339 injection for TAG measurement as an indicator of the secretion rate of the very low density lipoprotein (VLDL).

Tissue histology - Liver was harvested and fixed in 4% paraformaldehyde/0.2% gluteraldehyde for 48 hours. Liver was processed, paraffin embedded, sectioned at 5 μm, and stained with hemotoxylin and eosin as previously described [212]. For tumor analysis, whole liver was sectioned serially, and multiple sections per sample were examined by 2 veterinary pathologists from the Department of Laboratory Animal Medicine, UNC-Chapel Hill. High resolution images were collected using a Zeiss Axiovision A1 upright microscope.

Gamma Glutamyltransferase 1 (gGT1) - gGT1 levels were determined using ELISA (Cedarlane, Burlington, NC). Frozen liver samples from 1-yr-old mice were homogenized in ice cold PBS at pH 7.0 containing 10% protease inhibitors (Sigma) using an ultrasonic cell disruptor. The resulting suspension was centrifuged and protein levels were determined by the Lowry method [213]. Equal amounts of proteins were loaded onto the ELISA plate according to manufacturer's protocol. The optical density was read at 450nm on a Synergy 2 microplate reader (Biotek, Vermont).

Statistics - Statistical differences were determined using ANOVA, Tukey-Kramer HSD, and Student's *t*-test JMP version 6.0; SAS Institute, Cary, NC) and reported as means ± SEM.

3.4 RESULTS

Generation and validation of *Bhmt* knockout mice - *Bhmt*$^{-/-}$ mice were generated using a cre/loxP system to delete exons 6 and 7, which contain the zinc binding domain essential for BHMT activity. The mouse genotype was confirmed by PCR using genomic DNA (**Figure 3.1B**). *Bhmt*$^{-/-}$ mice also were validated by assaying hepatic BHMT activity (**Figure 3.1C)** and by Western blot (**Figure 3.1D**). Deletion of 1 allele of *Bhmt* resulted in a 46% reduction of activity, while deletion of both alleles resulted in the absence of activity. BHMT protein is predominantly found in mouse liver and was absent in *Bhmt*$^{-/-}$ liver.

***Bhmt* deletion had no effect on reproductive capacity or fetal viability -** Mating pairs of *Bhmt*$^{+/+}$, *Bhmt*$^{+/-}$, and *Bhmt*$^{-/-}$ mice produced offspring with similar litter size (7.5 pups/litter) with evenly distributed genders. *Bhmt*$^{+/-}$ breeding pairs were used to generate littermates of *Bhmt*$^{+/+}$, *Bhmt*$^{+/-}$, and *Bhmt*$^{-/-}$ mice for all experiments. *Bhmt*$^{+/-}$ breeding pairs produced offspring at the expected Mendelian ratio, with 24.5% *Bhmt*$^{+/+}$, 49.7% *Bhmt*$^{+/-}$, and 25.8% *Bhmt*$^{-/-}$ mice. The *Bhmt*$^{+/+}$ and *Bhmt*$^{-/-}$ mice appeared healthy and lived for at least 1 year.

***Bhmt*$^{-/-}$ mice had reduced body weight at early age -** Body length and weight of pups were monitored from 3.5 to 20 weeks of age. There was no significant difference in body length among *Bhmt*$^{+/+}$, *Bhmt*$^{+/-}$, and *Bhmt*$^{-/-}$ mice (data not shown), and in body weight between *Bhmt*$^{+/+}$ and *Bhmt*$^{+/-}$ mice (**Figure 3.1E**). *Bhmt*$^{-/-}$ mice started with similar body weights as did *Bhmt*$^{+/+}$ mice at weaning (3.5 wk), but gained less weight between 5 to 9 weeks of age ($p<0.05$). The weight difference did not persist after 9 weeks of age.

***Bhmt* deletion resulted in altered concentrations of choline and its metabolites -** Bhmt is predominantly found in the liver, however, complete deletion of *Bhmt* (*Bhmt*$^{-/-}$) resulted in a substantial increase in concentrations of betaine in liver (by 21-fold; $p<0.001$), kidney (by 5-fold; $p<0.001$), heart (by 14-fold; $p<0.001$), brain (by 5-fold; $p<0.001$), muscle (by 12-fold; $p<0.001$), adipose (by 2-fold; $p<0.001$), lung (by 11-fold; $p<0.001$), and plasma (by 16-fold; $p<0.001$) compared to *Bhmt*$^{+/+}$ mice (**Table 3.1**). Deletion of *Bhmt* resulted in reduced concentrations of choline in liver (by 82%; $p<0.01$), kidney (by 38%; $p<0.01$), heart (by 42%; $p<0.05$), and adipose (by 53%; $p<0.01$) compared to *Bhmt*$^{+/+}$ mice. Deletion of *Bhmt* resulted in reduced concentrations of PtdCho in liver (by 26%; $p<0.01$), kidney (by 21%; $p<0.05$), heart (by 25%; $p<0.01$), muscle (by 25%; $p<0.05$), and plasma (by 31%; $p<0.001$) compared to *Bhmt*$^{+/+}$ mice. Deletion of *Bhmt* resulted in reduced concentrations of phosphocholine (PCho) in liver (by 72%; $p<0.01$), heart (by 24%; $p<0.05$), muscle (by 65%; $p<0.001$), and adipose (by 68%; $p<0.01$) compared to *Bhmt*$^{+/+}$ mice. Deletion of *Bhmt* resulted in reduced concentrations of glycerophosphocholine (GPCho) in liver ($p<0.01$), kidney ($p<0.05$), heart ($p<0.001$), adipose ($p<0.05$) and lung ($p<0.01$), as well as reduced concentrations of sphingomyelin (SM) in kidney ($p<0.05$) and heart ($p<0.001$) compared to *Bhmt*$^{+/+}$ mice. In testis, there was no change in any choline metabolites in *Bhmt*$^{-/-}$ mice. Deletion of 1 copy of *Bhmt* (*Bhmt*$^{+/-}$) resulted in choline metabolite concentrations in tissues similar to those of *Bhmt*$^{+/+}$ mice (**Table 3.6**).

***Bhmt* deletion resulted in altered concentrations of Hcy, AdoMet, AdoHcy and related metabolites -** In liver, complete deletion of *Bhmt* resulted in a 43% decrease in AdoMet

concentrations ($p<0.01$), and a 2.6-fold increase in AdoHcy concentrations ($p<0.01$), resulting in a 76% reduction in methylation potential (AdoMet:AdoHcy) ratios (0.9 ± 0.1 in *Bhmt*$^{-/-}$ vs 3.6 ± 0.2 in *Bhmt*$^{+/+}$; $p<0.01$) (**Table 3.2**). *Bhmt*$^{-/-}$ mice also had reduced hepatic concentrations of DMG (by 95%; $p<0.001$), but had increased hepatic concentrations of tHcy (by 6-fold; $p<0.01$) and methylglycine (by 2.6-fold; $p<0.05$) compared to *Bhmt*$^{+/+}$ mice. Hepatic cystathionine, cysteine, methionine, and glycine did not differ among genotypes. In plasma, deletion of *Bhmt* resulted in increased concentrations of tHcy (by 7.8-fold; $p<0.001$), decreased concentrations of cysteine (by 48%; $p<0.01$), and decreased concentrations of total folate (by 35%; $p<0.01$) compared to plasma from *Bhmt*$^{+/+}$ mice. Deletion of 1 copy of *Bhmt* (*Bhmt*$^{+/-}$) did not result in changes in hepatic methylation potential, plasma tHcy, or plasma total folate compared to *Bhmt*$^{+/+}$ mice (**Table 3.7**). *Bhmt*$^{+/-}$ had plasma cysteine concentrations between those of *Bhmt*$^{+/+}$ and *Bhmt*$^{-/-}$ mice.

***Bhmt* deletion resulted in altered activities of enzymes involved in one-carbon metabolism -** Since *Bhmt*$^{-/-}$ mice (but not *Bhmt*$^{+/-}$ mice) had altered one-carbon metabolites, enzymes involved in one-carbon metabolism were measured in *Bhmt*$^{+/+}$ and *Bhmt*$^{-/-}$ mouse liver. Complete deletion of *Bhmt* resulted in increased hepatic CHDH (by 1.33 fold; $p<0.05$) and GNMT (by 1.13 fold; $p<0.05$) activities (**Figure 3.2**). Hepatic PEMT activity was not affected by *Bhmt* deletion.

***Bhmt* deletion resulted in increased hepatic fat accumulation and decreased phospholipids -** At 5 weeks of age, hepatic TAG concentrations were 6.5-fold higher in *Bhmt*$^{-/-}$ mice than in *Bhmt*$^{+/+}$ mice ($p<0.05$) (**Figure 3.3C**). *Bhmt*$^{+/-}$ mice had similar hepatic

TAG concentrations compared to that of *Bhmt*$^{+/+}$ mice (8.96 ± 1.92 ug/mg tissue in *Bhmt*$^{+/-}$ vs 11.75 ± 0.99 ug/mg tissue in *Bhmt*$^{+/+}$). The difference in hepatic steatosis between *Bhmt*$^{+/+}$ and *Bhmt*$^{-/-}$ mice was easily visible at the microscopic level (**Figure 3.3B**). Hepatic and plasma phospholipids were measured in *Bhmt*$^{+/+}$ and *Bhmt*$^{-/-}$ mouse liver due to their involvement with hepatic lipid storage and release. *Bhmt*$^{-/-}$ mice had lower concentrations of phospholipids in liver than did *Bhmt*$^{+/+}$ mice (**Figure 3.3A**); with a 40% reduction in PtdCho ($p<0.01$), and a 60% reduction in PtdIns ($p<0.01$). *Bhmt*$^{-/-}$ mice also had a 31% reduction in plasma concentrations of PtdCho compared to *Bhmt*$^{+/+}$ mice ($p<0.01$) (**Table 3.1**). PtdEth concentrations in liver and plasma were the same for both genotypes. *Bhmt*$^{-/-}$ mice had significantly reduced VLDL secretion rate (**Figure 3.3D**).

***Bhmt* deletion resulted in altered clinical analyses -** Plasma alanine aminotransferase activity, a measure of liver damage, was modestly increased in *Bhmt*$^{-/-}$ mice (34.7 ± 4.4 U/l in *Bhmt*$^{-/-}$ vs 20.6 ± 4.9 U/l in *Bhmt*$^{+/+}$; $p<0.05$) (**Table 3.3**). Plasma BUN, creatinine, CK, and LDH, tests of kidney and muscle function, showed no changes in the *Bhmt*$^{-/-}$ mice. Urine specific gravity was significantly reduced in *Bhmt*$^{-/-}$ mice (1.020 ± 0.002 mg/dL in *Bhmt*$^{-/-}$ vs 1.039 ± 0.005 mg/dL in *Bhmt*$^{+/+}$; $p<0.01$). Plasma TAG, glucose, NEFA, and β-hydroxybutyrate concentrations did not differ between genotypes. Compared to wildtype littermates, *Bhmt*$^{-/-}$ mice had significantly lower plasma total cholesterol concentrations (by 45%, $p<0.01$) and HDL-C (by 38%, $p<0.01$). Heterozygous mice had similar plasma ALT, BUN, creatinine, LDH, CK, TAG, glucose, NEFA, and β-hydroxybutyrate concentrations compared to wildtype mice (**Table 3.7)**. Heterozygous mice had no change in plasma cholesterol and HDL-C concentrations compared to *Bhmt*$^{+/+}$ mice.

***Bhmt* deletion resulted in preneoplastic, neoplastic, and regenerative lesions in the mouse liver -** Eleven *Bhmt*$^{+/+}$, and fourteen *Bhmt*$^{-/-}$ mice were maintained over the course of a year to determine one-year survival rates. At time of sacrifice, 64% (9 out of 14) of *Bhmt*$^{-/-}$ mice and 0% (0 out of 11) of *Bhmt*$^{+/+}$ mice had visible hepatic tumors (**Figure 3.4a**). Tumors observed in *Bhmt*$^{-/-}$ mice were solitary or multifocal, found in multiple liver lobes. The average liver weight of *Bhmt*$^{-/-}$ mice was heavier than that of *Bhmt*$^{+/+}$ mice (6.22 ± 2.11 %BW in *Bhmt*$^{-/-}$ vs 4.36 ± 0.26 %BW in *Bhmt*$^{+/+}$; $p<0.001$), attributable to tumor mass. A subset of the liver samples (4 out of 11 *Bhmt*$^{+/+}$ livers, 6 out of 9 *Bhmt*$^{-/-}$ livers with tumors, and 4 out of 5 *Bhmt*$^{-/-}$ livers without tumors) were serial-sectioned entirely, stained with H&E, and send to two veterinary pathologists for diagnosis. Microscopic analysis depicted a series of histological abnormalities from preneoplastic lesions (acidophilic/eosinophilic cell foci) to frank neoplasia visible only in the *Bhmt*$^{-/-}$ mice (**Table 3.4 & Figure 3.4b**). Hepatocellular adenomas (HCA) were found in 30% (3 out of 10) of the analyzed *Bhmt*$^{-/-}$ livers and none were found in the control animals. These benign lesions were represented by single or multiple nodules, sharply demarcated from the surrounding tissues, with a mild to moderate compression border and loss of lobular structure. Hepatocellular carcinomas (HCC) were found in 50% (5 out of 10) of the analyzed *Bhmt*$^{-/-}$ livers. HCC were represented by nodules of atypical, megalo-hepatocytes that were vacuolated or contained hyaline droplets. Indicative of malignancy, these lesions were organized in cords that were 5-6 cells wide, had poor or nonexisting interface with the surrounding tissues, and compressed mildly the adjacent normal cords. The portal triads and sinusoids were poorly or non-distinguishable in most of the nodules. Formation of HCA and HCC in *Bhmt*$^{-/-}$ mice were accompanied by

macro and micro vesicular steatosis, and stellate (Ito) cell and/or oval (bililary) cell hyperplasia (**Table 3.4**). We did not study *Bhmt*$^{+/-}$ mouse survival or carcinogenesis.

***Bhmt* deletion resulted in elevated gamma glutamyltransferase 1 in livers -** gGT1 is a highly sensitive marker of chronic liver disease, neoplasia. and HCC [214]. *Bhmt*$^{-/-}$ mice had hepatic gGT1 concentrations 3.3 fold higher than that of the control mice (0.815 ± 0.049 ng/mg tissue in *Bhmt*$^{-/-}$ vs 0.245 ± 0.085 ng/mg tissue in *Bhmt*$^{+/+}$; $p<0.01$).

Changes in choline and one-carbon metabolites at 5 weeks persisted at 1 year old *Bhmt*$^{-/-}$ mice - Choline deficiency and reduced methylation potential have been hypothesized as mechanisms underlying development of HCC. Compared to wildtype mice, *Bhmt*$^{-/-}$ mice had a 91% reduction in hepatic methylation potential (AdoMet:AdoHcy) compared to *Bhmt*$^{+/+}$ mice ($p<0.001$) at 1 year (**Table 3.5**), which was greater than the 76% reduction seen at 5 weeks of age (**Table 3.2**). The reduced methylation potential was due to reduced hepatic AdoMet (by 50%; $p<0.01$) and to elevated AdoHcy (by 5.5 fold; $p<0.001$) concentrations in *Bhmt*$^{-/-}$ mice compared to *Bhmt*$^{+/+}$ mice. Compared to wildtype littermates, *Bhmt*$^{-/-}$ mice had a 30-fold increase in hepatic betaine, a 73% reduction in GPCho, a 64% reduction in PCho, and an 18.8% reduction in PtdCho concentrations. At 1 yr old, *Bhmt*$^{-/-}$ mice still had elevated plasma tHcy concentration (by 6.9-fold; $p<0.01$), but no longer had decreased plasma cysteine concentration.

3.5 DISCUSSION

To our knowledge, this is the first report of the successful creation of *Bhmt*$^{-/-}$ mice. Deletion of *Bhmt* gene resulted in the complete loss of BHMT activity in liver, the organ where nearly all of activity resides in mice. Heterozygous mice had 53% of the hepatic BHMT activity measured in *Bhmt*$^{+/+}$, suggesting that the *Bhmt* gene is biallelically expressed. Mating pairs of *Bhmt*$^{+/+}$, *Bhmt*$^{+/-}$, and *Bhmt*$^{-/-}$ produced offspring with normal number of pups and evenly distributed genders, suggesting that BHMT is not essential for reproduction. This is interesting because mice in which choline dehydrogenase (*Chdh*; form betaine from choline, immediately upstream from *Bhmt* in choline pathway, **Figure 3.5**) was deleted are infertile [215]. Fetuses from heterozygous (*Bhmt*$^{+/-}$) mating pairs were born at the expected Mendelian ratio; they were viable and survived to at least one year of age, suggesting that BHMT is not essential for embryonic development or for the viability of mice.

Though a *Bhmt* knockout mouse has not been previously created, when S-(δ-carboxybutyl)-*DL*-homocysteine (CBHcy; a potent and specific inhibitor of BHMT) was administered intraperitoneally to wildtype mice [109] or fed to rats [110], it caused an elevation of plasma Hcy concentrations and a reduction in hepatic AdoMet:AdoHcy ratio. Our current study confirms the finding that inhibiting or ablating flux through BHMT affects one carbon metabolism. The changes are summarized in **Figure 3.5**. As expected, *Bhmt*$^{-/-}$ mice had significantly higher concentrations of the substrates for this enzyme (betaine and Hcy) in various tissues as compared to *Bhmt*$^{+/+}$ mice. Our data show that the transsulfuration and methionine synthase pathways do not have the capacity to remove the excess tHcy that

accumulates when BHMT is not present, indicating that BHMT has a critical role in Hcy homeostasis. *Bhmt*$^{-/-}$ mice also had a significant reduction in hepatic dimethylglycine concentrations, one of the products of BHMT. Methionine, the other reaction product, was not affected by the gene deletion, probably because dietary methionine and protein stores of methionine are so large that the loss of BHMT-catalyzed biosynthesis does not alter overall concentrations of this amino acid. However, AdoMet concentration, which is formed from methionine, was reduced in livers of *Bhmt*$^{-/-}$ mice, while AdoHcy concentrations were elevated. AdoMet is used by glycine *N*-methyltransferase (GNMT), to form methylglycine from glycine [216] (**Figure 3.5**). Methylglycine is also formed from dimethylglycine, the product of the BHMT catalyzed reaction. Since *Bhmt*$^{-/-}$ mice do not accumulate dimethylglycine, the elevated methylglycine observed in *Bhmt*$^{-/-}$ mice likely comes from the action of GNMT. GNMT is allosterically inhibited by methylTHF [198], which serves as the methyl-donor for methionine synthase, a parallel pathway to BHMT that catalyzes the conversion of Hcy to methionine [195]. It is possible that the *Bhmt*$^{-/-}$ mice rely heavily on the use of methylTHF to form the needed methionine. Hence, GNMT is released from methylTHF inhibition, resulting in increased methylglycine, reduced AdoMet and increased AdoHcy concentrations that we observed. This hypothesis is supported by elevated hepatic GNMT activity in *Bhmt*$^{-/-}$ mice (**Figure 3.2**), as well as the reduction in plasma concentrations of total folate (the predominant form contributing to plasma total folate is methylTHF) (**Table 3.2**). AdoHcy is cleaved by AdoHcy hydrolase, producing Hcy and adenosine. This reaction is reversible and thermodynamically favors the synthesis of AdoHcy [217]; this should occur in the presence of the high tHcy concentrations present in the *Bhmt*$^{-/-}$ mice.

Despite high plasma tHcy concentrations, *Bhmt*$^{-/-}$ mice had significantly lower plasma cysteine concentrations; we observed no differences in hepatic cysteine concentrations. Normally, high Hcy would be expected to result in increased cystathionine and cysteine concentrations. For example, MTHFR deficient mice had elevated plasma Hcy, accompanied by elevated plasma cysteine [218]. Supplemental betaine has been shown to increase the activity of liver CBS [219], thus the accumulation of this metabolite as well as tHcy in *Bhmt*$^{-/-}$ mice would be expected to increase concentrations of cysteine. However, AdoMet is an allosterically activator of CBS [220], and we suggest that reduced hepatic AdoMet concentrations inhibit the transsulfuration pathway. The flux of cysteine from liver to plasma must be rapid, perhaps explaining why plasma and not hepatic cysteine concentrations are altered.

Deletion of *Bhmt* results in a substantial accumulation of betaine in most tissues except testis. Betaine is either used as a methyl donor (which is blocked by *Bhmt* deletion) or as an osmolyte that regulates cellular volume and fluid balance. The accumulation of betaine in *Bhmt*$^{-/-}$ mice may affect osmoregulation. Tests of kidney function did not reveal any malfunction (**Table 3.3**). However, *Bhmt*$^{-/-}$ mice had reduced urinary specific gravity (USG) compared to that of *Bhmt*$^{+/+}$ mice (**Table 3.3**), suggesting reduced reabsorption of water by the kidney tubule. This finding is puzzling since high betaine should result in increased reabsorption of water and increased urine osmolality.

Surprisingly, the deletion of *Bhmt* does not result in accumulation of choline, the precursor of betaine. Choline is either oxidized to form betaine by the enzyme CHDH or it is used to form PtdCho. Since *Bhmt*$^{-/-}$ mice cannot utilize betaine, we expected to see product inhibition of CHDH resulting in increased choline availability for use in PtdCho synthesis. We observed the opposite, with lower choline and PtdCho concentrations in a number of tissues. Bhmt$^{-/-}$ mice had elevated hepatic expression of *Chdh* (data not shown) and hepatic CHDH activity (**Figure 3.2**), suggesting that this gene is induced by some factor in *Bhmt*$^{-/-}$ mice, possibly explaining increased use of choline to form betaine. The regulatory mechanisms for such an effect are not known.

At 5 weeks of age, *Bhmt*$^{-/-}$ mice developed a fatty liver, and had elevated plasma ALT activity (a measure of hepatic damage). The fatty liver is the result of decreased synthesis of PtdCho, which is essential for the secretion of VLDL from liver [221]. These findings are consistent with the literature. Rodents and humans fed a choline deficient diet develop fatty liver [222, 223], and have elevated plasma ALT activity because choline deficiency induces hepatocytes apoptosis [35]. Consistent with these observations in *Bhmt*$^{-/-}$ mice, others have reported administration of betaine or the induction of BHMT activity prevents fatty liver in *Mthfr*$^{-/-}$ mice [218], in non-alcoholic fatty liver [107] and in alcohol induced fatty livers [91, 100] in rodents. Together, these data suggest the importance of BHMT activity in modulating hepatic steatosis. In addition, *Bhmt*$^{-/-}$ mice had reduced plasma total cholesterol and HDL-C. The role of *Bhmt* deletion in cholesterol and lipoprotein homeostasis warrants further studies.

At 1 year of age, 64% of *Bhmt*$^{-/-}$ mice developed hepatic tumors. Histopathology confirmed that these tumors were either hepatocellular adenomas or carcinomas. Even those that did not have visible tumors had higher incidence of fat accumulation, cellular alteration and hyperplasia when compared to *Bhmt*$^{+/+}$ livers. Histological modifications were accompanied by elevation in gGT1 levels, a highly sensitive marker of HCC. In rodents, choline deficiency results in a higher incidence of spontaneous hepatocellular carcinomas [112]. Several mechanisms are suggested for these carcinogenic effects. Choline deficiency increases lipid peroxidation in the liver [113], which is a source of free radicals in the nucleus that could modify DNA and cause carcinogenesis. Choline deficiency perturbs protein kinase C (PKC) signaling, resulting in altered cell proliferation signals and cell apoptosis and eventually in carcinogenesis [114]. Methyl deficiency may also mediate the mechanisms that underlie the etiology of cancers. AdoMet level controls cell growth, and a persistent decrease in AdoMet concentrations leads to the development of HCC as observed in methionine adenosyltranferase 1A knockout mouse model (cannot make AdoMet from Met) [121]. Methyl deficiency may also alter epigenetic machinery by hypomethylating some genes but paradoxically hypermethylating specific genes (tumor suppressor genes) and consequently increasing the recruitment of methyl-binding proteins to the CpG islands. Consequently, the expression of tumor suppressor genes responsible for DNA repair (BRCA1, hMLH1), cell cycle regulation (p15, p16), carcinogenesis metabolism (GSTP1), hormonal response (RARβ2), apoptosis (DAPK, APAF-1), cell adherence (CDH1, CDH3) [118-120] are silenced, leading to tumor development. All the above mechanisms are potentially the underlying causes of HCC observed in *Bhmt*$^{-/-}$ mice since these mice are

essentially choline and methyl-group deficient. We plan to investigate each of these hypotheses in ongoing work in our laboratory.

Hepatocellular carcinoma is the fifth most common type of cancer worldwide [224]. In mouse models harboring genetic defects, HCC occurs spontaneously in a very limited number of cases [225]. For the first time, we present evidence that the *Bhmt* gene dysfunction links a metabolic defect to spontaneous neoplastic transformation in rodent livers. *Bhmt*$^{-/-}$ mice model marks the upper boundary for an effect of a lost-of-function gene variant in humans. Our studies in the *Bhmt*$^{-/-}$ mice suggest that humans with lost-of-function mutation in the *BHMT* gene may have important consequences, including hyperhomocysteinemia, altered choline metabolites, fatty liver, and hepatocellular carcinomas. It would be interesting to explore whether enhanced BHMT activity would reverse these symptoms.

3.6 FIGURES

Figure 3.1. Confirmation of *Bhmt*$^{-/-}$ mice.

A. *Bhmt* chimeric mice were generated using a gene targeting vector that removed exons 6 and 7 of the gene as described under "Experimental Procedures". loxP, locus of X-over P1; frt, flippase recognition target; neo, neomycin cassette; flp, flippase recombination enzyme; cre, cyclization recombination enzyme. **B.** PCR analysis of genomic DNA isolated from *Bhmt*$^{+/+}$, *Bhmt*$^{+/-}$, and *Bhmt*$^{-/-}$ mice. The PCR product of the WT allele was 1600 bp, while the KO allele was 545 bp. **C.** Hepatic BHMT activity was measured using a radiometric assay in *Bhmt*$^{+/+}$ (black bar), *Bhmt*$^{+/-}$ (hatched bar), and *Bhmt*$^{-/-}$ (white bar) mice. Data are presented as mean ± SEM, n=4-8 per group. Different letters differ significantly ($p<0.01$) by ANOVA and Tukey-Kramer HSD test. **D.** BHMT protein in liver from *Bhmt*$^{+/+}$ and *Bhmt*$^{-/-}$ mice were probed by Western blot analysis. The size of BHMT protein is 45 kDa. **E.** Body weights of *Bhmt*$^{+/+}$ (black square), *Bhmt*$^{+/-}$ (grey square), and *Bhmt*$^{-/-}$ (white square) mice were measured using a scale from age 3.5 to 20 weeks old. Data are presented as mean ± SEM, n=10-25 per group.*$p<0.05$, different from *Bhmt*$^{+/+}$ by Students' *t* test.

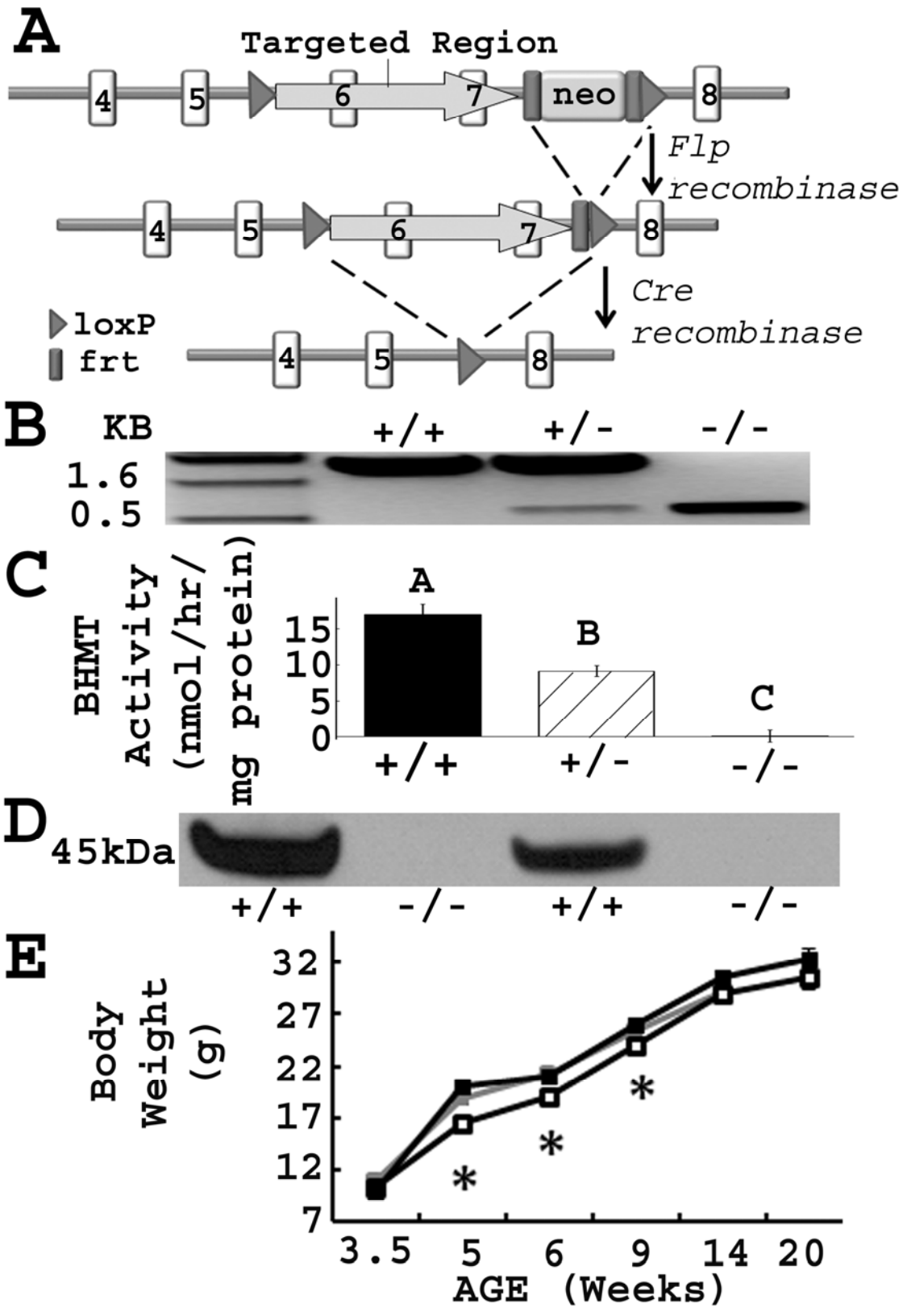
A
Targeted Region
4
5
6
7
neo
8
Flp
recombinase
loxP
frt
Cre
recombinase
B
KB
+/+
+/-
-/-
1.6
0.5
C
BHMT
Activity
(nmol/hr/
mg protein)
A
B
C
15
10
5
0
+/+
+/-
-/-
D
45kDa
+/+
-/-
+/+
-/-
E
Body
Weight
(g)
32
27
22
17
12
7
3.5
5
6
9
14
20
AGE (Weeks)
*
*
*

Figure 3.2. *Bhmt*$^{-/-}$ mice have altered activities of enzymes involved in one-carbon metabolism.

CHDH, GNMT and PEMT activities were measured in 5 week old *Bhmt*$^{+/+}$ (black bar) and *Bhmt*$^{-/-}$ mice (white bar) mouse liver using radiometric assays. Data are presented as mean ± SEM, n=6-8 per group. *$p<0.05$, different from *Bhmt*$^{+/+}$ by Students' *t* test. CHDH, choline dehydrogenase; GNMT, glycine-N-methyltransferase; PEMT, phosphatidylethanolamine methyltransferase.

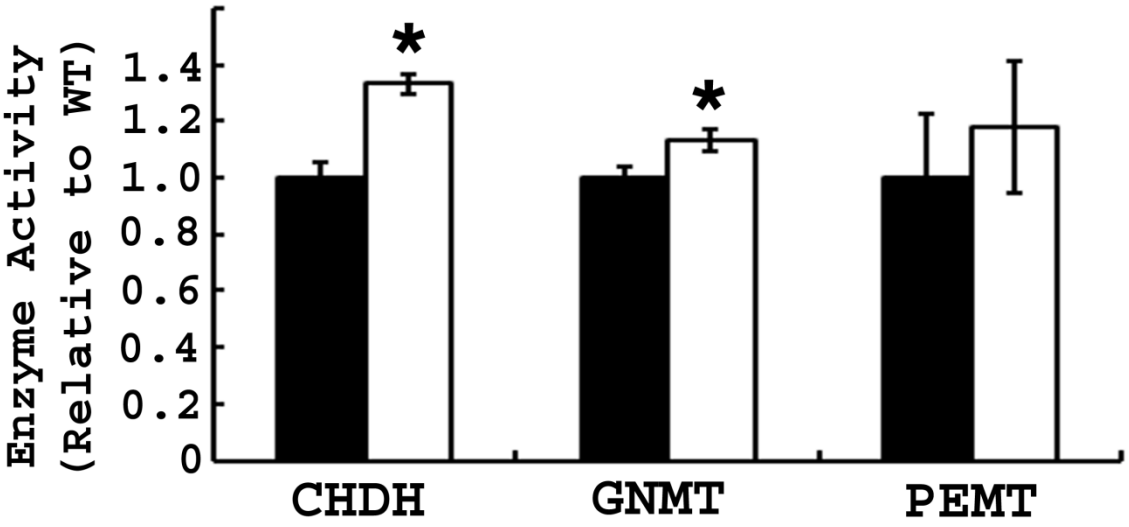
Enzyme Activity
(Relative to WT)
0
0.2
0.4
0.6
0.8
1.0
1.2
1.4
*
*
CHDH
GNMT
PEMT

Figure 3.3. *Bhmt*$^{-/-}$ mice have fatty liver and reduced hepatic phospholipid concentrations.

A. Hepatic phospholipids of 5 week *Bhmt*$^{+/+}$ (black bar) and *Bhmt*$^{-/-}$ mice (white bar) mice were analyzed by a thin layer chromatography - phosphate assay method. Data are presented as mean ± SEM, n=5 per group. *p<0.01, different from *Bhmt*$^{+/+}$ by Students' *t* test. **B.** Morphology of liver from 5 week old mice was shown by hematoxylin-eosin (H&E) staining at 100X magnification. Scale bar = 50 μm. **C.** Hepatic TAG of 5 week old *Bhmt*$^{+/+}$ (black bar) and *Bhmt*$^{-/-}$ (white bar) mice was extracted and quantitated by a colorimetric assay. Data are presented as mean ± SEM, n=6-8 per group. *p<0.05, different from *Bhmt*$^{+/+}$ by Students' *t* test. **D.** VLDL secretion rate of 5 week old *Bhmt*$^{+/+}$ (black square) and *Bhmt*$^{-/-}$ (white square) mice was determined by measuring the plasma TAG after lipoprotein lipase inhibitor injection. Data are presented as mean ± SEM, n=6 per group. *p<0.05, different from *Bhmt*$^{+/+}$ by Students' *t* test. TAG, triacylglycerol; PLs, phospholipids; PtdCho, phosphatidylcholine; PtdEth, phosphatidylethanolamine; PtdIns, phosphatidylinositol; PtdSer, phosphatidylserine; VLDL, very low density lipoprotein

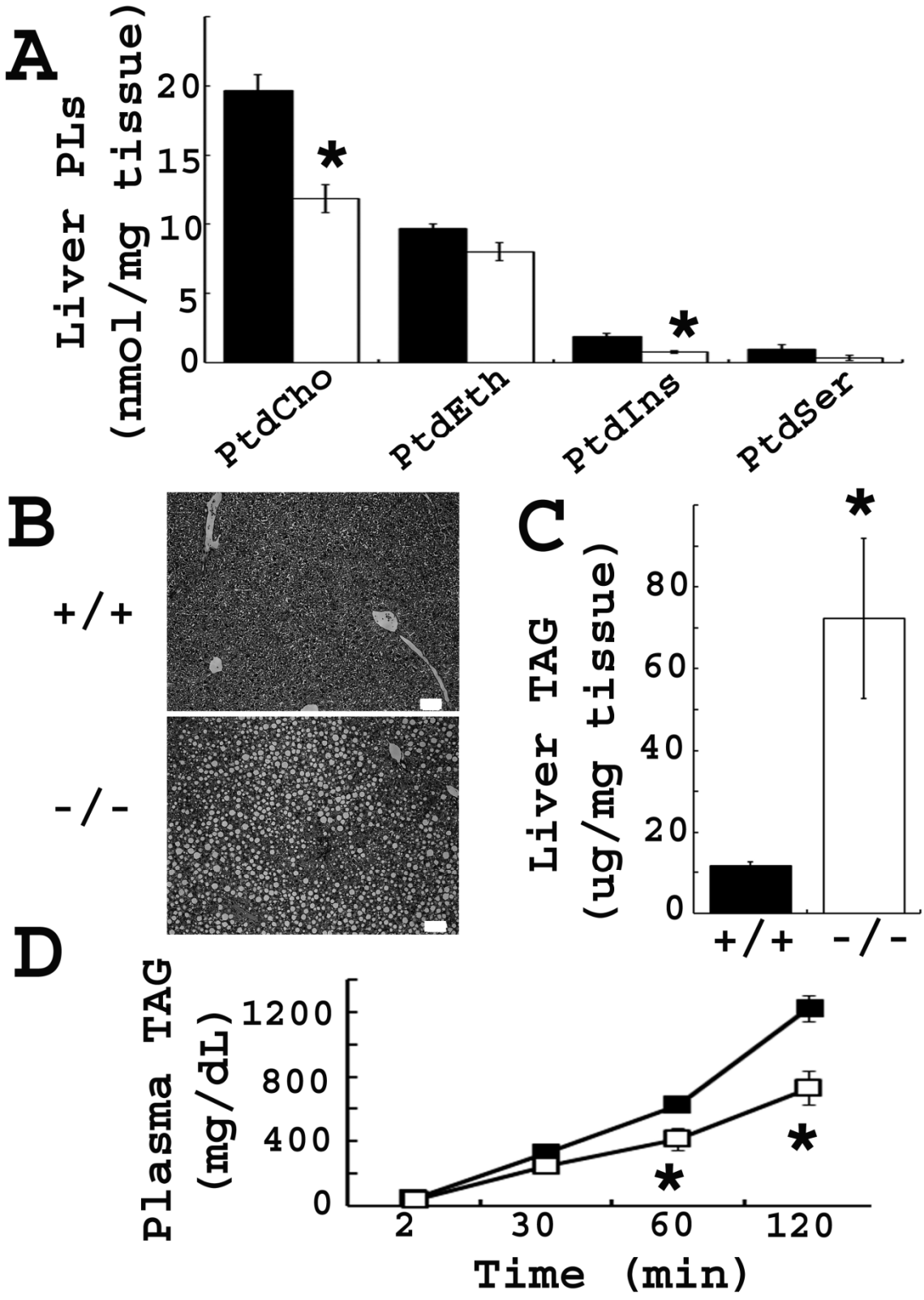
A
Liver PLs
(nmol/mg tissue)
20
15
10
5
0
*
*
PtdCho
PtdEth
PtdIns
PtdSer
B
+/+
-/-
C
Liver TAG
(ug/mg tissue)
80
60
40
20
0
*
+/+
-/-
D
Plasma TAG
(mg/dL)
1200
800
400
0
*
*
2
30
60
120
Time (min)

Figure 3.4. *Bhmt* deletion results in liver tumors at 1 year of age.

A. Visible hepatic tumors in one year old *Bhmt*$^{-/-}$ male mice. The inspection of liver specimens at 4X magnification revealed single or multiple nodules up to 8 mm in diameter. **B.** H&E images of tumor bearing livers at 400X magnification, showing representative hepatocellular carcinoma and adenoma morphology. Scale bar = 50 μm. *1*. Regenerative hyperplastic nodule containing streams of proliferative oval and biliary cells; *2*. Hepatocellular adenoma (* - center of the nodule) well-circumscribed with lobular structure absent, compressive borders, eosinophilic hepatocytes; *3*. Hepatocellular carcinoma represented by a large mass of abnormal vacuolated hepatocytes, containing poorly demarcated areas of smaller hepatocytes with less vacuolization, amphophilic cytoplasm, and a streaming growth pattern (arrow); *4*. Hepatocellular carcinoma nodule of variably sized hepatocytes exhibiting cytomegaly with hyaline droplets, small hepatocytes with streaming growth pattern, oval cell proliferation, Ito cell proliferation between cords (unlabeled arrow), infiltration of leukocytes.

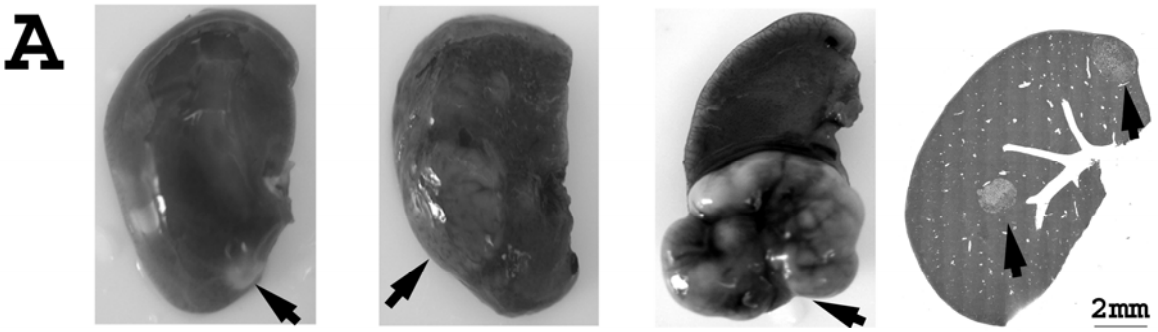

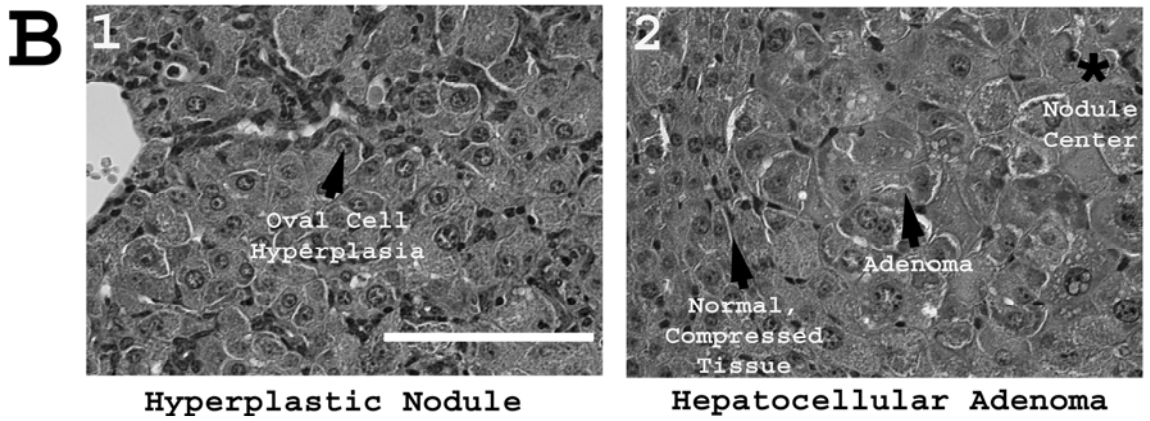

Hyperplastic Nodule

Hepatocellular Adenoma

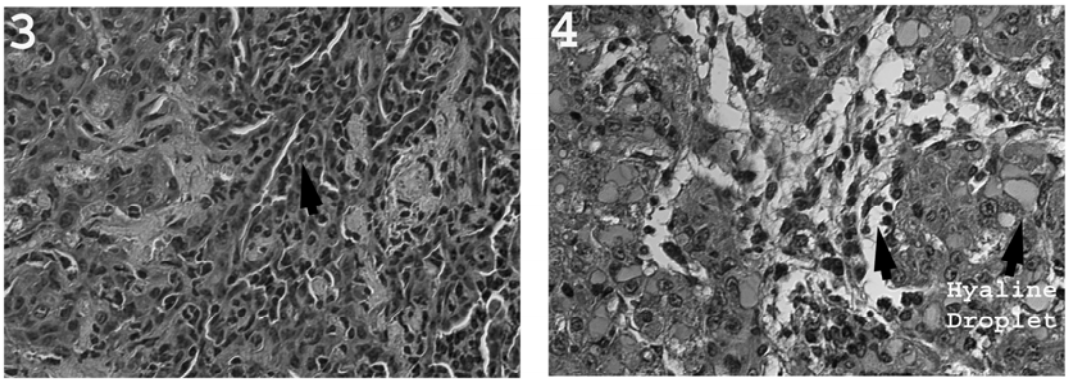

Hepatocellular Carcinoma

Carcinoma, Ito hyperlasia

Figure 3.5. Changes in one-carbon metabolism due to *Bhmt* deletion.

Deletion of *Bhmt* resulted in changes in the concentrations of the metabolites or activities of enzymes involved in homocysteine and one-carbon metabolism in tissues. AdoMet, S-adenosylmethionine; AdoHcy, S-adenosylhomocysteine; PtdCho, phosphatidylcholine; PtdEth, phosphatidylethanolamine; BHMT, betaine homocysteine methyl-transferase; PEMT, phosphatidylethanolamine methyltransferase; GNMT, glycine methyltransferase; CHDH, choline dehydrogenase.

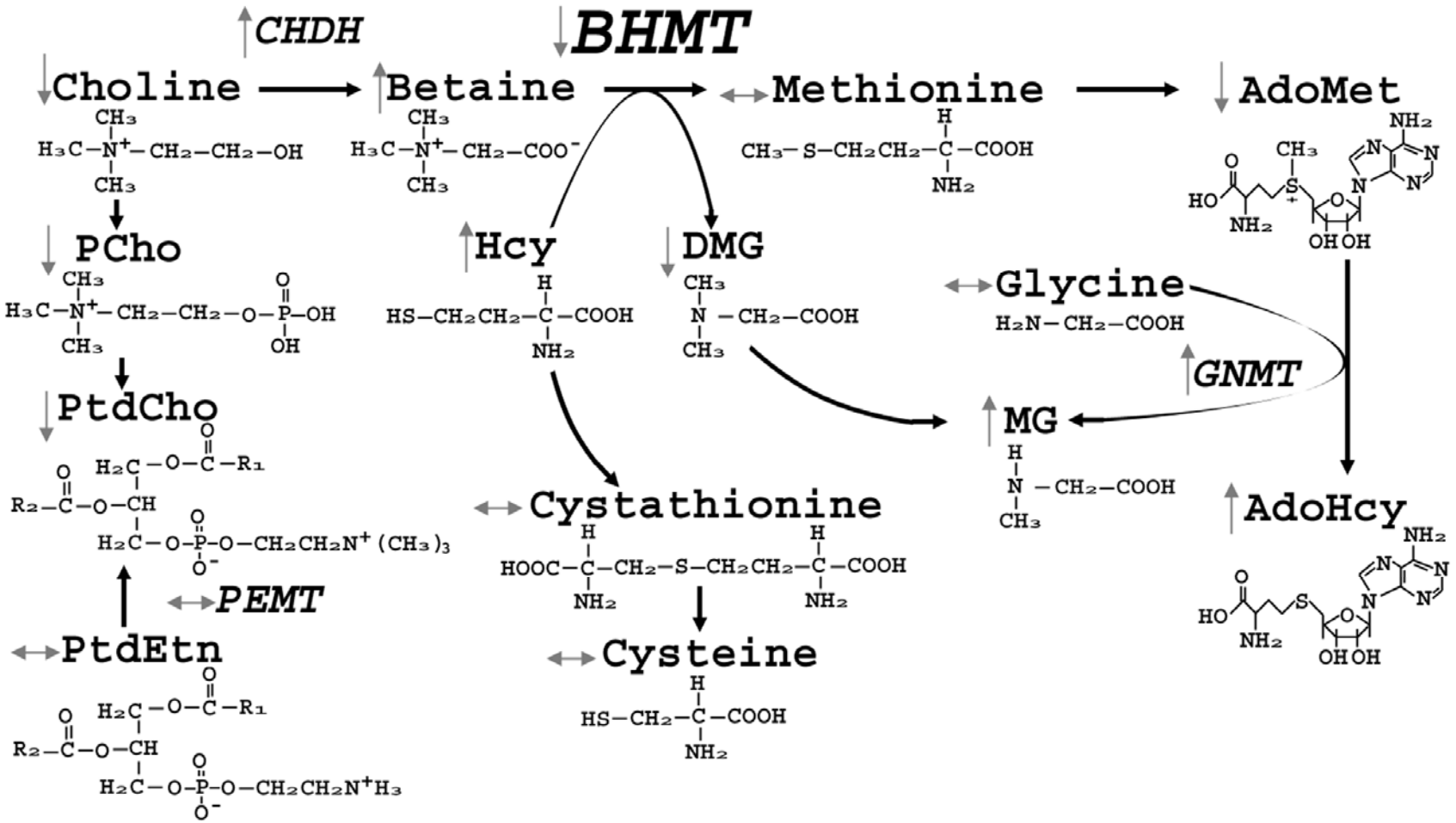
CHDH
BHMT
Choline
Betaine
Methionine
AdoMet
PCho
Hcy
DMG
Glycine
GNMT
PtdCho
MG
Cystathionine
AdoHcy
PEMT
PtdEtn
Cysteine

3.7 TABLES

Table 3.1. Deletion of *Bhmt* results in altered choline metabolites in various tissues.

Tissues were harvested from 5 week old *Bhmt*$^{+/+}$ and *Bhmt*$^{-/-}$ mice. Choline metabolites were extracted and quantified by liquid chromatography-electrospray ionization-isotope dilution mass spectrometry (LC–ESI–IDMS). Data are presented as mean ± SEM, n=5-10 animals/group. *p<0.05, ¥p<0.01,£p<0.001 different from *Bhmt*$^{+/+}$ by Students' *t* test. Concentrations are expressed as nmol/g, except for plasma, which is nmol/ml. PCho, phosphocholine; PtdCho, phosphatidylcholine; GPho, glycerophosphocholine; SM,sphingomyelin; ND, not detected.

		Betaine	Choline	GPCho	PCho	PtdCho	SM
Liver	*Bhmt*$^{+/+}$	1,321 ± 254	154 ± 36	1,730 ± 554	294 ± 67	15,897 ± 1,200	1,018 ± 131
	Bhmt$^{-/-}$	27,314 ± 2,001£	28 ± 8¥	266 ± 38¥	81 ± 7¥	11,686 ± 305¥	838 ± 37
Kidney	*Bhmt*$^{+/+}$	1,151 ± 91	779 ± 60	15,608 ± 1,475	853 ± 37	16,088 ± 1,025	3,373 ± 277
	Bhmt$^{-/-}$	5,424 ± 505£	481 ± 48¥	10,948 ± 672*	792 ± 41	12,707 ± 304*	2,685 ± 74*
Heart	*Bhmt*$^{+/+}$	77 ± 11	84 ± 12	164 ± 7	199 ± 12	11,111 ± 535	879 ± 50
	Bhmt$^{-/-}$	1,070 ± 131£	49 ± 6*	88 ± 10£	151 ± 14*	8,381 ± 455¥	583 ± 44£
Brain	*Bhmt*$^{+/+}$	22 ± 2	183 ± 26	1,208 ± 52	579 ± 33	22,856 ± 1,147	2,191 ± 149
	Bhmt$^{-/-}$	100 ± 10£	174 ± 15	1,120 ± 57	502 ± 9	21,020 ± 271	1,834 ± 52
Muscle	*Bhmt*$^{+/+}$	44 ± 3	67 ± 15	67 ± 4	51 ± 6	7,893 ± 655	411 ± 15
	Bhmt$^{-/-}$	529 ± 36£	28 ± 3*	58 ± 6	18 ± 3£	5,942 ± 238*	390 ± 13
Adipose	*Bhmt*$^{+/+}$	142 ± 25	73 ± 12	802 ± 223	90 ± 6	2,500 ± 217	156 ± 14
	Bhmt$^{-/-}$	284 ± 18£	34 ± 5¥	246 ± 79*	29 ± 7*	2,288 ± 271	144 ± 18
Lung	*Bhmt*$^{+/+}$	206 ± 17	198 ± 24	3,586 ± 348	551 ± 26	14,693 ± 344	2,389 ± 65
	Bhmt$^{-/-}$	2,237 ± 123£	188 ± 23	2,063 ± 82£	465 ± 42	14,437 ± 192	2,387 ± 47
Plasma	*Bhmt*$^{+/+}$	48 ± 3	20 ± 4	ND	ND	1,590 ± 81	145 ± 10
	Bhmt$^{-/-}$	772 ± 173£	13 ± 2	ND	ND	1,098 ± 71£	114 ± 77
Testis	*Bhmt*$^{+/+}$	2,014 ± 312	298 ± 51	809 ± 26	3,831 ± 270	5,760 ± 387	886 ± 74
	Bhmt$^{-/-}$	2,018 ± 111	241 ± 10	565 ± 47	3,706 ± 234	5,942 ± 233	954 ± 38

Table 3.2. Deletion of *Bhmt* results in reduced methylation potential and increased homocyteine concentrations.

Tissues were harvested from 5 week old *Bhmt*$^{+/+}$ and *Bhmt*$^{-/-}$ mice. Hepatic homocysteine metabolites were quantified by capillary stable isotope dilution gas chromatography/mass spectrometry. Hepatic AdoMet, AdoHcy and plasma total homocysteine and cysteine were quantified by high pressure liquid chromatography. Plasma total folate was quantified by a microbial (*Lactobacillus casei*) assay. Data are presented as mean± SEM, n=5-6 per group. *p<0.05, **p<0.01, different from *Bhmt*$^{+/+}$ by Students' *t* test. AdoMet, S-adenosylmethionine; AdoHcy, S-adenosylhomocysteine.

Organ	Metabolites	*Bhmt*$^{+/+}$	*Bhmt*$^{-/-}$
Liver	AdoMet [nmol/g tissue]	76.4 ± 3.7	43.5 ± 5.7**
	AdoHcy [nmol/g tissue]	21.8 ± 1.7	54.4 ± 7.7**
	AdoMet:AdoHcy	3.6 ± 0.2	0.9 ± 0.1**
	tHomocysteine [nmol/g tissue]	4.2 ± 0.3	26.5 ± 5.5**
	Methionine [nmol/g tissue]	223 ± 26	242 ± 23
	Dimethylglycine [nmol/g tissue]	48.2 ± 19.0	2.2 ± 0.2**
	Methylglycine [nmol/g tissue]	20.2 ± 8.9	52.7 ± 12.2*
	Cystathionine [nmol/g tissue]	32.0 ± 15.7	20.3 ± 5.8
	Cysteine [nmol/g tissue]	247 ± 25	291 ± 25
	Glycine [nmol/g tissue]	1,659 ± 128	1,561 ± 135
Plasma	tHomocysteine [μM]	6.5 ± 0.7	50.8 ± 5.9**
	Cysteine [μM]	131.1 ± 9.9	68.4 ± 9.3**
	tFolate [ng/ml]	81.7 ± 6.4	52.8 ± 5.1**

Table 3.3. Deletion of *Bhmt* results in altered metabolic markers

Plasma was collected from 5 week old $Bhmt^{+/+}$ and $Bhmt^{-/-}$ mice after 4 h fasting. Concentrations of plasma ALT, BUN, creatinine and activities of LDH and CK were quantitated by the Animal Clinical Chemistry and Gene Expression Facility, UNC-Chapel Hill. Plasma triacylglycerol, cholesterol, HDL cholesterol, glucose, NEFA, hydroxybutyrate were measured colorimetrically. Urine specific gravity was measured by the Department of Laboratory Animal Medicine Veterinary and Technical Services Facility, UNC- Chapel Hill. Data are presented as mean ± SEM, n=5-7 per group. *p<0.05, **p<0.01, different from $Bhmt^{+/+}$ by Students' *t* test. ALT, alanine transaminase; BUN, plasma urea nitrogen; LDH, lactate dehydrogenase; CK, creatinine kinase; HDL-C, high density lipoprotein cholesterol; NEFA, non-esterified fatty acids.

Organ	Clinical Markers	$Bhmt^{+/+}$	$Bhmt^{-/-}$
Plasma	ALT [U/I]	20.6 ± 4.9	34.7 ± 4.4*
	BUN [mg/dL]	12.5 ± 0.8	13.0 ± 1.8
	Creatinine [mg/dL]	<0.1	<0.1
	LDH [U/I]	841 ± 67	689 ± 80
	CK [U/I]	741 ± 147	511 ± 147
	Triacylglycerol [mg/dL]	60.9 ± 7.7	47.2 ± 7.9
	Cholesterol [mg/dL]	57.8 ± 4.3	31.6 ± 4.3**
	HDL-Cholesterol [mg/dL]	45.8 ± 3.2	26.7 ± 5.7**
	Glucose [mg/dL]	292.5 ± 33.2	226.0 ± 15.9
	NEFA [mM]	0.44 ± 0.08	0.28 ± 0.07
	Hydroxybutyrate [mM]	0.39 ± 0.08	0.29 ± 0.03
Urine	Specific Gravity [mg/dL]	1.039 ± 0.005	1.020 ± 0.002**

Table 3.4. Pathology in livers from a subset of 1 year old *Bhmt*$^{+/+}$ and *Bhmt*$^{-/-}$ mice.

A subset of 1 year old *Bhmt*$^{+/+}$ (4 out of 11, none had visible tumors) and *Bhmt*$^{-/-}$ mouse liver (6 out of 9 that had visible tumors, 4 out of 5 that did not have visible tumors) were serial-sectioned, H&E stained, and send to 2 veterinary pathologists for diagnosis. Dots indicated the changes observed in a particular sample. HCA, hepatocellular adenoma; HCC, hepatocellular carcinoma; Fat Accu., fat accumulation.

Genotype	Visible Tumor	HCA	HCC	Fat Accu.	Cellular Alteration	Hyperplasia
Bhmt$^{+/+}$				•	•	
Bhmt$^{+/+}$						
Bhmt$^{+/+}$						
Bhmt$^{+/+}$						
Bhmt$^{-/-}$	•	•		•	•	•
Bhmt$^{-/-}$	•	•		•	•	•
Bhmt$^{-/-}$	•	•	•			•
Bhmt$^{-/-}$	•		•		•	
Bhmt$^{-/-}$	•		•	•		•
Bhmt$^{-/-}$	•		•			
Bhmt$^{-/-}$				•	•	•
Bhmt$^{-/-}$					•	
Bhmt$^{-/-}$						•
Bhmt$^{-/-}$					•	

Table 3.5. Metabolites in 1-yr-old mouse tissues

Tissues were harvested from 1 year old *Bhmt*$^{+/+}$ and *Bhmt*$^{-/-}$ mice. Hepatic AdoMet, AdoHcy and plasma homocysteine and cysteine were quantified by high pressure liquid chromatography. Choline metabolites were extracted and quantified by liquid chromatography-electrospray ionization-isotope dilution mass spectrometry (LC–ESI–IDMS). Data are presented as mean± SEM, n=8 per group. **p<0.01, different from *Bhmt*$^{+/+}$ by Students' *t* test. AdoMet, S-adenosylmethionine; AdoHcy, S-adenosylhomocysteine; GPCho, glycerophosphocholine; PC, phosphocholine; PtdCho, phosphatidylcholine; SM, sphingomyeline.

Organ	**Metabolites**	***Bhmt*$^{+/+}$**	***Bhmt*$^{-/-}$**
Liver	AdoMet [nmol/g tissue]	113.1 ± 14.7	56.8 ± 3.9**
	AdoHcy [nmol/g tissue]	31.9 ± 5.3	176.3 ± 22.1**
	AdoMet:AdoHcy	4.05 ± 0.65	0.35 ± 0.03**
	Betaine [nmol/g tissue]	1,158 ± 330	34,976 ± 2,700**
	Choline [nmol/g tissue]	84 ± 13	144 ± 26
	GPCho [nmol/g tissue]	803 ± 121	218 ± 21**
	PC [nmol/g tissue]	674 ± 90	243 ± 59**
	PtdCho [nmol/g tissue]	17,317 ± 683	14,075 ± 795**
	SM [nmol/g tissue]	1,788 ± 127	1,976 ± 85
Plasma	tHomocysteine [μM]	5.5 ± 0.7	37.7 ± 8.6**
	Cysteine [μM]	150.8 ± 17.4	134.6 ± 23.1

3.8 SUPPLEMENTS

Table 3.6. Choline metabolites in *Bhmt*$^{+/-}$ tissues

Tissues were harvested from 5 week old *Bhmt*$^{+/-}$ mice. Data are presented as mean ± SEM, n=6 animals. *p<0.05, different from *Bhmt*$^{+/+}$ by Students' *t* test. Concentrations are expressed as nmol/g. PCho, phosphocholine; PtdCho, phosphatidylcholine; GPho, glycerophosphocholine; SM,sphingomyelin; ND, not detected. Choline metabolites in adipose and plasma were not measured in *Bhmt*$^{+/-}$ mice.

	Betaine	Choline	GPCho	PCho	PtdCho	SM
Liver	1,923 ± 364	154 ± 36	1,730 ± 554	294 ± 67	15,897 ± 1,200	1,018 ± 131
Kidney	1,296 ± 192	834 ± 28	15,786 ± 748	885 ± 31	14,035 ± 420	2,768 ± 60
Heart	95 ± 29	102 ± 7	212 ± 65	193 ± 13	9,877 ± 471	738 ± 48
Muscle	49 ± 4	67 ± 15	84 ± 10	41 ± 8	6,388 ± 174*	397 ± 11
Brain	18 ± 2	197 ± 36	1,322 ± 58	588 ± 35	20,441 ± 402	1,869 ± 84
Lung	239 ± 26	224 ± 26	3,432 ± 203	588 ± 20	14,777 ± 343	2,415 ± 63
Testis	2,334 ± 239	439 ± 30	859 ± 157	4,495 ± 193	6,581 ± 490	1,039 ± 61

Table 3.7. Other metabolites in *Bhmt*$^{+/-}$ tissues

Tissues were harvested from 5 week old *Bhmt*$^{+/-}$ mice. Data are presented as mean± SEM, n=3-6 per group. *p<0.05, different from *Bhmt*$^{+/+}$ by Students' *t* test. $^{\#}$p<0.05, different from *Bhmt*$^{-/-}$ by Students' *t* test. AdoMet, S-adenosylmethionine; AdoHcy, S-adenosylhomocysteine. ALT, alanine transaminase; BUN, plasma urea nitrogen; LDH, lactate dehydrogenase; CK, creatinine kinase; HDL-C, high density lipoprotein cholesterol; NEFA, non-esterified fatty acids.

Organ	**Metabolites**	***Bhmt*$^{+/-}$**
Liver	AdoMet [nmol/g tissue]	86.3 ± 22.8
	AdoHcy [nmol/g tissue]	35.4 ± 12.1
	AdoMet:AdoHcy	2.9 ± 0.4
Plasma	tHomocysteine [μM]	6.3 ± 0.3
	Cysteine [μM]	102.6 ± 8.4*$^{\#}$
	Total folate [ng/ml]	81.3 ± 17.7
	ALT [U/I]	31.0 ± 1.6
	BUN [mg/dL]	13.55 ± 0.3
	Creatinine [mg/dL]	<0.1
	LDH [U/I]	917.3 ± 165.5
	CK [U/I]	793.3 ± 51.3
	Triacylglycerol [mg/dL]	71.2 ± 5.8
	Cholesterol [mg/dL]	48.7 ± 20.1
	HDL-Cholesterol [mg/dL]	37.9 ± 14.9
	Glucose [mg/dL]	259.1 ± 13.1
	NEFA [mM]	0.29 ± 0.04
	Hydroxybutyrate [mM]	0.39 ± 0.02

CHAPTER IV

THE ROLE OF BHMT IN ENERGY HOMEOSTASIS

MOUSE BETAINE-HOMOCYSTEINE *S*-METHYLTRANSFERASE DEFICIENCY REDUCES BODY FAT VIA INCREASING ENERGY EXPENDITURE AND IMPAIRING FUEL USAGE AND STORAGE[1]

Ya-Wen Teng, Jessica M. Ellis, Rosalind A. Coleman, and Steven H. Zeisel

4.1 ABSTRACT

Betaine-homocysteine *S*-methyltransferase (BHMT) catalyzes the synthesis of methionine from homocysteine. In our initial report, we observed a reduced body weight in $Bhmt^{-/-}$ mice. We initiated this study to investigate the potential role of BHMT in energy metabolism. Compared to the controls ($Bhmt^{+/+}$), $Bhmt^{-/-}$ mice had less fat mass, smaller adipocytes, and better glucose and insulin sensitivities.

---

[1]Teng, Y., Ellis, J.M., Coleman, R.A., and Zeisel, S.H. (2011). Deletion of Murine Betaine-Homocysteine S-Methyltransferase Results in Decreased Body Fat Via Altering Energy Metabolism. Under Revision in *JBC*.

Compared to the controls, *Bhmt*$^{-/-}$ mice had increased energy expenditure and respiratory exchange ratio, with no changes in food intake, fat uptake or absorption, or in locomotor activity. The reduced adiposity in *Bhmt*$^{-/-}$ mice was not due to hyperthermogenesis. *Bhmt*$^{-/-}$ mice failed to maintain a normal body temperature upon cold exposure. *In vivo* and *ex vivo* tests showed that *Bhmt*$^{-/-}$ mice had normal lipolytic function. The rate of [^{14}C] fatty acid incorporated into [^{14}C] triacylglycerol was the same in *Bhmt*$^{+/+}$ and *Bhmt*$^{-/-}$ gonadal fat depots (GWAT), but was 62% lower in *Bhmt*$^{-/-}$ inguinal fat depots (IWAT) compared to that of *Bhmt*$^{+/+}$mice. The rate of [^{14}C] fatty acid oxidation was the same in both GWAT and IWAT from *Bhmt*$^{+/+}$ and *Bhmt*$^{-/-}$ mice. At basal level, *Bhmt*$^{-/-}$ GWAT had the same [^{14}C] glucose oxidation as did the controls. When stimulated with insulin, *Bhmt*$^{-/-}$ GWAT oxidized 2.4-fold more glucose than did the controls. Compared to the controls, the rate of [^{14}C] glucose oxidation was 2.4 and 1.8 fold higher respectively in *Bhmt*$^{-/-}$ IWAT without or with insulin stimulus. Our results show for the first time a role for BHMT in energy homeostasis.

4.2 INTRODUCTION

Betaine-homocysteine *S*-methyltransferase (BHMT) catalyzes the formation of methionine from homocysteine using the choline metabolite betaine as the methyl donor. BHMT is an enzyme predominantly found in liver in rodents [18], and plays an essential role in regulating homocysteine, choline, and one-carbon metabolism. BHMT also influences hepatic lipid accumulation via altering phosphatidylcholine (PtdCho) concentration. BHMT exerts this effect through two mechanisms. Firstly, choline, the precursor of betaine, can

alternatively be used to make PtdCho via Kennedy pathway. Secondly, methionine, the end product of BHMT, is the precursor of *S*-adenosylmethionine (AdoMet), which is required for the synthesis of PtdCho from phosphatidylethanolamine (PtdEtn) by the enzyme PtdEtn methyltransferase (PEMT). BHMT overexpression increases PtdCho synthesis, leading to reduced hepatic lipid accumulation [95], while BHMT deficiency leads to fatty liver [226]. While the role of BHMT in hepatic lipid metabolism has been elucidated, there is no evidence that BHMT plays a role in whole body energy metabolism and adiposity.

We observed that *Bhmt* deficient (*Bhmt*$^{-/-}$) mice had a lower body weight from 5 to 9 weeks of age compared to wildtype littermates [226]. Magnetic resonance image (MRI) analysis and dissection of adipose fat depots revealed that the reduced body weight observed in *Bhmt*$^{-/-}$ mice was due to reduced fat depots. These results suggested that *Bhmt* deficient mice might have problems with whole-body energy and lipid metabolism. This study aims to investigate the metabolic perturbations that lead to the reduced adiposity observed in *Bhmt*$^{-/-}$ mice. Homeostasis of energy stores is regulated by mechanisms including modulation of metabolic rate and thermogenesis, control of metabolite fluxes among various organs, and modulation of fuel synthesis and use within adipose tissue. We present evidence that *Bhmt*$^{-/-}$ mice have reduced adiposity due to increased whole-body metabolic rate, impaired triglyceride synthesis and enhanced glucose oxidation in white adipose tissue (WAT).

4.3 EXPERIMENTAL PROCEDURES

Generation and Maintenance of Mice – The strategy used to generate *Bhmt*$^{-/-}$ mice was as previously described [226]. *Bhmt*$^{-/-}$ mice and their wildtype littermates were of a C57Bl/6 x

sv 129 genetic background and were continuously backcrossed to C57Bl/6 mice. Generations F3 to F5 were used in this study. The animals were kept in a temperature-controlled environment at 24°C and exposed to a 12 hr light and dark cycle. All animals received AIN-76A pelleted diet with 1.1 g/kg choline chloride (Dyets, Bethlehem, PA). The Institutional Animal Care and Use Committee of the University of North Carolina at Chapel Hill approved all experimental protocols.

BHMT Western Blot - Mice were anesthetized by inhalation of isoflurane (Hospira, Lake Forest, IL). Tissues were harvested, snap frozen, pulverized under liquid nitrogen and stored at -80^{o}C until used. Western blot analysis was performed in liver and adipose homogenates as previously described [196].

Metabolic Studies - Body composition was determined in 14-wk-old mice by MRI (EchoMRI-100, Echo Medical Systems, LLC, Houston). Core temperature was measured in 7-wk-old mice using a rectal probe thermometer (Thermalert TH-5, Physitemp, Clifton, NJ). Food intake, oxygen consumption (VO_2), carbon dioxide release (VCO_2), heat production, and locomotor activity were measured every 27 minutes from individually housed mice (7-wk-old) using indirect calorimetry (TSE Systems, Germany) with an airflow of 0.25 liter/min. Locomotor activity was measured using infrared technology as the counts of three dimensional beam breaking (X total, Y total and Z total). Respiratory exchange ratio (RER) was calculated as VCO_2/VO_2. Mice were acclimated to the chambers for 24 hr, and data were collected during the following 24 hr. Stool samples were collected, and TAG was extracted using the Folch method [211] and measured colorimetrically (Sigma, St. Louis, MO). For

cold tolerance tests, 7-wk-old mice were fasted for 4 hr before being exposed to cold (4°C) without food or bedding. Core temperature was measured using a rectal probe thermometer (Thermalert TH-5) at baseline and every 15 min. Mice were removed from the cold-room when body temperature dropped below 28°C.

Biochemical Assays – An oral fat load test was performed by gavaging 7-wk-old mice with 10 μL/g B.W. olive oil after an overnight fast. Blood was collected retroorbitally at baseline, 1, 2, 4, and 6 hr, and plasma triacylglycerol (TAG) was measured with a colorimetric assay (Sigma). Glucose and insulin tolerance tests were performed by intraperitoneally injecting either glucose (2.5 g/kg B.W.) or human insulin (1 U/kg B.W., Novo Nordisk Inc., Princeton, NJ) to 7-wk-old mice after a 6 or 4 hr fast, respectively. Blood glucose was measured at baseline, 15, 30, 60, and 120 min by tail nick using a glucometer (One Touch Ultra, LifeScan, Inc., Milpitas, CA).

Plasma Metabolites - Plasma insulin (Ultra-Sensitive Mouse Insulin ELISA Kit, Crystal Chem Inc., Downers Grove, IL), total thyroxine (T4), total triiodothyronine (T3) (Alpha Diagnostic International, San Antonio, TX), and growth hormone (Millipore) levels were determined using commercially available ELISA kits according to the manufacturer's protocol. Plasma fibroblast growth factor 21 (FGF21) was determined using an RIA kit (Phoenix Pharmaceuticals Inc., Burlingame, CA) according to the manufacturer's protocol. Plasma creatine kinase (CK) was measured using an automatic chemical analyzer (Johnson and Johnson VT250, Rochester, NY) at the Animal Clinical Chemistry and Gene Expression Facility, UNC-Chapel Hill. Plasma TAG, glycerol (Sigma), and non-esterified fatty acids

(NEFA) (Wako, Richmond, VA) were measured colorimetrically per manufacturers' instructions. Plasma glucose was measured using a glucometer (One Touch Ultra).

Tissue Metabolites – Hepatic free glucose and glycogen were measured using an adopted acid hydrolysis method [227]. Liver was collected from 5-wk-old or 48-wk-old mice after a 4 hr fast. Briefly, 40 mg pulverized liver was homogenized in 1 ml of 1N HCl. Half of the homogenate was neutralized with 0.5 ml of 1M NaOH (non-hydrolyzed group). The other half was incubated at 95°C for 90 min before being neutralized with NaOH (hydrolyzed group). Glucosyl units released in both groups were measured using a colorimetrical glucose kit (Wako). Non-hydrolyzed group represented the free glucose measurement, while the difference between the hydrolyzed and the non-hydrolyzed groups represented the glycogen measurement. For bile acids and steroids, liver and gonadal fat pads were collected from 5-wk-old mice after a 4 hr fast. Tissues were sent to Metabolon (Research Triangle Park, NC), where the metabolites were measured using gas chromatography/mass spectrometry (GC/MS) and liquid chromatography/mass spectrometry (LC/MS) platforms as previously described [228-231]. Data was extracted and analyzed by Metabolon, and expressed as fold change relative to wildtype controls. For ATP/AMP/ADP, tissues were collected from 7-wk-old mice and immediately snap frozen in liquid nitrogen. Tissues were processed, and ATP, AMP and ADP measured using a high pressure liquid chromatography (HPLC) method as previously described [232].

Reverse Transcription-PCR – Total RNA was isolated from tissue using RNeasy Mini kit (Qiagen, Valencia, CA), and cDNA was synthesized using high-capacity cDNA reverse

transcription kit (Applied Biosystems, Calsbad, CA). cDNA was amplified by real-time PCR using SsoFast EvaGreen Supermix (Bio-Rad, Hercules, CA) with primers specific to the gene of interest. Results were normalized to the housekeeping genes (cyclophilin A or GAPDH) and calculated relatively to the controls by the $2^{-\Delta\Delta CT}$ method. For mitochondrial DNA analysis, genomic DNA was isolated by phenol/chloroform/isoamyl alcohol extraction. Relative amounts of mitochondria and nuclear DNA were determined by real-time PCR using cytochrome b and H19 respectively using genomic DNA as template.

Lipolysis – For *in vivo* lipolysis, mice were injected intraperitoneally with lipolytic stimuli (10 mg isoproterenol/1 kg B.W. or 1 mg CL316243/1 kg B.W.) (Sigma). Plasma was collected retroorbitally at baseline and 1.5 hr after injection. Plasma glycerol (Sigma) and NEFA (Wako) were measured colorimetrically, and glucose measured using a glucometer (One Touch Ultra). Gonadal and inguinal adipose explants were used for *ex vivo* lipolysis measurement as previously described [233, 234]. Briefly, pieces of fat explants (20 mg) were incubated in 0.5 ml Krebs Ringer Buffer (KRB) (12 mM HEPES, 121 mM NaCl, 4.9 mM KCl, 1.2 mM $MgSO_4$, and 0.33 mM $CaCl_2$) supplemented with 3.5% fatty acid free bovine serum albumin (FFF-BSA) and 0.1% glucose with or without 10 μM isoproterenol at 37°C. Twenty-five μL of buffer was collected at various time points to measure the release of glycerol colorimetrically (Sigma).

Adipocyte Isolation – Mature adipocytes were isolated from gonadal or inguinal fat depots from 12-16 wk-old mice and used for incorporation and oxidation studies [235]. Briefly, gonadal or inguinal fat depots were removed under sterile conditions, minced and incubated

at 37°C with shaking for 1 hr in KRB supplemented with 1% FFF-BSA, 2.5 mM glucose, and 200 nM adenosine, containing 1 mg/ml collagenase I. The digested tissues were filtered through a sterile 250 μm mesh and washed 3 times with supplemented KRB. Adipocytes were diluted with supplemented KRB to reach 10% adipocytes solution, and maintained for 30 min in polypropylene tube before the start of the assay. Due to the small fat mass in *Bhmt*$^{-/-}$ mice, the same fat depots from two *Bhmt*$^{-/-}$ mice were pooled together to get enough adipocytes per sample.

Incorporation and Oxidation - For fatty acid incorporation into TAG, 500 μL of 10% adipocyte solution were incubated with a 125 μL reaction mixture containing 15 μM [1-^{14}C] oleate (50 μCi/500 μL; Perkin Elmer) and 200 μM unlabeled oleate complexed to BSA for 2 hr at 37°C. [^{14}C] TAG was extracted [236], isolated by TLC, and detected and quantified with a Bioscan AR2000 Image System (Bioscan Inc., Washington, DC). The chromatoplate was run in chloroform/methanol/ammonium hydroxide (65:25:4; v:v:v) to 8 cm from the top. After residual solvents evaporated, the plate was rerun in heptane/isopropyl ether/acetic acid (60:40:4; v:v:v) to the top of the plate. For oxidation, 250 μL of 10% adipocytes solution were incubated with a 125 μL reaction mixture containing either 15 μM [1-^{14}C] oleate and 200 μM unlabeled oleate or 4 μM [^{14}C] glucose (50 μCi/500 μl; Perkin Elmer) and 4 mM unlabeled glucose (in KRB) for 1.5 hr at 37°C. The reaction mixture was incubated in a 13 mL polypropylene tube that contained a center well filled with folded filter paper. The tube was sealed with a rubber stopper. After 1.5 hr incubation, the reaction mixture was acidified with 150 μL of 70% perchloric acid, and 300 μL of 1 M NaOH was added to the center well. The sealed tubes were incubated at RT for an additional 45 min. The center well (containing

[^{14}C] CO_2 trapped by base) was then collected and placed into scintillation fluid and counted. The acidified reaction mixture (~400 μL) was incubated overnight at 4°C with 200 μL of 20% BSA. The mixture was centrifuged at 13,200 rpm for 20 min, and an aliquot of the supernatant was counted to determine [^{14}C]-labeled acid soluble metabolites (ASM). [^{14}C] CO_2 represents complete fatty acid or glucose oxidation, and [^{14}C] ASM represents incomplete fatty acid oxidation. For some experiments, 0.01 U insulin (Novo Nordisk Inc., Princeton, NJ) was added.

Tissue histology - Adipose tissues were collected from 12-wk-old mice and fixed in 4% paraformaldehyde in 0.1M phosphate buffer for 24 hr. Tissues were processed, paraffin embedded, sectioned at 5 μm, and stained with hemotoxylin and eosin as previously described [212]. For adipocyte size analysis, three images (200X) per sample were taken, and the average adipocyte cell areas were analyzed using AxioVision 4.8 software (Zeiss, USA).

Statistics - Statistical differences were determined using ANOVA, Tukey-Kramer HSD, and Student's *t*-test (JMP version 6.0; SAS Institute, Cary, NC) and reported as means ± SEM.

4.4 RESULTS

BHMT Deficiency Resulted in Reduced Fat Mass and Smaller Adipocytes – Our previous publication reported that *Bhmt*$^{-/-}$ mice gained less body weight between 5 to 9 weeks of age than did their wildtype littermates ($p<0.05$) [226]. To determine whether the reduced weight gain of *Bhmt*$^{-/-}$ mice was associated with reduced fat or lean mass, we measured body composition of these mice using MRI scan analysis. *Bhmt*$^{-/-}$ mice had 30% less fat mass than did *Bhmt*$^{+/+}$ mice ($p<0.01$), with no difference in lean mass (**Figure 4.1A**). The difference in fat mass was confirmed by collecting the individual fat pads. The two major white adipose tissues (WAT), gonadal (GWAT) and inguinal (IWAT), of *Bhmt*$^{-/-}$ mice were significantly smaller than those of *Bhmt*$^{+/+}$ mice at all ages (**Figure 4.1B**). The disparity in fat mass was exacerbated as mice aged, such that by 48 weeks of age, *Bhmt*$^{-/-}$ mice had a fat mass that was 41% of that of *Bhmt*$^{+/+}$ mice. To determine whether the reduced fat mass in *Bhmt*$^{-/-}$ mice was due to fewer fat cells and/or smaller fat cells, the sizes of individual adipocytes in GWAT and IWAT of *Bhmt*$^{+/+}$ and *Bhmt*$^{-/-}$ mice were analyzed. Histological images showed that both GWAT and IWAT from *Bhmt*$^{-/-}$ mice contained a larger number of smaller adipocytes (**Figure 4.1C**). We observed a 43% reduction in adipocyte size in GWAT ($p<0.05$) and an 80% reduction in adipocyte size in IWAT ($p<0.001$) in *Bhmt*$^{-/-}$ mice compared to those of *Bhmt*$^{+/+}$ mice (**Figure 4.1D**). These data suggested that *Bhmt*$^{-/-}$ mice likely had normal adipocyte differentiation, and that the *Bhmt*$^{-/-}$ adipocytes either stored less and/or used more lipids than did *Bhmt*$^{+/+}$ adipocytes. *Bhmt* is predominantly expressed in rodent liver. Western blotting confirmed that BHMT protein was specific to the liver and was absent in the adipose

tissue from both *Bhmt*$^{+/+}$ and *Bhmt*$^{-/-}$ mice (**Figure 4.1E**), suggesting that the reduced fat mass in *Bhmt*$^{-/-}$ mice was due to an indirect effect of the lack of hepatic BHMT activity.

BHMT Deficiency Resulted in Enhanced Glucose Tolerance and Insulin Sensitivity - Changes in adiposity are often associated with alterations in glucose and insulin homeostasis. *Bhmt*$^{-/-}$ mice had normal basal blood glucose levels (**Figure 4.1F, 4.1G**). Upon intraperitoneal injection of either glucose (**Figure 4.1F**) or insulin (**Figure 4.1G**), *Bhmt*$^{-/-}$ mice exhibited a faster glucose removal rate than did wildtype controls. *Bhmt*$^{-/-}$ mice also had a basal plasma insulin concentration that was 50% of that of the controls ($p<0.05$) (**Table 4.1**), indicating enhanced insulin sensitivity.

***Bhmt*$^{-/-}$ Mice Had Increased Energy Expenditure** – To investigate the mechanisms that elicit the reduced fat mass in *Bhmt*$^{-/-}$ mice, elements of energy metabolism, including food intake, lipid uptake and absorption, body temperature, energy expenditure and activity, were determined. *Bhmt*$^{+/+}$ and *Bhmt*$^{-/-}$ mice consumed similar amounts of food per day (**Figure 4.2A**). Fat load test (**Figure 4.2B**) and fecal lipid content (**Figure 4.2C**), tests for lipid uptake and absorption respectively, displayed no differences between *Bhmt*$^{+/+}$ and *Bhmt*$^{-/-}$ mice. *Bhmt*$^{+/+}$ and *Bhmt*$^{-/-}$ mice had similar rectal temperatures (**Figure 4.2D**). Compared to wildtype controls, *Bhmt*$^{-/-}$ mice had increased O_2 consumption (**Figure 4.2E**), increased CO_2 release (**Figure 4.2F**) and increased heat production (**Figure 4.2G**) throughout the light and dark phases. *Bhmt*$^{-/-}$ mice were not hyperactive (**Figure 4.2I**), suggesting that the increase in metabolic rate was independent of activity. The respiratory exchange ratio (RER), an indicator of metabolic fuel preference, was significantly elevated in *Bhmt*$^{-/-}$ mice during the

light phase (and there was a trend of increasing RER during the dark phase), (**Figure 4.2H**), implying that *Bhmt*$^{-/-}$ mice may rely more on the oxidation of glucose and less on fatty acids, consistent with improved insulin sensitivity and glucose tolerance.

Thermogenesis Was Not Increased in *Bhmt*$^{-/-}$ Mice – We next investigated whether the reduced adiposity observed in *Bhmt*$^{-/-}$ mice was due to increased thermogenesis. We predicted that *Bhmt*$^{-/-}$ mice would maintain a higher body temperature during a cold challenge if they had increased thermogenesis. After 6 hours of cold exposure, the wildtype controls dropped body temperature by 7.4% (from 38.18 ± 0.14 ºC to 35.36 ± 0.07 ºC), while *Bhmt*$^{-/-}$ mice dropped body temperature by 28.9% (from 37.92 ± 0.09 ºC to 26.98 ± 2.15 ºC) (**Figure 4.3A**). Mice were removed from the cold room when body temperature was less than 28 ºC. Brown adipose tissue (BAT) is a major site of nonshivering adaptive thermogenesis. We found no significant difference in the morphology or the weight of interscapular BAT between wildtype and knockout mice (data not shown). Real-time PCR analysis revealed normal thermogenic gene responses in *Bhmt*$^{-/-}$ BAT tissue during cold exposure, with elevated *Pgc1* (peroxisome proliferator activated receptor γ coactivator), *Lpl* (lipoprotein lipase), *Ucp1* (uncoupling protein 1), and *Mcpt1* (muscle-type carnitine palmitoyltransferase 1) expression levels similar to those of *Bhmt*$^{+/+}$ *mice* (**Figure 4.3B**), indicating that the adrenergic signaling was intact and similar between genotypes. *Bhmt*$^{+/+}$ and *Bhmt*$^{-/-}$ mice had similar BAT TAG concentration before and after cold exposure, suggesting similar fuel storage and usage (**Figure 4.3C**). Mice were also able to maintain body temperature using exogenous fuels derived from organs such as white adipose tissue and liver, and through adaptive thermogenesis involving shivering in skeletal muscle to increase energy output.

Upon cold exposure, *Bhmt*$^{-/-}$ mice had significantly lower plasma glucose (by 46%), glycerol (by 46%), and NEFA (by 17%) concentrations compared to those of wildtype controls (**Figure 4.3D-F**), suggesting a restricted supply of exogenous fuels. *Bhmt*$^{-/-}$ mice also had a significantly elevated plasma creatine kinase activity (by 1.76 fold), a marker for muscle breakdown, perhaps because of increased shivering (**Figure 4.3G**).

BHMT Deficiency Resulted in Altered Clinical Measurements in Plasma - We examined whether genotypic differences in energy balance were accompanied by changes in plasma clinical measurements. Basal plasma glycerol, NEFA, glucose, and TAG concentrations were similar for the two genotypes (**Figure 4.3D-4.3F**) as previously published [226]. Basal plasma insulin concentration was 50% lower in *Bhmt*$^{-/-}$ mice than in controls ($p<0.05$) (**Table 4.1**). Because of the prominent role of thyroid hormone in controlling metabolic rate, we investigated whether increased thyroid hormone concentration contributed to the hypermetabolic phenotype in *Bhmt*$^{-/-}$ mice. Indeed, *Bhmt*$^{-/-}$ mice had a 33% increase in plasma T4 (the major form of thyroid hormone in blood) concentration compared to that of wildtype controls ($p<0.05$). Concentration of fibroblast growth factor 21 (FGF21), a recently discovered metabolic and glucose regulator, was found to be 1.75-fold higher in *Bhmt*$^{-/-}$ plasma than in *Bhmt*$^{+/+}$ plasma ($p<0.01$). The increase in plasma FGF21 concentration observed in *Bhmt*$^{-/-}$ mice was accompanied by a 3.35-fold increase in hepatic *Fgf21* expression (where FGF21 is predominantly produced) compared to that of *Bhmt*$^{+/+}$ mice ($p<0.05$). Growth hormone and T3 concentrations were not different between genotypes.

BHMT Deficiency Resulted in Increased Bile Acids in Liver and Adipose Tissue – A novel concept indicating a signaling role of bile acids (BAs) in the control of energy metabolism has emerged [132, 133]. Increasing BA pool size in mice increased energy expenditure [133], while decreasing BA pool size reduced energy expenditure, resulting in weight gain and insulin resistance [132]. Since *Bhmt*$^{-/-}$ mice had reduced plasma cholesterol (the precursor of BAs) [226], we investigated whether *Bhmt* deletion altered the concentrations of BAs. Cholic acid and chenodeoxycholic acid are the primary BAs and often conjugated with taurine (as taurocholate or taurochenodeoxycholate) or glycine (as glycocholate or glycochenodeoxycholate) forming bile salts. Compared to wildtype littermates, *Bhmt* deletion resulted in 9.50-fold and 3.41-fold increases respectively in cholate ($p<0.01$) and taurocholate ($p<0.05$) in adipose tissue, and in 2.33-fold and 1.62-fold increases respectively in taurocholate ($p<0.05$) and glycocholate ($p<0.01$) in liver (**Table 4.2**). Cholesterol is hydrolyzed to form 7 hydroxycholesterol, the precursor of bile acids. Compared to the controls, *Bhmt*$^{-/-}$ mice had reduced cholesterol (by 20%, $p<0.05$) and increased 7-β-hydroxycholesterol (by 2.98-fold, $p<0.05$) concentrations in the liver, and increased 7-α-hydroxycholesterol (by 2.17-fold, $p<0.01$) concentrations in the adipose tissue. These data suggested that *Bhmt* deletion enhanced the synthesis of bile acids from cholesterol, and that the bile acids may contribute to the increased energy expenditure observed in *Bhmt*$^{-/-}$ mice.

BHMT Deficiency Resulted in Reduced Cellular ATP/AMP Ratio in Liver But Not in Adipose Tissues, and in Reduced Hepatic Glucose and Glycogen – Because *Bhmt*$^{-/-}$ mice displayed signs of lipodystrophy (fatty liver [226] and reduced fat pads), we measured ATP

and AMP in these organs (**Table 4.1**). *Bhmt*$^{+/+}$ and *Bhmt*$^{-/-}$ mice had the same energy levels (ATP, AMP, ATP/AMP) in both GWAT and IWAT. However, in the liver, where *Bhmt* is predominantly expressed, *Bhmt*$^{-/-}$ mice had a reduced ATP/AMP level (by 65.7%, $p<0.05$) compared to *Bhmt*$^{+/+}$ mice. The reduced ATP/AMP ratio was due to a 42% reduction in ATP concentration and a 61% increase in AMP concentration in *Bhmt*$^{-/-}$ liver compared to those of *Bhmt*$^{+/+}$ liver ($p<0.05$). The reduced ATP/AMP ratio in *Bhmt*$^{-/-}$ liver was not due to decreased mitochondria content as there was no difference in mitochondria DNA in liver between wildtype and knockout mice. *Bhmt*$^{-/-}$ mice had reduced hepatic glucose (by 22% at 5 weeks of age and by 53% at 48 weeks of age) and glycogen (by 17% at 5 weeks of age and by 87% at 48 weeks of age) concentrations compared to those of *Bhmt*$^{+/+}$ mice (**Table 4.1**). These data indicated that *Bhmt*$^{-/-}$ mice might be oxidizing more glucose (hence not storing them as glycogen), perhaps in an attempt to maintain the cellular ATP/AMP level. These data were consistent with the increased RER in *Bhmt*$^{-/-}$ mice, and perhaps explained why these mice were cold intolerant (due to lack of external glucose fuel).

***Bhmt*$^{-/-}$ Mice Did Not Have Altered Lipolytic Rate –** To investigate whether the markedly decreased adiposity observed in *Bhmt*$^{-/-}$ mice was due to increased lipolysis, we measured lipolytic rate in both *in vivo* and *ex vivo* models whereby lipolytic stimuli were given, and glycerol released was measured as the indicator of lipolytic rate. Plasma TAG and glucose were also measured in the *in vivo* model to determine the whole-body response to adrenergic stimuli. During the *in vivo* experiment, when CL316243 (β3 adrenergic specific lipolytic stimulus) was administered, *Bhmt*$^{+/+}$ and *Bhmt*$^{-/-}$ mice had similar levels of plasma TAG, glycerol, and glucose release (**Figure 4.4A-C**). When isoproterenol (non-specific lipolytic

stimulus) was administered, *Bhmt*$^{+/+}$ and *Bhmt*$^{-/-}$ mice had similar levels of plasma TAG and glycerol (**Figure 4.4A-B**), but a 50% decreased plasma glucose concentration compared to wildtype controls (**Figure 4.4C**). Lipolysis was further analyzed in isolated GWAT and IWAT explants from *Bhmt*$^{+/+}$ and *Bhmt*$^{-/-}$ mice. The explants from *Bhmt*$^{-/-}$ mice released similar amounts of glycerol as did those from *Bhmt*$^{+/+}$ mice under basal or stimulated conditions (**Figure 4.4D-E**), suggesting normal lipolytic machinery in *Bhmt*$^{-/-}$ mice.

BHMT Deficiency Resulted in Impaired TAG Synthesis and Enhanced Glucose Oxidation in Isolated Mature Adipocytes – Since TAG breakdown was not defective, we assessed whether TAG synthesis and FA oxidation were altered within the fat cells. We isolated mature adipocytes from both GWAT and IWAT from *Bhmt*$^{-/-}$ mice and their littermate controls and measured the rates of [1-^{14}C]oleate incorporation into TAG (for TAG synthesis), into CO_2 (for complete FA oxidation) and acid soluble metabolites (for incomplete FA oxidation). Mature adipocytes isolated from *Bhmt*$^{+/+}$ and *Bhmt*$^{-/-}$ GWAT had the same rate of TAG synthesis (**Figure 4.4F**). Interestingly, mature adipocytes isolated from *Bhmt*$^{-/-}$ IWAT made less TAG (by 62%) compared to that of *Bhmt*$^{+/+}$ mice ($p<0.001$). GWAT and IWAT adipocytes from *Bhmt*$^{+/+}$ and *Bhmt*$^{-/-}$ mice had the same FA oxidation rate (**Figure 4.4G**), indicating normal β oxidation machinery. Since several lines of evidence (RER, enhanced glucose tolerance and insulin sensitivity, reduced glucose upon cold exposure and isoproterenol stimulus, reduced hepatic glucose and glycogen concentrations) suggested an increased reliance on glucose in *Bhmt*$^{-/-}$ mice, we assessed whether their mature adipocytes used more glucose. At basal level (without insulin), mature adipocytes isolated from *Bhmt*$^{+/+}$ and *Bhmt*$^{-/-}$ GWAT had the same glucose oxidation rate (**Figure 4.4H**). However, with

insulin treatment, *Bhmt*$^{-/-}$ GWAT oxidized 2.38-fold more glucose than did *Bhmt*$^{+/+}$ GWAT ($p<0.05$). Mature adipocytes isolated from *Bhmt*$^{-/-}$ IWAT oxidized 2.4-fold and 1.78-fold more glucose than did *Bhmt*$^{+/+}$ IWAT without and with insulin treatment (**Figure 4.4I**). Compared to basal level, insulin treatment induced glucose oxidation by 1.87-fold, 4.17-fold, 3.21-fold, and 3.79-fold respectively for *Bhmt*$^{+/+}$ GWAT, *Bhmt*$^{-/-}$ GWAT, *Bhmt*$^{+/+}$ IWAT, and *Bhmt*$^{-/-}$ IWAT, confirming the viability of the isolated mature adipocytes, and indicating a higher response to insulin in *Bhmt*$^{-/-}$ mice, particularly in GWAT (**Figure 4.4H, 4.4I**).

4.5 DISCUSSION

BHMT is one of the most abundant proteins in the liver, representing 0.6-1.6% of the total protein [43]. However, its known functions are limited to its roles in choline and one-carbon metabolism. Our current studies establish a unique role for BHMT in energy homeostasis. These findings are remarkable given that these mice had reduced adiposity and better insulin sensitivity and glucose tolerance when fed a diet containing 5% fat.

Previously, we found that *Bhmt*$^{-/-}$ mice had reduced body weight from 5 to 9 weeks of age compared to wildtype littermates, although the difference in body weight disappeared after 9 weeks [226]. MRI and dissection of fat pads revealed that the reduced body weight in *Bhmt*$^{-/-}$ mice was due to lower fat mass. Different from changes in body weight, *Bhmt*$^{-/-}$ mice had fat pad mass smaller up to 1 year of age compared to the controls. *Bhmt*$^{-/-}$ mice were able to maintain body weight in light of the reduced fat mass perhaps due to the fact that they had heavier liver (fatty liver and liver tumor) that made up the difference in weights [226].

BHMT is a liver-specific enzyme in rodents [18]. Since BHMT protein is absent in normal adipose tissue, this observation indicates that the reduced fat mass in *Bhmt*$^{-/-}$ mice was due to an indirect effect of the lack of hepatic BHMT activity. How could lack of a hepatic enzyme result in reduced fat mass? One possibility is diminished lipid transport from the liver to adipose tissue via very low density lipoprotein (VLDL). Our previous work showed that *Bhmt*$^{-/-}$ mice had reduced hepatic PtdCho concentration, resulting in decreased VLDL secretion and increased hepatic fat accumulation [226]. However, the amount of fat missing in fat pads exceeds the excess amount accumulated in the liver. In addition, adipose should be able to store lipid obtained from the diet instead of depending solely on hepatic lipid sources. Thus, decreased VLDL secretion is unlikely to account for all the fat absence. Homeostasis of energy stores is regulated by mechanisms that include modulation of metabolic rate and thermogenesis, control of metabolite fluxes among various organs, and modulation of fuel synthesis and usage within adipose tissue. Examination of each of these parameters in *Bhmt*$^{-/-}$ mice showed that multiple factors might contribute to the reduced adiposity observed in this mouse model.

Bhmt$^{-/-}$ mice had normal food intake, fat clearance rate, and fecal fat content, indicating that the reduced adiposity was not due to reduced energy intake or fat malabsorption. *Bhmt*$^{-/-}$ mice had increased rates of O_2 consumption, CO_2 release, and heat production, suggesting that the reduced fat mass was partially due to hypermetabolism. Because locomotor activity did not differ between genotypes, the increased energy expenditure exhibited by *Bhmt*$^{-/-}$ mice was not due to increased physical activity. The increased RER suggested that *Bhmt*$^{-/-}$ mice were oxidizing more glucose, instead of FA, as

fuel to maintain whole body metabolism, particularly during the fasting period. We investigated whether the reduced adiposity was due to increased thermogenesis. Upon cold exposure, *Bhmt*$^{-/-}$ mice failed to maintain their body temperature. *Bhmt*$^{-/-}$ mice exhibited normal induction of genes involved in mitochondrial biogenesis, uncoupling, and fatty acid oxidation in BAT. Furthermore, *Bhmt*$^{-/-}$ mice had normal BAT TAG storage and functional lipolytic machinery in peripheral tissues. However, during prolonged cold exposure, *Bhmt*$^{-/-}$ mice had lower plasma glucose, glycerol, and NEFA and higher plasma CK (marker of muscle breakdown). These data indicate that *Bhmt*$^{-/-}$ mice were not hyperthermogenic. In fact, these animals were cold sensitive due to lack of exogenous fuel, and had to depend on shivering thermogenesis in an attempt to maintain body temperature. The reduced plasma glucose in *Bhmt*$^{-/-}$ mice during cold exposure was probably because they had less glucose and glycogen stored in the liver or increased demand of glucose as fuel supply. The reduced plasma glycerol and NEFA in *Bhmt*$^{-/-}$ mice during cold exposure was probably because they had less TAG stored in the adipose tissue to be released during energy needs. It was also possible that *Bhmt*$^{-/-}$ mouse liver was taking up glycerol and NEFA more efficiently for synthesizing glucose to make up the lack of glucose and glycogen stores.

Within the adipose tissue, we observed that *Bhmt*$^{-/-}$ IWAT, but not GWAT, made 62% less TAG than did the controls. Although *Bhmt*$^{-/-}$ had normal lipolytic and FA oxidation machinery in both fat depots, the mice might have less TAG stored at a time when fuel was needed. On the other hand, the energy level (ATP/AMP) in GWAT and IWAT did not differ for the two genotypes. These data together suggest that *Bhmt*$^{-/-}$ mice may be utilizing more glucose instead of FA to maintain the cellular ATP/AMP ratio. Indeed, we observed

increased glucose oxidation in *Bhmt*$^{-/-}$ GWAT with insulin stimulus, and increased glucose oxidation in *Bhmt*$^{-/-}$ IWAT with or without insulin stimulus. This hypothesis was further supported by the elevated RER obtained from the indirect calorimetry, the enhanced glucose and insulin sensitivities observed in *Bhmt*$^{-/-}$ mice, the reduced plasma glucose during cold exposure and ß-adrenergic stimulation, and the reduced hepatic glucose and glycogen concentrations. These data also suggest that the altered glucose metabolism in *Bhmt*$^{-/-}$ mice was not limited to adipose tissue, but also occurred in the liver. Enhanced whole-body glucose oxidation could limit the availability of acetyl-CoA forming fatty acids and the availability of the glycerol backbone forming TAG.

It is intriguing that the observed effects were more pronounced in IWAT as compared to GWAT in *Bhmt*$^{-/-}$ mice. The size of *Bhmt*$^{-/-}$ GWAT adipocytes was 57% that of controls, while IWAT adipocytes size was 20% the size of that in controls. Adipocytes from *Bhmt*$^{-/-}$ IWAT synthesized 62% less TAG and oxidized 2.4-fold more glucose than did control IWAT, while no changes were detected in adipocytes from GWAT. It is commonly accepted that visceral (GWAT) and subcutaneous (IWAT) fat pads are different. GWAT is considered to be the "pure WAT", while IWAT is a "convertible WAT" that may convert to BAT [237]. Compared to visceral fat, subcutaneous fat cells express more thyroid hormone receptors [238] and mitochondrial *Ucp1* [239, 240], have more efficient insulin signaling and *Glut4* [241], and is more responsive to *Pparγ* thiazolidinedione ligand [242, 243]. When subcutaneous fat was transplanted into visceral cavity of mice, it reduced body weight and fat mass, and enhanced insulin and glucose sensitivities [244], suggesting an intrinsic difference between the two fat pads. These differences in GWAT and IWAT may explain why effects in

Bhmt$^{-/-}$ IWAT are more pronounced. Similar findings have been observed in a different mouse model [245].

Bhmt$^{-/-}$ mice had reduced adiposity due to increased energy expenditure, enhanced glucose oxidation, and reduced TAG synthesis (**Figure 4.5**). The next question was how *Bhmt* deficiency could exert these differences, and we identified several candidates that may be responsible. Coinciding with increased energy expenditure, *Bhmt*$^{-/-}$ mice had elevated plasma T4 (the major form of thyroid hormone in the blood), a well-known energy metabolism regulator. *Bhmt*$^{-/-}$ mice also over-expressed hepatic *Fgf21* and plasma FGF21 concentration was elevated, possibly contributing to the elevated energy expenditure and the enhanced glucose sensitivity. FGF21 is a novel metabolic regulator that is preferentially expressed in the liver [140]. FGF21 increases glucose uptake [142, 144] and decreased intracellular TAG content in adipocytes [144]; it lowers plasma glucose and TAG when administered to diabetic mice [142]; and it increases energy expenditure and improves insulin sensitivity in diet-induced obese mice [145, 146]. Furthermore, *Bhmt*$^{-/-}$ mice had increased bile acids concentrations in both liver and adipose tissue. Recent progress suggested a role of bile acids in glucose and energy homeostasis. Mice fed a cholic acid (a bile acid) supplemented diet had increased energy expenditure, preventing obesity and insulin resistance [133], while mice with reduced bile acids had decreased energy expenditure [132]. *Bhmt* deletion resulted in increased cholate and taurocholate in adipose tissue, and in increased taurocholate and glycocholate in liver. *Bhmt*$^{-/-}$ mice had reduced hepatic and serum cholesterol [226]. This was perhaps due to an increased conversion of cholesterol to cholic acid. Indeed, the concentration of 7-hydroxycholesterol, the precursor to bile acid from

cholesterol, was significantly elevated in both liver and adipose in *Bhmt*$^{-/-}$ mice. A growing body of evidence suggested an interaction among bile acids, thyroid hormone and FGF21. Thyroid hormone induced cholesterol 7α hydroxylase (CYP7A1), the rate-limiting enzyme in bile-acid synthesis from cholesterol [138, 139], and there was an inverse relationship between thyroid hormone level and serum cholesterol [136]. Thyroid hormone also induced hepatic *Fgf21* expression in mice [147]. Bile acids enhanced the conversion of T4 to T3 within tissues, resulting in increased energy expenditure in mice [133]. Both bile acids and FGF21 concentrations were elevated in patients with nonalcoholic fatty liver [149]. Bile acids, thyroid hormone and FGF21 all induce similar metabolic changes, and these data together suggested that there was an interaction among these factors and *Bhmt* deficiency. All of these were altered in *Bhmt*$^{-/-}$ mice and could contribute to the reduced adiposity observed in *Bhmt*$^{-/-}$ mice. However, more studies are required to elucidate the interaction among these factors and their roles in reduced adiposity in *Bhmt*$^{-/-}$ mice.

Aside from the increased bile acids, thyroid hormone and FGF21, deletion of hepatic *Bhmt* may cause reduced adiposity via changes in choline metabolites. As mentioned previously, BHMT is a major regulator of choline metabolism. Deletion of *Bhmt* resulted in altered choline metabolites, including a 21-fold and 2-fold increase in hepatic and adipose tissue betaine concentration and an 82% and 53% decrease in hepatic and adipose tissue choline concentration [226]. Recently, studies suggested that manipulation of dietary choline or alteration of pathways in choline metabolism may influence energy expenditure and adiposity. Mice fed a methionine and choline deficient diet (MCDD) were hypermetabolic, lost weight [150], and had better insulin sensitivity and glucose tolerance [154]. Mice with

the *Pemt* gene (making PtdCho from PtdEtn) deleted had normal metabolic parameters on a regular chow diet compared to wildtype controls, however, when fed a high fat diet, they had increased oxygen consumption and RER, accumulated less body fat and had increased glucose sensitivity [155]. The lack of weight gain in $Pemt^{-/-}$ mice disappeared when mice were supplemented with choline. These observations suggest a potential role of choline deficiency in modulating energy metabolism. Similar to MCCD fed mice and the $Pemt^{-/-}$ mice, $Bhmt^{-/-}$ mice had reduced choline and PtdCho concentrations, enhanced glucose and insulin sensitivities, increased energy expenditure and reduced adiposity.

Bhmt ablation also resulted in a significant accumulation of betaine, which serves as a methyl donor and osmolyte. Betaine is commercially available as a feed additive; it is widely discussed as a "carcass modifier" due to its lipotropic and growth-promoting effects, generating leaner meat [156]. Dietary betaine supplementation resulted in reduced abdominal fat in poultry, and reduced carcass fat (by 10-18%) in pigs [156-181]. The exact mechanism by which betaine modulates carcass quality is still unclear but has been suggested to involve interactions of betaine with growth factors and thyroid hormones [172, 175, 179, 181, 187-191]. We did not observe increased growth hormone, but did observe enhanced plasma T4 and FGF21 concentration and consequently hypermetabolism in $Bhmt^{-/-}$ mice. Betaine may also have a role as a glucose sensitizer. Betaine supplementation enhanced insulin sensitivity in diet-induced-obese mice and increased insulin signaling pathway in isolated adipocytes [99].

To summarize (**Figure 4.5**), *Bhmt* deletion resulted in reduced adiposity, enhanced insulin sensitivity and glucose tolerance. The reduction in fat mass in *Bhmt* deficient mice could be attributed to (1) increased whole body energy expenditure (2) decreased mobilization of lipids from the liver (VLDL) to be stored in adipose tissues (3) decreased TAG synthesis within adipocytes, and (4) increased glucose oxidation. Deletion of *Bhmt* resulted in a panel of abnormalities, including elevated thyroid hormone, bile salts, FGF21, and betaine concentrations, and reduced choline and PtdCho concentrations. Many of these have been related to elevated energy metabolism, reduced adiposity, and enhanced glucose tolerance and insulin sensitivity. How these parameters interact with each other warrant further studies. This study suggests the importance of *Bhmt* in regulating energy metabolism and adiposity.

4.6 FIGURES

Figure 4.1. *Bhmt*$^{-/-}$ mice have reduced adiposity and better insulin & glucose sensitivities. **A.** Body mass was measured in 14-week-old *Bhmt*$^{+/+}$ (black bar) and *Bhmt*$^{-/-}$ (white bar) mice using magnetic resonance image (MRI). *p<0.01, different from *Bhmt*$^{+/+}$ mice by Students' *t* test; n=6 per group. **B.** Two major fat pads, gonadal (GWAT) and inguinal (IWAT) white adipose tissues, were harvested from from *Bhmt*$^{+/+}$ (black square) and *Bhmt*$^{-/-}$ (white square) mice at various age. *p<0.01, different from *Bhmt*$^{+/+}$ of the same age by Students' *t* test; n=10-16 per group for 5-12 week old mice and n=5 per group for 20-48 week old mice. **C.** Morphology of GWAT and IWAT from 3-month-old mice was shown by hematoxylin-eosin staining. Scale bar = 50 μm. **D.** The adipocyte cell area of GWAT and IWAT from *Bhmt*$^{+/+}$ (black bar) and *Bhmt*$^{-/-}$ (white bar) mice was analyzed using Zeiss AxioVision software. *p<0.05, **p<0.01, different from *Bhmt*$^{+/+}$ mice by Students' *t* test; n=3-5 per group. **E.** BHMT protein in liver and adipose tissue from *Bhmt*$^{+/+}$ and *Bhmt*$^{-/-}$ mice were probed by Western blot analysis. The size of BHMT protein is 45 kDa. **F-G.** Glucose tolerance test (F) and insulin tolerance test (G) was done in 7-week-old *Bhmt*$^{+/+}$ (black square) and *Bhmt*$^{-/-}$ (white square) mice via intraperitonal injection of either glucose or insulin and measuring tail blood glucose at various time points. *p<0.05, different from *Bhmt*$^{+/+}$ by Students' *t* test; n=7 per group. Data is presented as mean ± SEM.

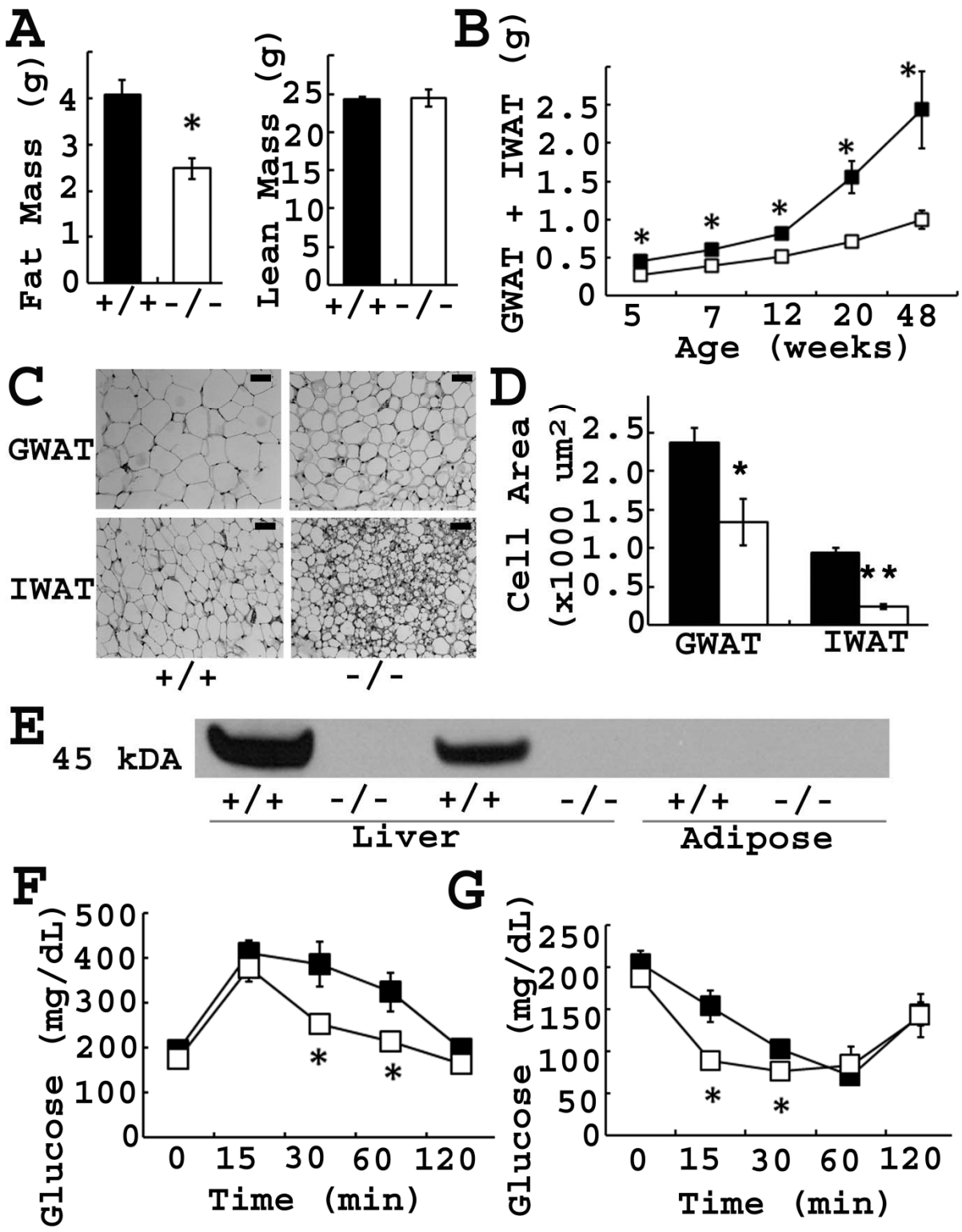
A
Fat Mass (g)
Lean Mass (g)
+/+ -/-
B
GWAT + IWAT (g)
Age (weeks)
C
GWAT
IWAT
+/+
-/-
D
Cell Area (x1000 um²)
GWAT
IWAT
E
45 kDA
+/+ -/- +/+ -/- +/+ -/-
Liver
Adipose
F
Glucose (mg/dL)
Time (min)
G
Glucose (mg/dL)
Time (min)

Figure 4.2. *Bhmt*$^{-/-}$ mice have altered energy metabolism. A. Food intake was measured in 7-week-old *Bhmt*$^{+/+}$ (black bar) and *Bhmt*$^{-/-}$ (white bar) mice using indirect calorimetry; n=8 per group. **B.** A fat tolerance test was performed in 7-week-old *Bhmt*$^{+/+}$ (black square) and *Bhmt*$^{-/-}$ (white square) mice via oral gavage of olive oil and measuring plasma TAG at various time points; n=3 per group. **C.** Fecal fat from *Bhmt*$^{+/+}$ (black bar) and *Bhmt*$^{-/-}$ (white bar) mice was extracted and measured using a colorimetric assay; n=7 per group. **D.** Rectal temperature of 7-week-old *Bhmt*$^{+/+}$ (black bar) and *Bhmt*$^{-/-}$ (white bar) mice was measured using a rectal probe thermometer at room temperature; n=6-7 per group. **E-I.** Oxygen consumption (E), carbon dioxide release (F), heat release (G), respiratory exchange ratio (CO_2 release/O_2 used) (H), and locomotor activity (I) were measured in 7-week-old *Bhmt*$^{+/+}$ (black) and *Bhmt*$^{-/-}$ (white) using indirect calorimetry. Data was obtained after mice being acclimated to the chambers for 24 hr. *$p<0.05$, **$p<0.01$, different from *Bhmt*$^{+/+}$ mice by Students' *t* test; n=8 per group. Data is presented as mean ± SEM. TAG, triacylglycerol; VO_2, oxygen consumption; VCO_2, carbon dioxide release; RER, respiratory exchange ratio.

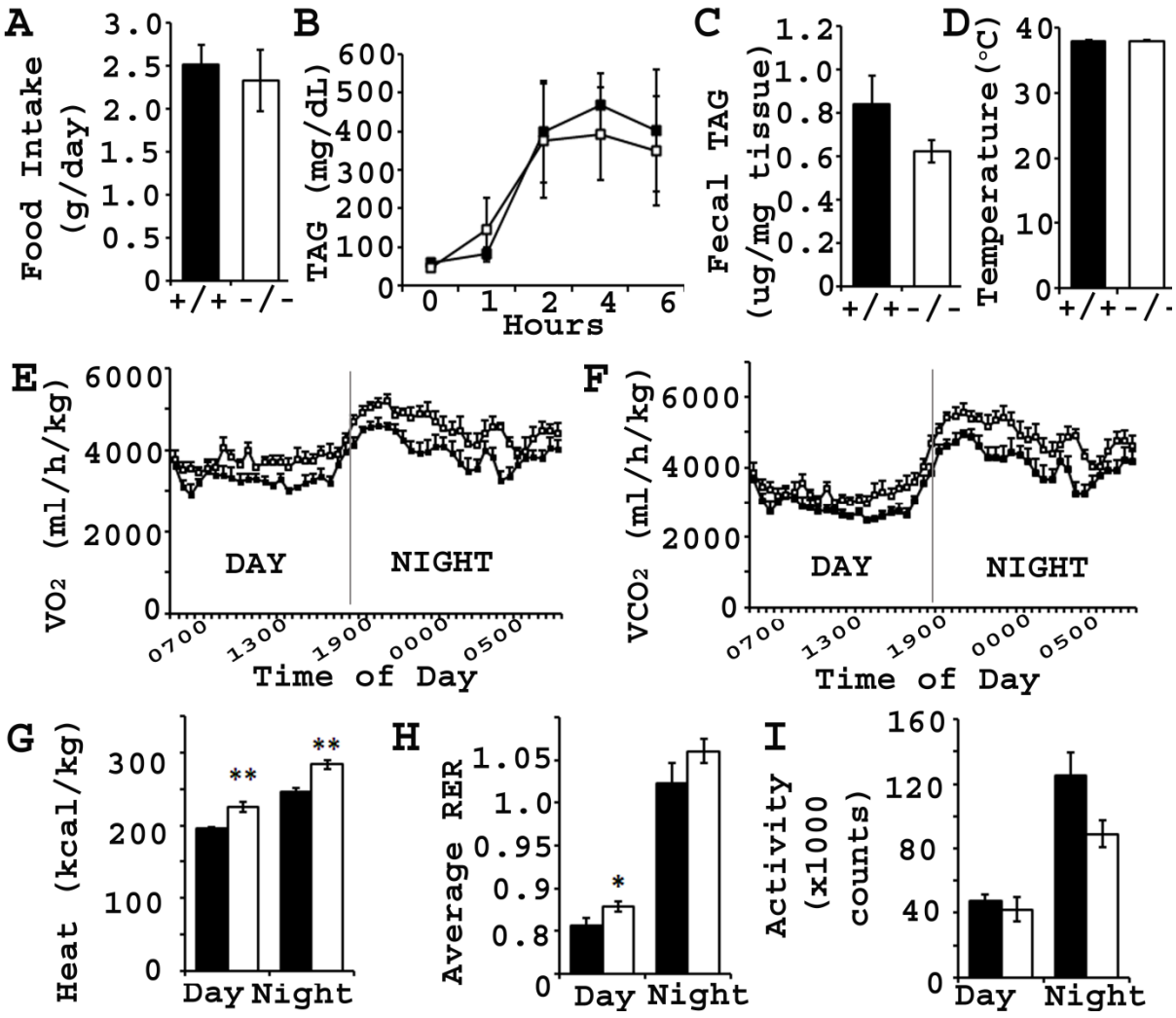
A
Food Intake (g/day)
3.0
2.5
2.0
1.5
1.0
0.5
0
+/+ -/-
B
TAG (mg/dL)
600
500
400
300
200
100
0
0 1 2 4 6
Hours
C
Fecal TAG (ug/mg tissue)
1.2
1.0
0.8
0.6
0.4
0.2
0
+/+ -/-
D
Temperature (°C)
40
30
20
10
0
+/+ -/-
E
VO2 (ml/h/kg)
6000
4000
2000
0
DAY
NIGHT
0700 1300 1900 0000 0500
Time of Day
F
VCO2 (ml/h/kg)
6000
4000
2000
0
DAY
NIGHT
0700 1300 1900 0000 0500
Time of Day
G
Heat (kcal/kg)
300
200
100
0
**
**
Day Night
H
Average RER
1.05
1.0
0.95
0.9
0.8
0
*
Day Night
I
Activity (x1000 counts)
160
120
80
40
0
Day Night

Figure 4.3. *Bhmt*$^{-/-}$ mice are cold sensitive. Seven-week-old mice were exposed to room temperature or 4°C, and tissues collected after 6 hour exposure. **A.** Body temperature of *Bhmt*$^{+/+}$ (black square) and *Bhmt*$^{-/-}$ (white square) mice exposed to 4°C was measured using a rectal probe thermometer at different time point. *p<0.05, **p<0.01, different from *Bhmt*$^{+/+}$ mice at the same time point by Students' *t* test; n=13-14 per group. **B.** Expression of genes involved in thermogenesis in the BAT of *Bhmt*$^{+/+}$ (black bar) and *Bhmt*$^{-/-}$ (white bar) mice at room temperature (n=3-4 per group) or 4°C (n=7-8 per group) exposure. **C.** TAG in BAT from room temperature (n=3-6 per group) or 4°C (n=13-14 per group) exposed *Bhmt*$^{+/+}$ (black bar) and *Bhmt*$^{-/-}$ (white bar) mice were extracted and measured colorimetrically. **D-G.** Plasma glucose (D), glycerol (E), NEFA (F), and CK (G) from room temperature (n=3-6 per group) or 4°C (n=13-14 per group) exposed *Bhmt*$^{+/+}$ (black bar) and *Bhmt*$^{-/-}$ (white bar) mice were measured colorimetrically. *p<0.05, different from *Bhmt*$^{+/+}$ mice under the same condition by Students' *t* test. Data is presented as mean ± SEM. BAT, brown adipose tissue; NEFA, non-esterified fatty acid; CK, creatine kinase; PGC1α, pparγ coactivator 1α; LPL, lipoprotein lipase; UCP1, uncoupling protein 1; MCPT1, muscle carnitine palmitoyl transferase 1.

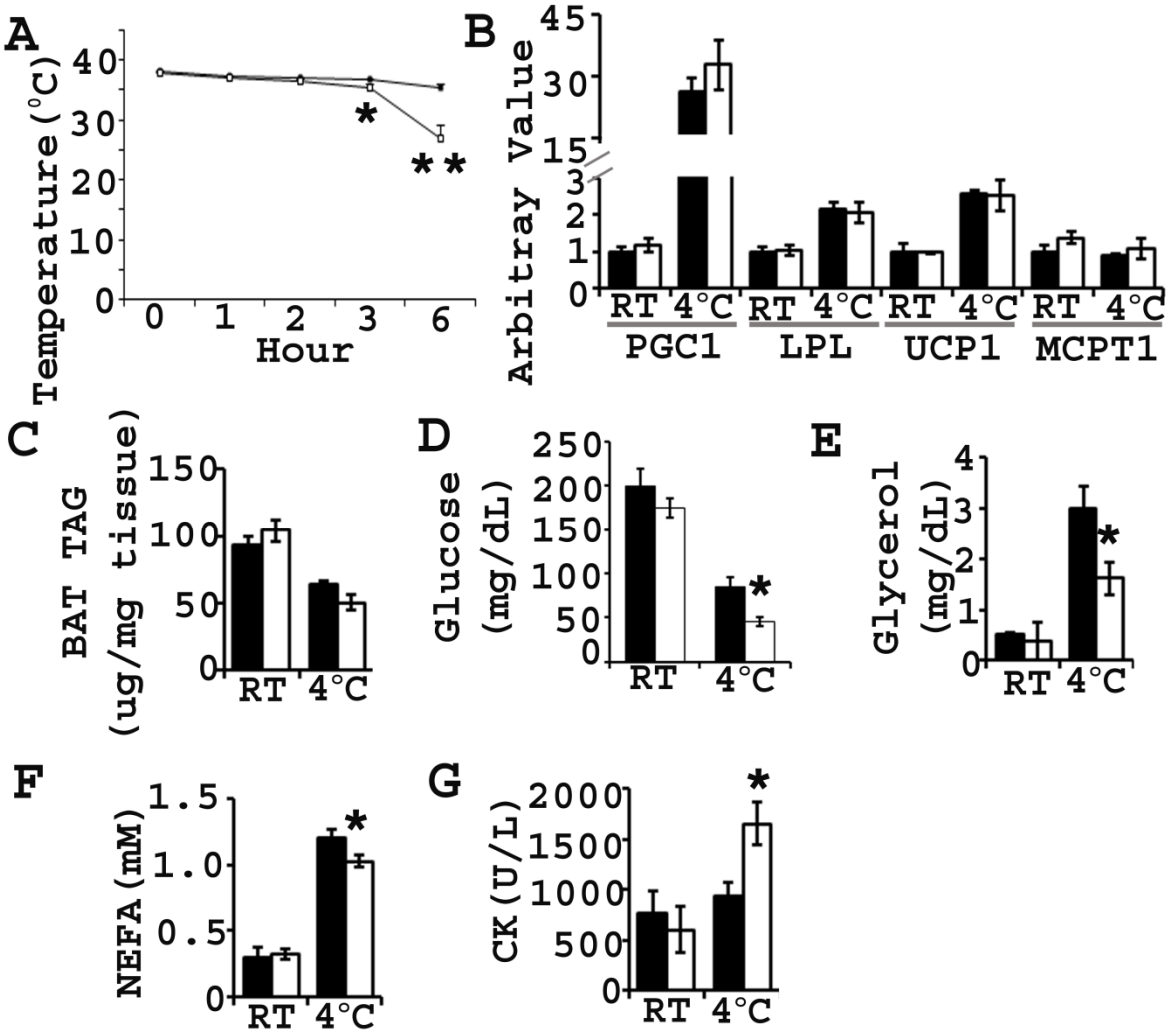
A
Temperature(°C)
40
30
20
10
0
0 1 2 3 6
Hour
*
**
B
Arbitray Value
45
30
15
3
2
1
0
RT 4°C RT 4°C RT 4°C RT 4°C
PGC1 LPL UCP1 MCPT1
C
BAT TAG
(ug/mg tissue)
150
100
50
0
RT 4°C
D
Glucose
(mg/dL)
250
200
150
100
50
0
*
RT 4°C
E
Glycerol
(mg/dL)
4
3
2
1
0
*
RT 4°C
F
NEFA(mM)
1.5
1.0
0.5
0
*
RT 4°C
G
CK(U/L)
2000
1500
1000
500
0
*
RT 4°C

Figure 4.4. *Bhmt*$^{-/-}$ mice have altered TAG synthesis and glucose oxidation. A-C. Plasma TAG (A), glycerol (B), and glucose (C) were measured in 7-week-old *Bhmt*$^{+/+}$ (black bar) and *Bhmt*$^{-/-}$ (white bar) mice before and after ip injection of lipolytic stimulus isoproterenol or CL316243; n= 5-7 per group. **D-E.** Gonadal (D) or inguinal (E) explants from *Bhmt*$^{+/+}$ (black square) and *Bhmt*$^{-/-}$ (white square) mice were used to measure glycerol release without (solid line) or with (dashed line) 10 μM lipolytic stimulus isoproterenol; n=4-6 per group. **F.** Mature adipocytes were isolated from *Bhmt*$^{+/+}$ (black bar) and *Bhmt*$^{-/-}$ (white bar) mice GWAT and IWAT and used to determine the rate of labeled fatty acid incorporated to triacylglycerol. **p<0.01, different from *Bhmt*$^{+/+}$ mice by Students' *t* test; n=4-5 per group. **G.** Mature adipocytes were isolated from *Bhmt*$^{+/+}$ and *Bhmt*$^{-/-}$ mice GWAT and IWAT and used to determine the rate of ^{14}C 18:1 oxidation: CO_2 (grey bar), ASM (white bar); n=10-13 per group. **H-I.** Mature adipocytes were isolated from *Bhmt*$^{+/+}$ (black bar) and *Bhmt*$^{-/-}$ (white bar) mice GWAT (H) and IWAT (I) and used to determine the rate of glucose oxidation with or without insulin. *p<0.05,**p<0.01 different from *Bhmt*$^{+/+}$ mice under the same treatment by Students' *t* test; n=7-10 per group without insulin, n=4-7 per group with insulin. Data is presented as mean ± SEM. GWAT, gonadal white adipose tissue; IWAT, inguinal white adipose tissue; ASM, acid soluble metabolites; TAG, triacylglycerol; Iso, isoproterenol; CL, CL CL316243.

A
Plasma TAG (mg/dL)
80
60
40
20
0
-Iso
+Iso
-CL
+CL
B
Plasma Glycerol (mg/dL)
10
8
6
4
2
0
-Iso
+Iso
-CL
+CL
C
Plasma Glucose (mg/dL)
200
150
100
50
0
*
-Iso
+Iso
-CL
+CL
D
Glycerol (ug/mg tissue)
1.6
1.2
0.8
0.4
0
+Iso
-Iso
0
30
120
240
Time (Min)
E
Glycerol (ug/mg tissue)
1.0
0.8
0.6
0.4
.2
0
+Iso
-Iso
0
30
120
240
Time (Min)
F
C14 TAG (pmol/mg protein/2hr)
600
400
200
0
**
GWAT
IWAT
G
FA Oxidation (pmol/mg protein/1.5hr)
400
300
200
100
0
+/+
-/-
+/+
-/-
GWAT
IWAT
H
CO2 (pmol/mg protein/1.5hr)
6000
5000
4000
3000
2000
1000
0
*
-
-
+
+
Insulin
GWAT
I
CO2 (pmol/mg protein/1.5hr)
2000
1500
1000
500
0
**
**
-
-
+
+
Insulin
IWAT

Figure 4.5. Overview of metabolic disturbances in *Bhmt*$^{-/-}$ mice. Increased energy expenditure, decreased lipid mobilization from the liver to adipose tissue, decreased TAG synthesis and enhanced glucose oxidation together resulted in reduced fat mass in *Bhmt*$^{-/-}$ mice. *Bhmt* deletion increased plasma FGF21 and T4 concentrations, and increased betaine and bile acids concentrations while decreased choline concentration in both liver and adipose tissue. All of these changes had been associated with increased energy expenditure, enhanced insulin sensitivity, and reduced adiposity, and might be interrelate with one-another. BHMT, betaine homocysteine *S*-methyltransferase; Cho, choline; Bet, betaine; PtdCho, phosphatidylcholine; VLDL, very low density lipoprotein; FA, fatty acid; TAG, triacylglycerol; FGF21, fibroblast growth factor 21; Chol, cholesterol; 7 hydroxychol, 7 hydroxycholesterol; BAs, bile acids; Glu, glucose; Gly, glycogen; G-6-P, glucose-6-phosphate; Dio2, deiodinase 2; T4, thyroxine; T3 triiodothyronine.

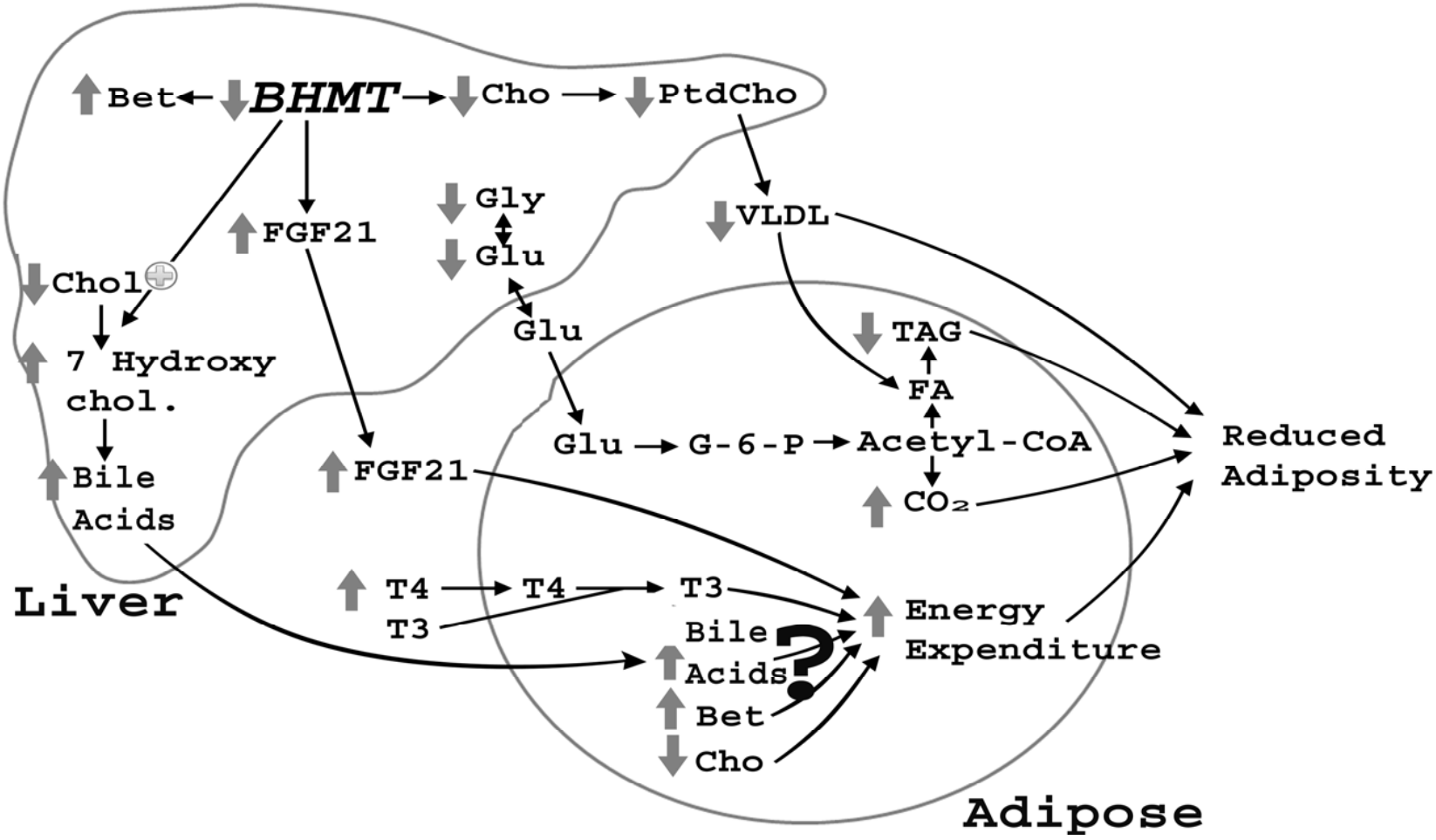
Bet
BHMT
Cho
PtdCho
Gly
Glu
FGF21
VLDL
Chol
7 Hydroxy chol.
Bile Acids
Glu
TAG
FA
Glu
G-6-P
Acetyl-CoA
CO2
Reduced Adiposity
FGF21
Liver
T4
T4
T3
T3
Bile Acids
Energy Expenditure
Bet
Cho
Adipose

4.7 TABLES

Table 4.1. Metabolites and Gene Expression of *Bhmt*$^{+/+}$ and *Bhmt*$^{-/-}$ mice in Tissues.

Plasma was collected from 7-12 week old *Bhmt*$^{+/+}$ and *Bhmt*$^{-/-}$ mice after 4 h fasting, and metabolites measured using commercial available kits; n=8-17 per group. Liver, GWAT, IWAT were collected from 7-week-old *Bhmt*$^{+/+}$ and *Bhmt*$^{-/-}$ mice unless otherwise indicated. *Fgf21* expression and mitochondria DNA were measured by real-time PCR, and expressed relatively to the controls; n=6-10 per group. ATP and AMP were measured using a high pressure chromatography method; n=4 for ATP and AMP measurement. Glucose and glycogen were measured using an acid hydrolysis method; n=6 per group. *p<0.05, **p<0.01, different from *Bhmt*$^{+/+}$ by Students' *t* test. Data is presented as mean ± SEM.

Organ	Measurement	*Bhmt*$^{+/+}$	*Bhmt*$^{-/-}$
Plasma	Insulin [ng/mL]	0.806 ± 0.120	0.405 ± 0.157*
	FGF21 [ng/mL]	1.49 ± 0.16	2.6 ± 0.3**
	T4 (thyroxine) [µg/dL]	4.61 ± 0.27	5.73 ± 0.22**
	T3 (triiodothyronine) [ng/dL]	69.92 ± 5.87	75.37 ± 9.87
	Growth hormone [ng/mL]	5.02 ± 1.23	4.66 ± 1.46
Liver	FGF21 expression [arbitrary value]	1.00 ± 0.24	3.35 ± 0.95*
	Glucose [µmol/g liver] [5-wk-old]	23.22 ± 0.91	18.22 ± 1.47*
	Glucose [µmol/g liver] [48-wk-old]	24.35 ± 2.06	11.53 ± 2.39*
	Glycogen [µmol/g liver] [5-wk-old]	100.13 ± 7.01	83.13 ± 4.21
	Glycogen [µmol/g liver] [48-wk-old]	56.64 ± 15.31	7.22 ± 2.56*
	ATP [nmol/mg protein]	132.8 ± 14.8	77.0 ± 13.0*
	AMP [nmol/mg protein]	104.9 ± 30.6	169.2 ± 27.6
	ATP/AMP	1.49 ± 0.33	0.51 ± 0.17*
	Mitochondria DNA [arbitrary value]	1.00 ± 0.23	1.23 ± 0.21
GWAT	ATP [nmol/mg protein]	74.6 ± 20.3	96.2 ± 28.4
	AMP [nmol/mg protein]	182.5 ± 28.2	220.8 ± 53.7
	ATP/AMP	0.50 ± 0.21	0.58 ± 0.31
	Mitochondria DNA [arbitrary value]	1.00 ± 0.08	1.26 ± 0.17
IWAT	ATP [nmol/mg protein]	51.5 ± 7.8	66.8 ± 16.9
	AMP [nmol/mg protein]	226.8 ± 23.3	258.1 ± 12.1
	ATP/AMP	0.23 ± 0.04	0.25 ± 0.05
	Mitochondria DNA [arbitrary value]	1.00 ± 0.14	1.30 ± 0.11

Table 4.2. Bile acids and sterols in *Bhmt* liver and adipose tissue.

Liver and gonadal adipose tissue were collected from 5-week-old *Bhmt*$^{+/+}$ and *Bhmt*$^{-/-}$ mice after 4 hour fasting; n=6 per group. The relative abundance of metabolites was measured and analyzed by liquid and gas chromatography by Metabolon (Research Triangle Park, NC). Dark grey=elevated relatively to controls, light grey=decreased relatively to controls, N/D=not-detected.

METABOLITES	**LIVER**			
	WT Mean	KO Mean	Fold Change	P Value
Cholate	0.84 ± 0.08	2.26 ± 0.78	2.71	0.184
Taurocholate	0.75 ± 0.09	1.21 ± 0.12	1.62	0.010
Glycocholate	0.88 ± 0.18	1.95 ± 0.43	2.33	0.021
Taurochenodeoxycholate	1.62 ± 0.44	0.88 ± 0.22	0.54	0.228
Cholesterol	1.19 ± 0.07	0.95 ± 0.06	0.80	0.036
7-ß-hydroxycholesterol	0.76 ± 0.45	2.26 ± 0.71	2.98	0.020
	ADIPOSE			
	WT Mean	KO Mean	Fold Change	P Value
Cholate	0.94 ± 0.23	8.93 ± 2.88	9.50	0.005
Taurocholate	1.14 ± 0.31	3.90 ± 0.96	3.41	0.020
Cholesterol	1.09 ± 0.08	1.25 ± 0.10	1.15	0.261
7-α-hydroxycholesterol	0.88 ± 0.19	1.92 ± 0.20	2.17	0.009
7-ß-hydroxycholesterol	1.03 ± 0.18	1.53 ± 0.21	1.48	0.075

CHAPTER V

SYNTHESIS

5.1 Overview

This dissertation describes two independent projects that examine the metabolic consequences of *Bhmt* deficiency. In this work, we generated the first mouse model with the gene encoding *Bhmt* deleted. The results of these studies confirm the importance of BHMT in the regulation of homocysteine and one-carbon metabolism. The results of these studies also reveal that BHMT has broader metabolic effects than we previously anticipated. We show for the first time that BHMT is involved in hepatic carcinogenesis and in energy metabolism. Although many questions remain to be addressed, this work is expected to stimulate further research. This chapter will discuss the key findings from these projects and their future implications for understanding and treatment of BHMT-related diseases.

5.2 *Bhmt* deficiency caused hyperhomocysteinemia

Elevation of Hcy has been associated with cardiovascular disease, neural tube defect, renal dysfunction, and cognitive impairment [43]. Although it is well established that BHMT functions to remethylate Hcy into methionine, this role has traditionally received little attention. This is due to the assumption that transsulfuration and methyl-folate pathways could potentially replace the lack of BHMT. Using *Bhmt* deficient mice, this dissertation provides compelling evidence that the role of BHMT in Hcy metabolism is not replaceable. $Bhmt^{-/-}$ mice have a substantial increase in hepatic (by 6-fold) and plasma Hcy (by 7.8-fold), suggesting that transsulfuration and methyl-folate pathways do not have the capacity to remove the excess Hcy due to *Bhmt* deficiency under normal conditions.

BHMT and MS share the function of remethylating Hcy to methionine. MS uses methyl-folate as the methyl donor. An interesting question to ask is whether folate supplementation can reverse, while folate deficiency can exacerbate, the elevated plasma Hcy caused by *Bhmt* deletion? My student, Ignacio Cerdena, and I are currently addressing this question. We are feeding 6 week old $Bhmt^{+/+}$ and $Bhmt^{-/-}$ female mice a folate deficient, a folate control or a folate supplemented diet for 4 weeks. We will collect plasma and tissues for analysis. Preliminary data from this study shows that $Bhmt^{-/-}$ mice have higher plasma homocysteine than do $Bhmt^{+/+}$ mice in all dietary groups (**Figure 5.1**). The data also shows that a 4-week folate supplementation does not ameliorate the elevated plasma Hcy caused by *Bhmt* deficiency, while folate deficiency exacerbates it. This ongoing project provides a valuable message – humans who have HHcy due to *BHMT* deficiency may not benefit from

dietary folate supplementation, but they would do worse if they are not taking in enough folate.

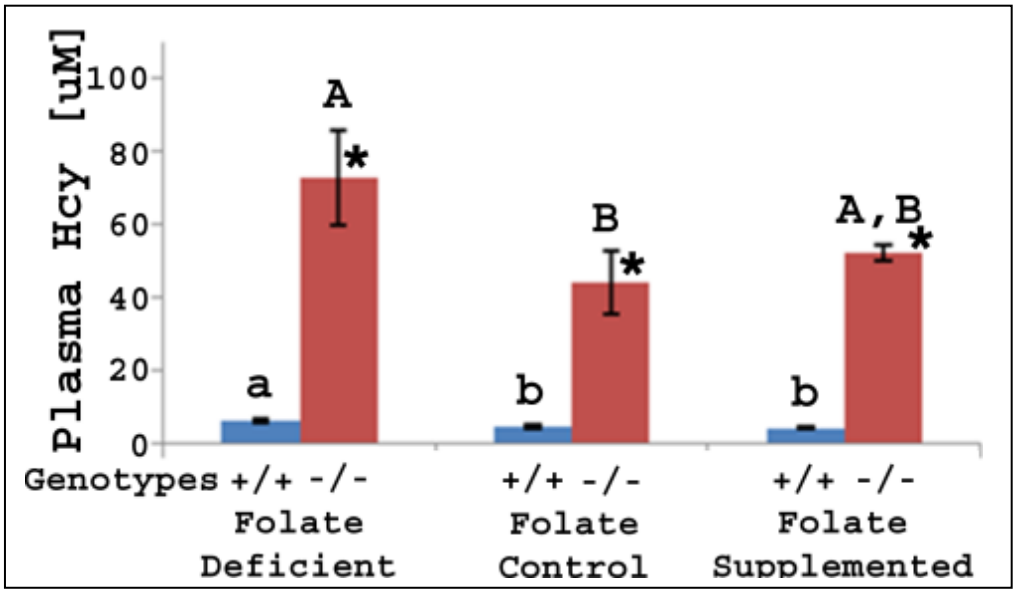

Figure 5.1 Plasma total homocysteine of *Bhmt*$^{+/+}$ or *Bhmt*$^{-/-}$ mice on varying folate diets. Six weeks old *Bhmt*$^{+/+}$ and *Bhmt*$^{-/-}$ mice were given a folate deficient, a folate control or a folate supplemented diet for four weeks. Plasma total homocysteine was quantified by high pressure liquid chromatography. Small letters, significantly different by diets within wildtype mice. Capitalized letters, significantly different by diets within knockout mice. *, significantly different by genotypes within the same diet.

The pressing question arising from these findings is whether the elevated Hcy levels in *Bhmt*$^{-/-}$ mice affect the pathology of HHcy-related diseases, particularly cardiovascular diseases. Several mouse models of HHcy have been engineered to study the vascular pathophysiology of hyperhomocysteinemia [42]. Those include mice with the gene encoding *Cbs, Mthfr* or *Mtr/Ms* deleted [246-248]. Mice with homozygous defects in these genes have poor growth and survival, making the study of vascular pathophysiology of HHcy difficult [246-248]. Instead, studies have been done in mice with heterozygous defect in these genes.

These mice are barely hyperhomocysteinemic (plasma Hcy of 6-9 μM, compared with 3-5 μM in wildtype littermates) and require additional diet manipulation to reach the HHcy state [249-251]. The *Bhmt*$^{-/-}$ mouse will be a valuable mouse model to examine the relationship between HHcy and vascular diseases because it survives to at least 1 year of age and is severely hyperhomocysteinemic. Future studies should examine whether deletion of *Bhmt* results in increased susceptibility to vascular diseases due to HHcy.

5.3 *Bhmt* deficiency disturbed choline metabolites

The results from this dissertation elucidate the effects of *Bhmt* deficiency on choline metabolites. As predicted, *Bhmt* deficiency results in a substantial accumulation of betaine in most tissues, except testis. Unexpectedly, *Bhmt* deficiency results in reduced choline and PtdCho concentrations in tissues, suggesting the complexity of the regulation of choline metabolism.

Deletion of *Bhmt* does not result in accumulation of choline, the precursor of betaine. Choline is either oxidized to form betaine by the enzyme CHDH or used to form PtdCho. Since *Bhmt*$^{-/-}$ mice cannot use betaine, we expected to see product inhibition of CHDH, resulting in increased choline availability for use in PtdCho synthesis. The opposite has been observed, with lower choline and PtdCho concentrations in a number of tissues. *Bhmt*$^{-/-}$ mice have elevated hepatic *Chdh* expression and CHDH activity, suggesting that this gene is induced by some factor present in *Bhmt*$^{-/-}$ mice, possibly explaining increased use of choline to form betaine. It is intriguing that nature would sacrifice the possibility of synthesizing PtdCho to make methyl donors. This further demonstrates the importance of betaine and

AdoMet. The questions that arise from these findings regard how CHDH is regulated and whether it is differentially regulated based on tissue types. Testis is the only tissue that maintains normal betaine and choline concentrations during *Bhmt* deficiency. This finding suggests a rigid control of CHDH activity and the importance of maintaining choline metabolite homeostasis in the testis. Our laboratory finds that male mice with *Chdh* deficiency are infertile due to abnormal mitochondria in the testis [252]. Contrary to *Bhmt*$^{-/-}$ mice, *Chdh*$^{-/-}$ mice have high choline and low betaine concentrations, indicating a potential role of betaine in fertility. Amy Johnson in our laboratory is currently studying the role of *Chdh* in male infertility. Future studies examining the regulation of CHDH are needed to develop preventative strategies for male infertility.

In addition to being a methyl donor, betaine also serves as an osmolyte that regulates cellular volume and fluid balance [253]. Cells in the renal medulla are typically exposed to high extracellular osmolarity (NaCl and urea). High NaCl and urea cause water efflux from cells, resulting in reduced cellular volume and creating a hypertonic state that is damaging to cells [254]. Therefore, cells accumulate osmolytes such as betaine to counteract the hypertonicity by retaining water within cells. One would predict that betaine accumulation within renal cells would increase water retention, generating elevated urine osmolarity (lower urinary specific gravity). We observe the opposite, with *Bhmt*$^{-/-}$ mice have reduced urinary specific gravity. One possibility is that these mice are thirsty and consume extra fluid, leading to increased urinary output that consequently decreases urinary osmolarity. To test this hypothesis, fluid intake and urinary output need to be determined. Furthermore, within cells there are other organic osmolytes, such as glycerophosphocholine, taurine, sorbital, and

inositol. Whether betaine accumulation results in compensatory changes of other osmolytes remains to be answered. Future studies should examine the role of betaine in kidney function and betaine's relationship with other osmolytes.

The physiological consequences of accumulating excessive betaine within cells are not understood. Excessive levels of osmolytes could potentially result in cells swelling due to excess water retention and in altered intracellular ionic strength. The mitochondrion is the site of betaine formation (CHDH is a mitochondrial enzyme). Excess betaine accumulation and water retention could potentially result in swollen mitochondria, thereby altering oxidative and energy generating functions. This could potentially contribute to the altered energy metabolism and the fuel usage observed in *Bhmt*$^{-/-}$ mice. To examine the structure of organelles, various tissues from *Bhmt* mice have been collected and are now being processed for conducting transmission electron microscopy (TEM). If changes in organelles are observed, then cellular functions should be examined. It is essential for the future studies to examine the potential effects of betaine as an osmolyte in cellular functions.

5.4 *Bhmt* deficiency altered hepatic health

Alteration of one-carbon metabolism has been associated with liver diseases such as alcoholic and nonalcoholic fatty liver, human liver cirrhosis, and hepatocellular carcinoma for at least 50 years. Expression of genes involved in one-carbon metabolism, such as *BHMT*, is reduced significantly in human cirrhosis and hepatocellular carcinoma [255]. Betaine is used to treat both alcoholic and nonalcoholic fatty liver, while choline deficiency is the only nutrient deficiency that results in hepatocellular carcinoma (summarized in the background

section). Data from this dissertation demonstrates that *Bhmt* deficiency results in nonalcoholic fatty liver at an early age and hepatocellular carcinoma at 1 yr of age. Taken together, one-carbon metabolism plays a crucial role in hepatic health. However, the molecular bases of these findings are not fully elucidated.

Bhmt$^{-/-}$ mice have a 6-fold increase in hepatic triacylglycerol concentration compared to their wildtype littermates. We show that *Bhmt*$^{-/-}$ mice have reduced hepatic PtdCho concentration (by 36%) and VLDL secretion, explaining the fatty liver. However, *Bhmt* may have more roles in hepatic lipid metabolism. Cultured hepatocytes overexpressing *Bhmt*, and rat livers following an *in vivo* induction of *Bhmt*, have increased apolipoprotein B expression, suggesting an additional role of betaine/BHMT system on lipoprotein homeostasis [101-103]. BHMT catalyzes the synthesis of methionine, which is the precursor of AdoMet. The cells need carnitine to transfer fatty acids to mitochondria, where fatty acid oxidation takes place. Carnitine is synthesized from lysine or methionine via methylation, in which AdoMet is required. Deletion of *Bhmt* could possibly reduce carnitine synthesis (by reducing methionine and AdoMet), resulting in limited fatty acid oxidation and a consequent fat accumulation in the liver. Fatty acid oxidation can be tested by incubating hepatocytes or liver homogenates with labeled fatty acid and collecting labeled CO_2. This hypothesis probably does not apply to adipose tissue as *Bhmt*$^{-/-}$ mice have reduced fat mass and no change in fatty acid oxidation.

Bhmt deficiency results in HHcy, which has been associated with altering several biological functions. HHcy has been shown to induce endoplasmic reticulum (ER) stress [108]. ER is an essential organelle, which provides a specialized environment for the

production and post-translational modifications of secretory and membrane proteins. Studies suggest that Hcy can be wrongly incorporated to proteins, causing protein misfolding and unfolding in the ER and increasing ER stress [93, 95, 101, 108]. Increased ER stress activates *Srebp1c* (sterol regulatory element binding protein 1c), an ER bound transcription factor that induces lipid synthesis, which further contributes to fatty liver. Transgenic mice overexpressing human *BHMT* are resistant to HHcy induced ER stress and are protected from alcohol induced fatty liver [95]. This hypothesis can be tested by measuring ER stress markers such as GRP78 (glucose regulated protein 78) and CHOP (C/EBP homologous protein) in tissue. HHcy is also associated with alteration in sterol metabolism. Mice with one allele of *Mthfr* deleted ($Mthfr^{+/-}$, gene in the methyl-folate pathway) have HHcy and increased mRNA and protein levels of CYP7A1, an enzyme that mediates the synthesis of bile acids from cholesterol. $Bhmt^{-/-}$ mice have reduced cholesterol concentration in liver and increased bile acid concentrations in liver and adipose tissue. These data suggest that *Bhmt* deletion enhances the synthesis of bile acids from cholesterol. It is unclear whether HHcy in $Bhmt^{-/-}$ mice is the underlying mechanism for this phenotype.

Bhmt deficiency may also result in oxidative stress. Oxidative stress plays a key role in the development of liver injury, and glutathione attenuates oxidative stress by scavenging free radicals. Glutathione (GSH) is made from cysteine, the synthesis of which requires AdoMet (**Figure 2.4**). GSH becomes glutathione disulfide (GSSG) when oxidized. The ratio of GSH and GSSG within a cell measures cellular toxicity. Since *Bhmt* deficiency reduces AdoMet by 50%, the synthesis of glutathione may be affected. Although we do not see a change in hepatic cysteine level in $Bhmt^{-/-}$ *mice*, plasma cysteine concentration is

significantly reduced during *Bhmt* deficiency. In addition, a side project looking at the metabolomics of *Bhmt*$^{-/-}$ mice reveals that *Bhmt* deficiency reduces both GSH and GSSG in the liver (**Table 5.1**). Compared to the controls, *Bhmt*$^{-/-}$ mice have reduced GSH (by 89%) and GSSG (by 20%) concentrations, leading to an 86% reduction in GSH:GSSG ratio. These data suggest that *Bhmt*$^{-/-}$ mice might be under cellular oxidative stress. The cellular stress may contribute to the later liver injury (fibrosis and HCC) observed in *Bhmt*$^{-/-}$ mice. The mitochondria are the primary intracellular site of oxygen consumption and the major source of reactive oxygen species. Glutathione maintains the redox balance in mitochondria. Future studies should examine how the reduced GSH:GSSG in *Bhmt*$^{-/-}$ mice affects the function of mitochondria, whose primary roles are to oxidize fuels and to generate ATP.

Table 5.1 Glutathione Levels in *Bhmt* Mouse Liver

	WT Mean	KO Mean	Fold Change	P Value
Glutathione, reduced (GSH)	6.53 ± 2.62	0.71 ± 0.12	0.11	0.0184
Glutathione, oxidized (GSSG)	1.11 ± 0.02	0.88 ± 0.03	0.80	<0.001
GSH:GSSG	5.95 ± 2.43	0.80 ± 0.13	0.14	<0.01

Liver was collected from 5-week-old *Bhmt*$^{+/+}$ and *Bhmt*$^{-/-}$ mice after 4 hour fasting; n=6 per group. The relative abundance of metabolites was measured and analyzed by liquid and gas chromatography by Metabolon (Research Triangle Park, NC).

At 1 year of age, 64% of *Bhmt*$^{-/-}$ mice develop hepatic tumors. Histopathology confirms that these tumors are either hepatocellular adenomas or carcinomas. Even those samples that do not have visible tumors have a higher incidence of fat accumulation, cellular alteration and hyperplasia when compared to *Bhmt*$^{+/+}$ livers. The pressing question arising

from these findings is the underlying mechanisms of *Bhmt* deletion in hepatocarcinogenesis. Understanding the role of BHMT in mitigating liver injury may help to develop effective and safe therapies for fatty liver diseases. Several mechanisms have been proposed linking choline deficiency to HCC (summarized in the background section). Those include increased lipid peroxidation, perturbed PKC pathway, and altered DNA methylation of genes involved in tumor genesis. We plan to investigate each of these hypotheses in ongoing work in our laboratory.

To summarize, this dissertation shows that *Bhmt* deficiency results in adverse hepatic effects such as fatty liver and hepatocellular carcinoma. In the future studies, the metabolic basis of these findings needs to be addressed. In addition, the roles of *Bhmt* deficiency in ER stress, oxidative stress, apolipoprotein B synthesis, and sterol metabolism need to determined.

5.5 *Bhmt* deficiency altered methylation potential

Compared to wildtype mice, $Bhmt^{-/-}$ mice have a significant reduction in hepatic methylation potential (AdoMet:AdoHcy) - by 76% at 5 weeks of age, and by 91% at 1 year of age. Decreased hepatic AdoMet/AdoHcy could affect all methylation reactions, including the epigenetic modification DNA methylation. Alteration in DNA methylation may alter the expression of genes involved in tumor genesis, leading to altered cancer risks (summarized in the background section). *Mat1A* and *Gnmt* knockout mouse models are two examples with disturbed methyl group metabolism that leads to tumor genesis [121, 123].

To determine whether methyl group deficiency in *Bhmt*$^{-/-}$ mice results in altered DNA methylation pattern, and consequently, altered gene expression profile, I use CpG methylation and gene expression arrays. *Bhmt*$^{-/-}$ mice have a significant reduction in overall DNA methylation (**Figure 5.2)**. However, when closely examining individual probes for CpG sites, no single CpG sites has been significantly different between genotypes with a false discovery rate less than 0.05. Several factors could contribute to this lack of finding: (1) a small N (n=5) per group, (2) variable methylation pattern within each group, particularly in the *Bhmt*$^{-/-}$ mice group, and (3) a lack of established bioinformatics methods specific for analyzing CpG arrays. To determine whether the methylation of a CpG site is altered, a methylation-specific-PCR or pyrosequencing for the particular CpG site may be better a approach. In conclusion, I believe there would be epigenetic effect due to *Bhmt* deficiency. However, I have failed to prove this using CpG methylation arrays. Future studies examining this question require better methods.

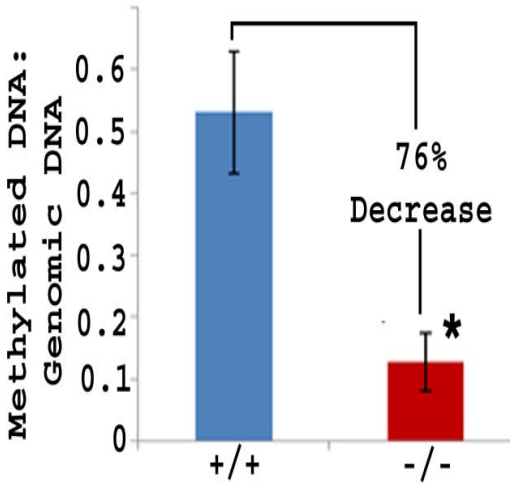

Figure 5.2 Ratio between methylated and total DNA in *Bhmt*$^{+/+}$ and *Bhmt*$^{-/-}$ mice. Genomic DNA was extracted from 5 week old *Bhmt*$^{+/+}$ and *Bhmt*$^{-/-}$ mouse livers. A portion of the DNA was immunoprecipitated using an antibody specific against 5-methylcytidine. The pulled-down methylated DNA and its own genomic DNA were labeled with cyanine (3 and 5 respectively) and cohybridized onto the CpG methylation array. Compared to the controls, *Bhmt*$^{-/-}$ mice had similar signal intensity for total genomic DNA, but less methylated DNA signal intensity. The data suggested that *Bhmt*$^{-/-}$ mice had DNA hypomethylation.

5.6 *Bhmt* deficiency altered fuel metabolism within adipocytes

Bhmt$^{-/-}$ mice have smaller adipocytes in both gonadal and inguinal depots than do the controls. Factors that contribute to the size of an adipocyte include reduced lipid synthesis (FA and TAG synthesis) and increased lipid breakdown (lipolysis and FA oxidation). We show that *Bhmt*$^{-/-}$ mice have normal lipolytic and FA oxidation functions. In contrast, *Bhmt*$^{-/-}$ mice have reduced triacylglycerol synthesis in the isolated mature adipocytes from inguinal depots. These data suggest that the smaller adipocytes in *Bhmt*$^{-/-}$ mice are due to a problem in lipid synthesis rather than breakdown. However, this study does not define the mechanism by which *Bhmt* deletion reduces TAG synthesis. In addition, whether *Bhmt* deficiency results in reduced FA synthesis remains to be determined. Compared to the controls, *Bhmt*$^{-/-}$ mice oxidize more glucose in the whole body (by indirect calorimetry) and in the isolated adipocytes. Glucose undergoes glycolysis, generating pyruvate, which becomes the fatty acid precursor acetyl CoA. Increased glucose oxidation in *Bhmt*$^{-/-}$ mice may result in reduced acetyl CoA available for the synthesis of FA that is subsequently incorporated into TAG. Increased glucose oxidation in *Bhmt*$^{-/-}$ mice may also result in reduced glucose available in the adipose tissue for generating glycerol-3-phosphate, the glucose backbone required for TAG synthesis. To confirm the rate of FA synthesis, the incorporation of radiolabeled acetate or glucose into lipid can be measured in isolated primary adipocytes from *Bhmt* mice. To confirm the rate of glucose incorporation to lipid, glucose can be given to mice intravenously, and tissues collected for lipid extraction.

This study also does not determine the rate of adipocyte differentiation. The histology of both gonadal and inguinal fat pads shows that *Bhmt*$^{-/-}$ mice have a larger number of smaller adipocytes, so it is assumed that the reduced adiposity in *Bhmt*$^{-/-}$ mice is more likely due to problems in making or storing lipids, rather than problems in adipocyte differentiation. To study adipocyte differentiation, I have attempted to isolate and differentiate preadipocytes from *Bhmt* mice. However, *Bhmt*$^{-/-}$ mice have small fat pads, making preadipocyte isolation exceedingly difficult. In addition, the differentiation rate varies significantly from sample to sample such that I have failed to draw any reliable conclusions.

This study has identified the possible metabolic bases that contribute to the reduced adiposity in *Bhmt*$^{-/-}$ mice, such as reduced TAG synthesis and increased glucose oxidation. Future studies need to investigate the direct links between *Bhmt* deletion and these changes. The FA synthesis rate and adipocyte differentiation in *Bhmt* mice may also need to be determined.

5.7 *Bhmt* deficiency altered glucose metabolism

Many lines of evidence from this study suggest that *Bhmt* deficiency alters glucose metabolism. Indirect calorimetry shows that *Bhmt*$^{-/-}$ mice oxidizes more glucose than fatty acids in the whole body system. Adipocytes isolated from *Bhmt*$^{-/-}$ mice oxidize more glucose than do those from *Bhmt*$^{+/+}$ mice. We do not examine the underlying mechanisms of such findings. Is the increased glucose oxidation in *Bhmt*$^{-/-}$ mice caused by increased glucose uptake by tissues? Future studies should examine the uptake of labeled glucose into tissues. In addition, glucose metabolism in other tissues in these mice, particularly the liver, has not

been closely investigated. *Bhmt*$^{-/-}$ mice have reduced hepatic glucose concentration and glycogen storage, which is assumed to be the consequence of an increased demand of glucose. However, I have not tested whether the reduced glycogen in *Bhmt*$^{-/-}$ mice is due to decreased glycogen synthesis from glucose or increased glycogen breakdown to release glucose.

Whether or not *Bhmt* deficiency alters glucose metabolism via altering the insulin signaling pathway remains to be examined. Insulin binds to the insulin receptor (IR), which recruits insulin receptor substrates (IRS). IRS activates the PKB/Akt pathway, resulting in inhibition of gluconeogenesis and induction of glycogen synthesis. Several studies provide evidence that betaine/BHMT is associated with altered insulin homeostasis. A study demonstrates that betaine supplementation alleviates insulin resistance in high-fat-fed mouse model by activating Akt and ERK, two major kinases in the insulin signaling pathway, in the adipose tissues [99]. Another study demonstrates that betaine treatment enhances hepatic insulin signaling in high-fat-fed mouse model by activating hepatic IRS1, leading to enhanced glycogen synthesis [98]. Zucker diabetic fatty rats (model for type 2 diabetes) [256] and streprozotocin-diabetic rats (model of type 1 diabetes) [257] both have increased hepatic BHMT activity and *Bhmt* mRNA levels, implying a correlation between BHMT and insulin sensitivity. These studies, together with the evidence from this dissertation, suggest a role of betaine and BHMT in insulin signaling and glucose metabolism. The insulin-signaling pathway in both *Bhmt*$^{-/-}$ liver and adipose tissue requires additional attention. I have preliminary data showing that *Bhmt*$^{-/-}$ mice have increased protein levels of hepatic insulin receptors (**Figure 5.3**). Increased insulin receptors are often associated with increased

glycogen synthesis, which does not seem to be the case in *Bhmt*$^{-/-}$ mice. However, it is possible that the increased protein levels of hepatic insulin receptors are responses to the reduced hepatic glucose and glycogen concentrations observed in *Bhmt*$^{-/-}$ mice. The exact interaction between betaine/BHMT and insulin and glucose metabolism requires additional study.

Future studies need to investigate the roles of betaine/BHMT in insulin and glucose homeostasis in closer detail. Does the *Bhmt*$^{-/-}$ mouse liver take up more glucose? Does the *Bhmt*$^{-/-}$ mouse have altered insulin signaling pathway? Why does the *Bhmt*$^{-/-}$ mouse have less glucose and glycogen stored in the liver?

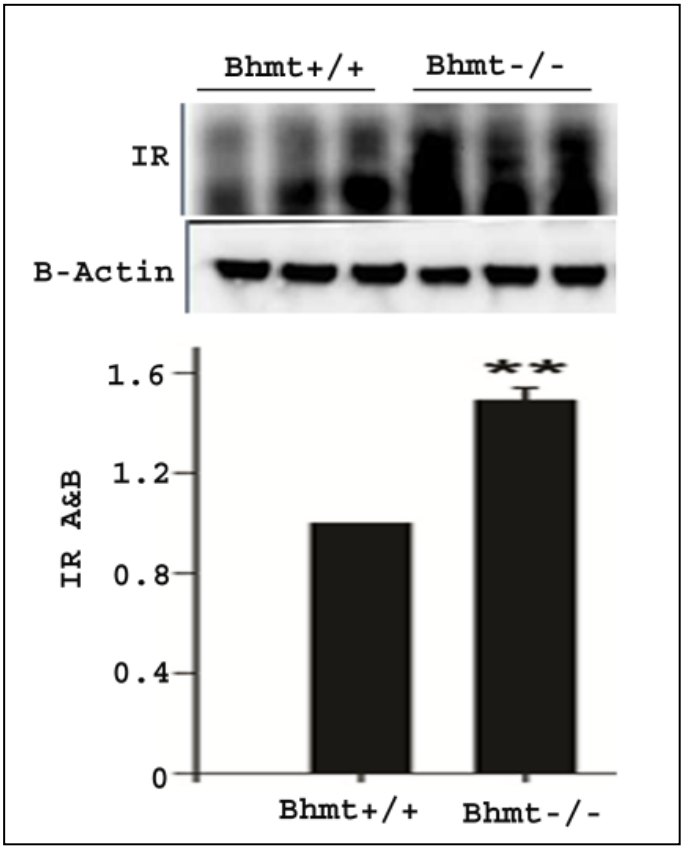

Figure 5.3 Insulin receptor (IR) α and ß in *Bhmt* mouse liver. Livers were collected from 7 week old *Bhmt*$^{+/+}$ and *Bhmt*$^{-/-}$ mice. Insulin receptor α and ß protein levels were quantified using a Western blotting analysis. *Bhmt*$^{-/-}$ mice expressed higher hepatic insulin receptor protein than did *Bhmt*$^{+/+}$ mice.

5.8 *Bhmt* deficiency increased energy expenditure

Bhmt$^{-/-}$ mice have reduced adiposity in part due to increased energy expenditure. Although we have not identified a direct relationship between *Bhmt* deficiency and energy expenditure, we find several factors that could contribute to this phenotype. These factors include bile acids, FGF21, thyroid hormone, betaine and choline (summarized in the background section). All of these are altered in *Bhmt*$^{-/-}$ mice, and there seem to be an interaction among these factors. The question for future study is to identify which one of these is the key element to the reduced adiposity observed in *Bhmt*$^{-/-}$ mice? To answer this, one could alter one of these elements in *Bhmt*$^{-/-}$ mice and see if the alteration reverses the reduced adiposity. For example, one can feed *Bhmt*$^{-/-}$ mice a high choline diet to determine whether it can reverse the phenotype, under the assumption that *Bhmt*$^{-/-}$ mice will not use all choline to make betaine. One could inhibit CYP7A1, the enzyme that synthesizes bile acids from cholesterol to determine whether reduced bile acids can reverse this phenotype, under the assumption that reduced bile acids will not kill the mice. Figuring out how to moderately change one of these elements at a time remains a challenge finding the underlying mechanism of the reduced adiposity in *Bhmt*$^{-/-}$ mice. Another goal for future studies is to find the interactions among these factors. As discussed in the background section, thyroid hormone can induce the synthesis of bile acids and FGF21. Bile acids can transform prohormone T4 to the active thyroid hormone T3. Both bile acids and FGF21 concentrations increase in patients with nonalcoholic fatty liver disease. Future studies need to examine the underlying mechanisms of how *Bhmt* deletion alters the concentrations of these molecules, and how they interrelate with one another.

5.9 Are *Bhmt*$^{-/-}$ mice resistant to a high fat diet?

Bhmt$^{-/-}$ mice have reduced body fat when fed a regular diet. However, it remains a question whether *Bhmt* deficiency are protected from diet-induced obesity. It is possible that a high-fat diet could override the increased energy expenditure and glucose oxidation in *Bhmt*$^{-/-}$ mice. This would be important to discover, since many Americans are facing an obesity problem due to the high-fat Western diets.

5.10 Public Health Significance

Elevated plasma total homocysteine in humans is associated with numerous diseases, particularly cardiovascular disease. Nonalcoholic fatty liver disease affects around 20% of the general global population, around 50% of diabetic subjects, >50% of obese persons, and 90% of morbidly obese persons [258]. It can progress to steatohepatitis (fatty inflammation), fibrosis (excessive fibrous tissue), cirrhosis (serious liver damage), and eventually hepatic tumor [259]. Liver cancer is among the most lethal cancers (five-year survival rates under 14%) in the United States. About 20,000 Americans are estimated to die of liver cancer in 2011 [111]. There has been a striking increase in the prevalence of obesity in the United States during the past 20 years [260]. About 33% U.S. adults are obese, and 17% (12.5 million) of children and adolescents are obese [260]. The medical costs of obesity in the United States are staggering, estimated to be $147 billion dolor per year [260]. The data presented in this dissertation provide novel evidence the important roles of BHMT in homocysteine homeostasis, in hepatic health, and in energy metabolism. Humans who have *BHMT* SNPs that result in drastically reduced BHMT activity may at higher risk for

cardiovascular diseases and hepatocellular carcinoma, and may have decreased body fat. More importantly, this dissertation reveals novel insights into the potential roles of choline and betaine in regulating hepatic health and adiposity. Although future studies are warranted, dietary intake of choline and betaine may be potential candidates as treatments for these related diseases.

REFERENCES

1. Castro, C., et al., *Dissecting the catalytic mechanism of betaine-homocysteine S-methyltransferase by use of intrinsic tryptophan fluorescence and site-directed mutagenesis.* Biochemistry, 2004. **43**(18): p. 5341-51.

2. Finkelstein, J.D., B.J. Harris, and W.E. Kyle, *Methionine metabolism in mammals: kinetic study of betaine-homocysteine methyltransferase.* Arch Biochem Biophys, 1972. **153**(1): p. 320-4.

3. Park, E.I. and T.A. Garrow, *Interaction between dietary methionine and methyl donor intake on rat liver betaine-homocysteine methyltransferase gene expression and organization of the human gene.* J Biol Chem, 1999. **274**(12): p. 7816-24.

4. Sunden, S.L., et al., *Betaine-homocysteine methyltransferase expression in porcine and human tissues and chromosomal localization of the human gene.* Arch Biochem Biophys, 1997. **345**(1): p. 171-4.

5. Neece, D.J., M.A. Griffiths, and T.A. Garrow, *Isolation and characterization of a mouse betaine-homocysteine S-methyltransferase gene and pseudogene.* Gene, 2000. 250(1-2): p. 31-40.

6. Gonzalez, B., et al., *Crystal structure of rat liver betaine homocysteine s-methyltransferase reveals new oligomerization features and conformational changes upon substrate binding.* J Mol Biol, 2004. **338**(4): p. 771-82.

7. Evans, J.C., et al., *Betaine-homocysteine methyltransferase: zinc in a distorted barrel.* Structure, 2002. **10**(9): p. 1159-71.

8. Bose, N. and C. Momany, *Crystallization and preliminary X-ray crystallographic studies of recombinant human betaine-homocysteine S-methyltransferase.* Acta Crystallogr D Biol Crystallogr, 2001. **57**(Pt 3): p. 431-3.

9. Miller, C.M., S.S. Szegedi, and T.A. Garrow, *Conformation-dependent inactivation of human betaine-homocysteine S-methyltransferase by hydrogen peroxide in vitro.* Biochem J, 2005. **392**(Pt 3): p. 443-8.

10. Millian, N.S. and T.A. Garrow, *Human betaine-homocysteine methyltransferase is a zinc metalloenzyme.* Arch Biochem Biophys, 1998. **356**(1): p. 93-8.

11. Fisher, M.C., et al., *Perturbations in choline metabolism cause neural tube defects in mouse embryos in vitro.* FASEB J, 2002. **16**(6): p. 619-21.

12. Feng, Q., et al., *Betaine-homocysteine methyltransferase: human liver genotype-phenotype correlation.* Mol Genet Metab. **102**(2): p. 126-33.

13. McKeever, M.P., et al., *Betaine-homocysteine methyltransferase: organ distribution in man, pig and rat and subcellular distribution in the rat.* Clin Sci (Lond), 1991. **81**(4): p. 551-6.

14. Garrow, T.A., *Purification, kinetic properties, and cDNA cloning of mammalian betaine-homocysteine methyltransferase.* J Biol Chem, 1996. **271**(37): p. 22831-8.

15. Martin, J.J. and J.D. Finkelstein, *Enzymatic determination of betaine in rat tissues.* Anal Biochem, 1981. **111**(1): p. 72-6.

16. Finkelstein, J.D., et al., *Regulation of hepatic betaine-homocysteine methyltransferase by dietary methionine.* Biochem Biophys Res Commun, 1982. **108**(1): p. 344-8.

17. Finkelstein, J.D., et al., *Regulation of hepatic betaine-homocysteine methyltransferase by dietary betaine.* J Nutr, 1983. **113**(3): p. 519-21.

18. Szegedi, S.S., et al., *Betaine-homocysteine S-methyltransferase-2 is an S-methylmethionine-homocysteine methyltransferase.* J Biol Chem, 2008. **283**(14): p. 8939-45.

19. Chadwick, L.H., et al., *Betaine-homocysteine methyltransferase-2: cDNA cloning, gene sequence, physical mapping, and expression of the human and mouse genes.* Genomics, 2000. **70**(1): p. 66-73.

20. Li, F., et al., *Human betaine-homocysteine methyltransferase (BHMT) and BHMT2: common gene sequence variation and functional characterization.* Mol Genet Metab, 2008. **94**(3): p. 326-35.

21. Scheibler, C., *Ueber dad Betain, eine im Safte der Zuckerruben (Beta vulgaris) vorkommende Pflanzenbase.* Ber Dtsch Chem Ges, 1869. **2**: p. 292-295.

22. Scheibler, C., *Ueber dad Betain und seine Constitution.* Ber Dtsch Chem GesDtsch Chem Ges, 1870. **3**: p. 155-161.

23. Zeisel, S.H., et al., *Concentrations of choline-containing compounds and betaine in common foods.* J Nutr, 2003. **133**(5): p. 1302-7.

24. Schwahn, B.C., et al., *Pharmacokinetics of oral betaine in healthy subjects and patients with homocystinuria.* Br J Clin Pharmacol, 2003. **55**(1): p. 6-13.

25. Ueland, P.M., *Choline and betaine in health and disease.* J Inherit Metab Dis. **34**(1): p. 3-15.

26. Zeisel, S.H. and J.K. Blusztajn, *Choline and human nutrition.* Ann. Rev. Nutr., 1994. **14**: p. 269-296.

27. Zeisel, S.H., *Choline: an essential nutrient for humans.* Nutrition, 2000. **16**(7-8): p. 669-71.

28. Yates, A.A., S.A. Schlicker, and C.W. Suitor, *Dietary Reference Intakes: the new basis for recommendations for calcium and related nutrients, B vitamins, and choline.* J Am Diet Assoc, 1998. **98**(6): p. 699-706.

29. Lekim, D. and H. Betzing, *Intestinal absorption of polyunsaturated phosphatidylcholine in the rat.* Hoppe Seylers Z. Physiol. Chem., 1976. **357**: p. 1321-1331.

30. Cheng, W.-L., et al., *Bioavailability of choline and choline esters from milk in rat pups.* J. Nutr. Biochem., 1996. **7**: p. 457-464.

31. Blusztajn, J.K., S.H. Zeisel, and R.J. Wurtman, *Developmental changes in the activity of phosphatidylethanolamine N-methyltransferases in rat brain.* Biochem. J., 1985. **232**(2): p. 505-11.

32. Ueland, P.M., P.I. Holm, and S. Hustad, *Betaine: a key modulator of one-carbon metabolism and homocysteine status.* Clin Chem Lab Med, 2005. **43**(10): p. 1069-75.

33. Zeisel, S.H., *Choline: critical role during fetal development and dietary requirements in adults.* Annu Rev Nutr, 2006. **26**: p. 229-50.

34. Yao, Z.M. and D.E. Vance, *The active synthesis of phosphatidylcholine is required for very low density lipoprotein secretion from rat hepatocytes.* J. Biol. Chem., 1988. **263**(6): p. 2998-3004.

35. da Costa, K.A., et al., *Elevated serum creatine phosphokinase in choline-deficient humans: mechanistic studies in C2C12 mouse myoblasts.* Am J Clin Nutr, 2004. **80**(1): p. 163-170.

36. da Costa, K.A., et al., *Choline deficiency increases lymphocyte apoptosis and DNA damage in humans.* Am J Clin Nutr, 2006. **84**(1): p. 88-94.

37. da Costa, K.A., et al., *Choline deficiency in mice and humans is associated with increased plasma homocysteine concentration after a methionine load.* Am J Clin Nutr, 2005. **81**(2): p. 440-444.

38. Vance, D.E., *Boehringer Mannheim Award lecture. Phosphatidylcholine metabolism: masochistic enzymology, metabolic regulation, and lipoprotein assembly.* Biochem. Cell. Biol., 1990. **68**(10): p. 1151-1165.

39. DeLong, C.J., et al., *Molecular distinction of phosphatidylcholine synthesis between the CDP- choline pathway and phosphatidylethanolamine methylation pathway.* J Biol Chem, 1999. **274**(42): p. 29683-8.

40. Walkey, C.J., et al., *Biochemical and evolutionary significance of phospholipid methylation.* J Biol Chem, 1998. **273**(42): p. 27043-6.

41. Zhu, X., et al., *Phosphatidylethanolamine N-methyltransferase (PEMT) knockout mice have hepatic steatosis and abnormal hepatic choline metabolite concentrations despite ingesting a recommended dietary intake of choline.* Biochem J, 2003. **370**(Pt 3): p. 987-93.

42. Dayal, S. and S.R. Lentz, *Murine models of hyperhomocysteinemia and their vascular phenotypes.* Arterioscler Thromb Vasc Biol, 2008. **28**(9): p. 1596-605.

43. Pajares, M.A. and D. Perez-Sala, *Betaine homocysteine S-methyltransferase: just a regulator of homocysteine metabolism?* Cell Mol Life Sci, 2006. **63**(23): p. 2792-803.

44. Finkelstein, J.D., *Homocysteine: a history in progress.* Nutr Rev, 2000. **58**(7): p. 193-204.

45. Finkelstein, J.D. and J.J. Martin, *Methionine metabolism in mammals. Distribution of homocysteine between competing pathways.* J Biol Chem, 1984. **259**(15): p. 9508-13.

46. Kloor, D. and H. Osswald, *S-Adenosylhomocysteine hydrolase as a target for intracellular adenosine action.* Trends Pharmacol Sci, 2004. **25**(6): p. 294-7.

47. Varela-Moreiras, G., C. Ragel, and J. Perez de Miguelsanz, *Choline deficiency and methotrexate treatment induces marked but reversible changes in hepatic folate concentrations, serum homocysteine and DNA methylation rates in rats.* J. Amer. Coll. Nutr., 1995. **14**(5): p. 480-485.

48. Zeisel, S.H., et al., *Effect of choline deficiency on S-adenosylmethionine and methionine concentrations in rat liver.* Biochem. J., 1989. **259**: p. 725-729.

49. Selhub, J., et al., *Effects of choline deficiency and methotrexate treatment upon liver folate content and distribution.* Cancer Res., 1991. **51**(1): p. 16-21.

50. Varela-Moreiras, G., et al., *Effect of chronic choline deficiency in rats on liver folate content and distribution.* J. Nutr. Biochem., 1992. **3**(October): p. 519-522.

51. da Costa, K.A., et al., *Common genetic polymorphisms affect the human requirement for the nutrient choline.* FASEB J, 2006. **20**(9): p. 1336-44.

52. Morin, I., et al., *Common variant in betaine-homocysteine methyltransferase (BHMT) and risk for spina bifida.* Am J Med Genet A, 2003. **119A**(2): p. 172-6.

53. Boyles, A.L., et al., *Neural tube defects and folate pathway genes: family-based association tests of gene-gene and gene-environment interactions.* Environ Health Perspect, 2006. **114**(10): p. 1547-52.

54. Zhu, H., et al., *Are the betaine-homocysteine methyltransferase (BHMT and BHMT2) genes risk factors for spina bifida and orofacial clefts?* Am J Med Genet A, 2005. **135**(3): p. 274-7.

55. Weisberg, I.S., et al., *Investigations of a common genetic variant in betaine-homocysteine methyltransferase (BHMT) in coronary artery disease.* Atherosclerosis, 2003. **167**(2): p. 205-14.

56. Heil, S.G., et al., *Betaine-homocysteine methyltransferase (BHMT): genomic sequencing and relevance to hyperhomocysteinemia and vascular disease in humans.* Mol Genet Metab, 2000. **71**(3): p. 511-9.

57. Giusti, B., et al., *Genetic analysis of 56 polymorphisms in 17 genes involved in methionine metabolism in patients with abdominal aortic aneurysm.* J Med Genet, 2008. **45**(11): p. 721-30.

58. Xu, X., et al., *Choline metabolism and risk of breast cancer in a population-based study.* FASEB J, 2008. **22**(6): p. 2045-52.

59. Xu, X., et al., *High intakes of choline and betaine reduce breast cancer mortality in a population-based study.* FASEB J, 2009.

60. Mudd, S.H., et al., *The natural history of homocystinuria due to cystathionine beta-synthase deficiency.* Am J Hum Genet, 1985. **37**(1): p. 1-31.

61. Wilcken, D.E. and B. Wilcken, *The natural history of vascular disease in homocystinuria and the effects of treatment.* J Inherit Metab Dis, 1997. **20**(2): p. 295-300.

62. Walter, J.H., et al., *Strategies for the treatment of cystathionine beta-synthase deficiency: the experience of the Willink Biochemical Genetics Unit over the past 30 years.* Eur J Pediatr, 1998. **157 Suppl 2**: p. S71-6.

63. Yap, S., et al., *Vascular outcome in patients with homocystinuria due to cystathionine beta-synthase deficiency treated chronically: a multicenter observational study.* Arterioscler Thromb Vasc Biol, 2001. **21**(12): p. 2080-5.

64. Wendel, U. and H.J. Bremer, *Betaine in the treatment of homocystinuria due to 5,10-methylenetetrahydrofolate reductase deficiency.* Eur J Pediatr, 1984. **142**(2): p. 147-50.

65. Holme, E., B. Kjellman, and E. Ronge, *Betaine for treatment of homocystinuria caused by methylenetetrahydrofolate reductase deficiency.* Arch Dis Child, 1989. **64**(7): p. 1061-4.

66. Yaghmai, R., et al., *Progressive cerebral edema associated with high methionine levels and betaine therapy in a patient with cystathionine beta-synthase (CBS) deficiency.* Am J Med Genet, 2002. **108**(1): p. 57-63.

67. Devlin, A.M., et al., *Cerebral edema associated with betaine treatment in classical homocystinuria.* J Pediatr, 2004. **144**(4): p. 545-8.

68. Alfthan, G., et al., *The effect of low doses of betaine on plasma homocysteine in healthy volunteers.* Br J Nutr, 2004. **92**(4): p. 665-9.

69. Franken, D.G., et al., *Treatment of mild hyperhomocysteinemia in vascular disease patients.* Arterioscler Thromb, 1994. **14**(3): p. 465-70.

70. Schwab, U., et al., *Betaine supplementation decreases plasma homocysteine concentrations but does not affect body weight, body composition, or resting energy expenditure in human subjects.* Am J Clin Nutr, 2002. **76**(5): p. 961-7.

71. Olthof, M.R., et al., *Low dose betaine supplementation leads to immediate and long term lowering of plasma homocysteine in healthy men and women.* J Nutr, 2003. **133**(12): p. 4135-8.

72. Olthof, M.R., et al., *Effect of homocysteine-lowering nutrients on blood lipids: results from four randomised, placebo-controlled studies in healthy humans.* PLoS Med, 2005. **2**(5): p. e135.

73. Olthof, M.R., et al., *Effect of folic acid and betaine supplementation on flow-mediated dilation: a randomized, controlled study in healthy volunteers.* PLoS Clin Trials, 2006. **1**(2): p. e10.

74. Detopoulou, P., et al., *Dietary choline and betaine intakes in relation to concentrations of inflammatory markers in healthy adults: the ATTICA study.* Am J Clin Nutr, 2008. **87**(2): p. 424-30.

75. Bidulescu, A., et al., *Usual choline and betaine dietary intake and incident coronary heart disease: the Atherosclerosis Risk in Communities (ARIC) study.* BMC Cardiovasc Disord, 2007. **7**: p. 20.

76. Dalmeijer, G.W., et al., *Prospective study on dietary intakes of folate, betaine, and choline and cardiovascular disease risk in women.* Eur J Clin Nutr, 2008. **62**(3): p. 386-94.

77. Konstantinova, S.V., et al., *Divergent associations of plasma choline and betaine with components of metabolic syndrome in middle age and elderly men and women.* J Nutr, 2008. **138**(5): p. 914-20.

78. Lever, M., et al., *Plasma lipids and betaine are related in an acute coronary syndrome cohort.* PLoS One. **6**(7): p. e21666.

79. McGregor, D.O., et al., *Betaine supplementation decreases post-methionine hyperhomocysteinemia in chronic renal failure.* Kidney Int, 2002. **61**(3): p. 1040-6.

80. Zeisel, S.H., *Betaine supplementation and blood lipids: fact or artifact?* Nutr Rev, 2006. **64**(2 Pt 1): p. 77-9.

81. Paschos, P. and K. Paletas, *Non alcoholic fatty liver disease and metabolic syndrome.* Hippokratia, 2009. **13**(1): p. 9-19.

82. Miglio, F., et al., *Efficacy and safety of oral betaine glucuronate in non-alcoholic steatohepatitis. A double-blind, randomized, parallel-group, placebo-controlled prospective clinical study.* Arzneimittelforschung, 2000. **50**(8): p. 722-7.

83. Abdelmalek, M.F., et al., *Betaine, a promising new agent for patients with nonalcoholic steatohepatitis: results of a pilot study.* Am J Gastroenterol, 2001. **96**(9): p. 2711-7.

84. Abdelmalek, M.F., et al., *Betaine for nonalcoholic fatty liver disease: results of a randomized placebo-controlled trial.* Hepatology, 2009. **50**(6): p. 1818-26.

85. Cho, E., et al., *Choline and betaine intake and risk of breast cancer among post-menopausal women.* Br J Cancer. **102**(3): p. 489-94.

86. Kotsopoulos, J., S.E. Hankinson, and S.S. Tworoger, *Dietary betaine and choline intake are not associated with risk of epithelial ovarian cancer.* Eur J Clin Nutr. **64**(1): p. 111-4.

87. Cohen, J.C., J.D. Horton, and H.H. Hobbs, *Human fatty liver disease: old questions and new insights.* Science. **332**(6037): p. 1519-23.

88. Halsted, C.H., et al., *Folate deficiency disturbs hepatic methionine metabolism and promotes liver injury in the ethanol-fed micropig.* Proc Natl Acad Sci U S A, 2002. **99**(15): p. 10072-7.

89. Lu, S.C., H. Tsukamoto, and J.M. Mato, *Role of abnormal methionine metabolism in alcoholic liver injury.* Alcohol, 2002. **27**(3): p. 155-62.

90. Ji, C. and N. Kaplowitz, *Hyperhomocysteinemia, endoplasmic reticulum stress, and alcoholic liver injury.* World J Gastroenterol, 2004. **10**(12): p. 1699-708.

91. Barak, A.J., et al., *Dietary betaine promotes generation of hepatic S-adenosylmethionine and protects the liver from ethanol-induced fatty infiltration.* Alcohol Clin Exp Res, 1993. **17**(3): p. 552-5.

92. Barak, A.J., H.C. Beckenhauer, and D.J. Tuma, *Betaine, ethanol, and the liver: a review.* Alcohol, 1996. **13**(4): p. 395-8.

93. Ji, C. and N. Kaplowitz, *Betaine decreases hyperhomocysteinemia, endoplasmic reticulum stress, and liver injury in alcohol-fed mice.* Gastroenterology, 2003. **124**(5): p. 1488-99.

94. Kharbanda, K.K., et al., *Betaine administration corrects ethanol-induced defective VLDL secretion.* Mol Cell Biochem, 2009. **327**(1-2): p. 75-8.

95. Ji, C., et al., *Effect of transgenic extrahepatic expression of betaine-homocysteine methyltransferase on alcohol or homocysteine-induced fatty liver.* Alcohol Clin Exp Res, 2008. **32**(6): p. 1049-58.

96. Bacon, B.R., et al., *Nonalcoholic steatohepatitis: an expanded clinical entity.* Gastroenterology, 1994. **107**(4): p. 1103-9.

97. Sanyal, A.J., et al., *Nonalcoholic steatohepatitis: association of insulin resistance and mitochondrial abnormalities.* Gastroenterology, 2001. **120**(5): p. 1183-92.

98. Kathirvel, E., et al., *Betaine improves nonalcoholic fatty liver and associated hepatic insulin resistance: a potential mechanism for hepatoprotection by betaine.* Am J Physiol Gastrointest Liver Physiol. **299**(5): p. G1068-77.

99. Wang, Z., et al., *Betaine improved adipose tissue function in mice fed a high-fat diet: a mechanism for hepatoprotective effect of betaine in nonalcoholic fatty liver disease.* Am J Physiol Gastrointest Liver Physiol. **298**(5): p. G634-42.

100. Kharbanda, K.K., et al., *Betaine attenuates alcoholic steatosis by restoring phosphatidylcholine generation via the phosphatidylethanolamine methyltransferase pathway.* J Hepatol, 2007. **46**(2): p. 314-21.

101. Ji, C., et al., *Mechanisms of protection by the betaine-homocysteine methyltransferase/betaine system in HepG2 cells and primary mouse hepatocytes.* Hepatology, 2007. **46**(5): p. 1586-96.

102. Sowden, M.P., et al., *Apolipoprotein B mRNA and lipoprotein secretion are increased in McArdle RH-7777 cells by expression of betaine-homocysteine S-methyltransferase.* Biochem J, 1999. **341 (Pt 3)**: p. 639-45.

103. Sparks, J.D., et al., *Hepatic very-low-density lipoprotein and apolipoprotein B production are increased following in vivo induction of betaine-homocysteine S-methyltransferase.* Biochem J, 2006. **395**(2): p. 363-71.

104. Fernandez-Checa, J.C., A. Colell, and C. Garcia-Ruiz, *S-Adenosyl-L-methionine and mitochondrial reduced glutathione depletion in alcoholic liver disease.* Alcohol, 2002. **27**(3): p. 179-83.

105. Mari, M., et al., *Mitochondrial glutathione, a key survival antioxidant.* Antioxid Redox Signal, 2009. **11**(11): p. 2685-700.

106. Ganesan, B., R. Anandan, and P.T. Lakshmanan, *Studies on the protective effects of betaine against oxidative damage during experimentally induced restraint stress in Wistar albino rats.* Cell Stress Chaperones.

107. Kwon do, Y., et al., *Impaired sulfur-amino acid metabolism and oxidative stress in nonalcoholic fatty liver are alleviated by betaine supplementation in rats.* J Nutr, 2009. **139**(1): p. 63-8.

108. Ji, C., *Dissection of endoplasmic reticulum stress signaling in alcoholic and non-alcoholic liver injury.* J Gastroenterol Hepatol, 2008. **23 Suppl 1**: p. S16-24.

109. Collinsova, M., et al., *Inhibition of betaine-homocysteine S-methyltransferase causes hyperhomocysteinemia in mice.* J Nutr, 2006. **136**(6): p. 1493-7.

110. Strakova, J., et al., *Dietary intake of S-(alpha-carboxybutyl)-DL-homocysteine induces hyperhomocysteinemia in rats.* Nutr Res. **30**(7): p. 492-500.

111. *American cancer society.* www.cancer.org.

112. Newberne, P.M. and A.E. Rogers, *Labile methyl groups and the promotion of cancer.* Ann. Rev. Nutr., 1986. **6**(407): p. 407-432.

113. Rushmore, T., et al., *Rapid lipid peroxidation in the nuclear fraction of rat liver induced by a diet deficient in choline and methionine.* Cancer Lett., 1984. **24**: p. 251-5.

114. da Costa, K., et al., *Accumulation of 1,2-sn-diradylglycerol with increased membrane-associated protein kinase C may be the mechanism for spontaneous hepatocarcinogenesis in choline deficient rats.* J. Biol. Chem., 1993. **268**(3): p. 2100-2105.

115. Bird, A.P., *CpG-rich islands and the function of DNA methylation.* Nature, 1986. **321**(6067): p. 209-13.

116. Jeltsch, A., *Beyond Watson and Crick: DNA Methylation and Molecular Enzymology of DNA Methyltransferases.* Chembiochem, 2002. **3**(5): p. 382.

117. Fuks, F., *DNA methylation and histone modifications: teaming up to silence genes.* Curr Opin Genet Dev, 2005. **15**(5): p. 490-5.

118. Costello, J.F. and C. Plass, *Methylation matters.* J Med Genet, 2001. **38**(5): p. 285-303.

119. Esteller, M., *CpG island hypermethylation and tumor suppressor genes: a booming present, a brighter future.* Oncogene, 2002. **21**(35): p. 5427-40.

120. Momparler, R.L., *Cancer epigenetics.* Oncogene, 2003. **22**(42): p. 6479-83.

121. Lu, S.C. and J.M. Mato, *S-Adenosylmethionine in cell growth, apoptosis and liver cancer.* J Gastroenterol Hepatol, 2008. **23 Suppl 1**: p. S73-7.

122. Liu, S.P., et al., *Glycine N-methyltransferase-/- mice develop chronic hepatitis and glycogen storage disease in the liver.* Hepatology, 2007. **46**(5): p. 1413-25.

123. Martinez-Chantar, M.L., et al., *Loss of the glycine N-methyltransferase gene leads to steatosis and hepatocellular carcinoma in mice.* Hepatology, 2008. **47**(4): p. 1191-9.

124. Saltiel, A.R. and C.R. Kahn, *Insulin signalling and the regulation of glucose and lipid metabolism.* Nature, 2001. **414**(6865): p. 799-806.

125. Shi, Y. and P. Burn, *Lipid metabolic enzymes: emerging drug targets for the treatment of obesity.* Nat Rev Drug Discov, 2004. **3**(8): p. 695-710.

126. Rosen, E.D. and B.M. Spiegelman, *Adipocytes as regulators of energy balance and glucose homeostasis.* Nature, 2006. **444**(7121): p. 847-53.

127. Cannon, B. and J. Nedergaard, *Brown adipose tissue: function and physiological significance.* Physiol Rev, 2004. **84**(1): p. 277-359.

128. Morton, G.J., et al., *Central nervous system control of food intake and body weight.* Nature, 2006. **443**(7109): p. 289-95.

129. Khan, A.H. and J.E. Pessin, *Insulin regulation of glucose uptake: a complex interplay of intracellular signalling pathways.* Diabetologia, 2002. **45**(11): p. 1475-83.

130. Duntas, L.H., *Thyroid disease and lipids.* Thyroid, 2002. **12**(4): p. 287-93.

131. Yen, P.M., *Physiological and molecular basis of thyroid hormone action.* Physiol Rev, 2001. **81**(3): p. 1097-142.

132. Watanabe, M., et al., *Lowering bile acid pool size with a synthetic farnesoid X receptor (FXR) agonist induces obesity and diabetes through reduced energy expenditure.* J Biol Chem. **286**(30): p. 26913-20.

133. Watanabe, M., et al., *Bile acids induce energy expenditure by promoting intracellular thyroid hormone activation.* Nature, 2006. **439**(7075): p. 484-9.

134. Liu, Y.Y. and G.A. Brent, *Thyroid hormone crosstalk with nuclear receptor signaling in metabolic regulation.* Trends Endocrinol Metab. **21**(3): p. 166-73.

135. Zorzano, A., M. Palacin, and A. Guma, *Mechanisms regulating GLUT4 glucose transporter expression and glucose transport in skeletal muscle.* Acta Physiol Scand, 2005. **183**(1): p. 43-58.

136. Shin, D.J., et al., *Two uniquely arranged thyroid hormone response elements in the far upstream 5′ flanking region confer direct thyroid hormone regulation to the murine cholesterol 7alpha hydroxylase gene.* Nucleic Acids Res, 2006. **34**(14): p. 3853-61.

137. Friis, T. and L.R. Pedersen, *Serum lipids in hyper- and hypothyroidism before and after treatment.* Clin Chim Acta, 1987. **162**(2): p. 155-63.

138. Gullberg, H., et al., *Thyroid hormone receptor beta-deficient mice show complete loss of the normal cholesterol 7alpha-hydroxylase (CYP7A) response to thyroid hormone but display enhanced resistance to dietary cholesterol.* Mol Endocrinol, 2000. **14**(11): p. 1739-49.

139. Gullberg, H., et al., *Requirement for thyroid hormone receptor beta in T3 regulation of cholesterol metabolism in mice.* Mol Endocrinol, 2002. **16**(8): p. 1767-77.

140. Nishimura, T., et al., *Identification of a novel FGF, FGF-21, preferentially expressed in the liver.* Biochim Biophys Acta, 2000. **1492**(1): p. 203-6.

141. Badman, M.K., et al., *Hepatic fibroblast growth factor 21 is regulated by PPARalpha and is a key mediator of hepatic lipid metabolism in ketotic states.* Cell Metab, 2007. **5**(6): p. 426-37.

142. Kharitonenkov, A., et al., *FGF-21 as a novel metabolic regulator.* J Clin Invest, 2005. **115**(6): p. 1627-35.

143. Iizuka, K., J. Takeda, and Y. Horikawa, *Glucose induces FGF21 mRNA expression through ChREBP activation in rat hepatocytes.* FEBS Lett, 2009. **583**(17): p. 2882-6.

144. Li, K., et al., *The effects of fibroblast growth factor-21 knockdown and over-expression on its signaling pathway and glucose-lipid metabolism in vitro.* Mol Cell Endocrinol.

145. Coskun, T., et al., *Fibroblast growth factor 21 corrects obesity in mice.* Endocrinology, 2008. **149**(12): p. 6018-27.

146. Xu, J., et al., *Fibroblast growth factor 21 reverses hepatic steatosis, increases energy expenditure, and improves insulin sensitivity in diet-induced obese mice.* Diabetes, 2009. **58**(1): p. 250-9.

147. Adams, A.C., et al., *Thyroid hormone regulates hepatic expression of fibroblast growth factor 21 in a PPARalpha-dependent manner.* J Biol Chem. **285**(19): p. 14078-82.

148. Kalhan, S.C., et al., *Plasma metabolomic profile in nonalcoholic fatty liver disease.* Metabolism. **60**(3): p. 404-13.

149. Dasarathy, S., et al., *Elevated hepatic fatty acid oxidation, high plasma fibroblast growth factor 21, and fasting bile acids in nonalcoholic steatohepatitis.* Eur J Gastroenterol Hepatol. **23**(5): p. 382-8.

150. Rizki, G., et al., *Mice fed a lipogenic methionine-choline-deficient diet develop hypermetabolism coincident with hepatic suppression of SCD-1.* J Lipid Res, 2006. **47**(10): p. 2280-90.

151. Vetelainen, R., A. van Vliet, and T.M. van Gulik, *Essential pathogenic and metabolic differences in steatosis induced by choline or methione-choline deficient diets in a rat model.* J Gastroenterol Hepatol, 2007. **22**(9): p. 1526-33.

152. Rinella, M.E. and R.M. Green, *The methionine-choline deficient dietary model of steatohepatitis does not exhibit insulin resistance.* J Hepatol, 2004. **40**(1): p. 47-51.

153. Leclercq, I.A., et al., *Intrahepatic insulin resistance in a murine model of steatohepatitis: effect of PPARgamma agonist pioglitazone.* Lab Invest, 2007. **87**(1): p. 56-65.

154. Raubenheimer, P.J., M.J. Nyirenda, and B.R. Walker, *A choline-deficient diet exacerbates fatty liver but attenuates insulin resistance and glucose intolerance in mice fed a high-fat diet.* Diabetes, 2006. **55**(7): p. 2015-20.

155. Jacobs, R.L., et al., *Impaired de novo choline synthesis explains why phosphatidylethanolamine N-methyltransferase-deficient mice are protected from diet-induced obesity.* J Biol Chem, 2010. **285**(29): p. 22403-13.

156. Eklund, M., et al., *Potential nutritional and physiological functions of betaine in livestock.* Nutr Res Rev, 2005. **18**(1): p. 31-48.

157. Cromwell GL, L.M., Randolph JR, Monegue HJ, Laurent KM, Parker JR, *Efficacy of btaine as a carcass modifier in finishing pigs fed normal and reduced energy diets.* Journal of Animal Science, 1999. **77**(Suppl. 1, 179).

158. Cera, K.R., Schinckel, A.P., *Carcass and performance responses to feeding betaine in pigs.* Journal of Animal Science 1995. **73**(Suppl 1, 82).

159. Fernandez-Figares, I., et al., *Effect of dietary betaine on nutrient utilization and partitioning in the young growing feed-restricted pig.* J Anim Sci, 2002. **80**(2): p. 421-8.

160. Hanczakowska E, U.J., Swiatkiewycz M, *The efficiency of betaine and organic compounds of chromium in fattening of pigs with ad libitum or restricted feeding.* Roczniki Naukowe Zootechniki, 1999. **26**: p. 263-274.

161. Kitt SJ, M.P., Lewis AJ, Chen HY, *Effects of betaine and pen space allocation on growth performance, plasma urea concentration and carcass characteristics of growing and finishing barrows.* Journal of Animal Science, 1999. **77**(Suppl. I, 53).

162. Lawrence, B.V., et al., *Impact of betaine on pig finishing performance and carcass composition.* Journal of Animal Science, 2002. **80**(2): p. 475.

163. Matthews, J.O., et al., *Effects of betaine, pen space, and slaughter handling method on growth performance, carcass traits, and pork quality of finishing barrows.* J Anim Sci, 2001. **79**(4): p. 967-74.

164. Matthews, J.O., et al., *Effects of betaine on growth, carcass characteristics, pork quality, and plasma metabolites of finishing pigs.* J Anim Sci, 2001. **79**(3): p. 722-8.

165. Overland, M., K.A. Rorvik, and A. Skrede, *Effect of trimethylamine oxide and betaine in swine diets on growth performance, carcass characteristics, nutrient digestibility, and sensory quality of pork.* Journal of Animal Science, 1999. **77**(8): p. 2143.

166. Siljander-Rasi, H., et al., *Effect of equi-molar dietary betaine and choline addition on performance, carcass quality and physiological parameters of pigs.* ANIMAL SCIENCE-GLASGOW THEN PENICUIK-, 2003. **76**(1): p. 55-62.

167. Smith, J.W., et al., *The effects of supplementing growing finishing swine diets with betaine and (or) choline on growth and carcass characteristics.* 1995.

168. Smith, J.W., et al., *The effects of dietary carnitine, betaine, and chromium nicotinate supplementation on growth and carcass characteristics in growing-finishing pigs.* J. Anim. Sci, 1994. **72**(Suppl 1): p. 274.

169. Urbanczyk, J., *An attempt to decrease pig carcass fatness by nutritive factors.* Krmiva, 1997. **39**(6): p. 311-325.

170. Urbanczyk, J., E. Hanczakowska, and M. Swiatkiewicz, *Betaine and organic chromium as the feed additives in pig nutrition; Betaina i organiczne polaczenia chromu jako dodatki do paszy dla tucznikow.* Annals of Warsaw Agricultural University. Animal Science (Poland), 1999.

171. Urbanczyk, J., E. Hanczakowska, and M. Swiatkiewycz, *The efficiency of betaine and organic chromium compounds according to fattening pig genotype.* Biuletyn Naukowy Przemyslu Paszowego, 2000. **39**: p. 53?4.

172. Wang, Y.Z. and Z.R. Xu, *Effect of feeding betaine on weight gain and carcass trait of barrows and gilts and approach to mechanism.* J. Zhejiang Agric. Univ, 1999. **25**: p. 281-285.

173. Wang, Y.Z., Z.R. Xu, and J. Feng, *Study on the effect of betaine on meat quality and the mechanism in finishing pigs.* Scientia Agricultura Sinica, 2000. **33**: p. 94?9.

174. Webel, D.M., F.K. McKeith, and R.A. Easter, *The effects of betaine supplementation on growth performance and carcass characteristics in finishing pigs.* Journal of Animal Science, 1995. **73**(suppl 1): p. 82.

175. Yu, D., Feng, J., Xu, Z., *Effects of betaine on fat and protein metabolism in different stages of swine.* Chinese Journal of Veterinary Science, 2001. **21**: p. 200-203.

176. Esteve-Garcia, E. and S. Mack, *The effect of-methionine and betaine on growth performance and carcass characteristics in broilers* 1.* Animal feed science and technology, 2000. **87**(1-2): p. 85-93.

177. McDevitt, R.M., S. Mack, and I.R. Wallis, *Can betaine partially replace or enhance the effect of methionine by improving broiler growth and carcase characteristics?* British poultry science, 2000. **41**(4): p. 473-480.

178. Schutte, J.B., et al., *Replacement value of betaine for DL-methionine in male broiler chicks.* Poultry science, 1997. **76**(2): p. 321.

179. Wang, Y.Z., Xu, Z.R., Chen M.L., *Effect of betaine on carcass fat metabolism of meat duck.* Chinese Journal of Veterinary Science, 2000. **20**: p. 409-413.

180. Wang, Y.Z., *Effect of betaine on growth performance and carcass traits of meat ducks.* Journal of Zhejiang University Agricultural and Life Sciences, 2000. **26**: p. 347-352.

181. Zou, X.T. and J.J. Lu, *Effects of betaine on the regulation of the lipid metabolism in laying hen. Agrie.* Sci., China, 2002. **1**: p. 1043-1049.

182. Wray-Cahen, D., et al., *Betaine improves growth, but does not induce whole body or hepatic palmitate oxidation in swine (Sus scrofa domestica).* Comp Biochem Physiol A Mol Integr Physiol, 2004. **137**(1): p. 131-40.

183. Huang, Q., Xu, Z., Han, X., Li, W., *Changes in hormones, growth factor and lipid metabolism in finishing pigs fed betaine.* Livestock Science, 2006. **105**: p. 78-85.

184. Huang, Q., Xu, Z., Han, X., Li, W., *Effect of dietary betaine supplementation on lipogenic enzyme activities and fatty acid synthase mRNA expression in finishing pigs.* Anim. Feed Sci. Technol., 2008. **140**: p. 365-375.

185. Zhan, X.A., et al., *Effects of methionine and betaine supplementation on growth performance, carcase composition and metabolism of lipids in male broilers.* Br Poult Sci, 2006. **47**(5): p. 576-80.

186. Waterland, R.A., et al., *Methyl donor supplementation prevents transgenerational amplification of obesity.* Int J Obes (Lond), 2008. **32**(9): p. 1373-9.

187. Xu, Z., M. Wang, and M. Huai, *Approach of the mechanism of growth-promoting effect of betaine on swine.* Zhongguo shou yi xue bao= Chinese journal of veterinary science, 1999. **19**(4): p. 399.

188. Xu, Z. and X. Zhan, *Effects of betaine on methionine and adipose metabolism in broiler chicks.* Acta Veterinaria et Zootechnica Sinica, 1998. **29**: p. 212-219.

189. Yu, D.Y., Xu, Z.R., *Effects of methyl-donor on the performances and mechanisms of growth-promoting hormone in piglets.* Chinese Journal of Animal Science, 2000. **36**: p. 8-10.

190. Zou, X.T., *Effects of betaine on endocrinology of laying hens and its mechanism of action.* Chinese Journal of Veterinary Science, 2001. **21**: p. 300?03.

191. Zou, X.T., Y.L. Ma, and Z.R. Xu, *Effects of betaine and thyroprotein on laying performance and approach to mechanism of the effects in hens.* Acta Agriculturae Zhejiangensis, 1998. **10**: p. 144?49.

192. Shibata, T., et al., *Synthesis of betaine-homocysteine S-methyltransferase is continuously enhanced in fatty livers of thyroidectomized chickens.* Poult Sci, 2003. **82**(2): p. 207-13.

193. Konstantinova, S.V., et al., *Dietary patterns, food groups, and nutrients as predictors of plasma choline and betaine in middle-aged and elderly men and women.* Am J Clin Nutr, 2008. **88**(6): p. 1663-9.

194. Zeisel, S.H., *Choline: Critical Role During Fetal Development and Dietary Requirements in Adults.* Annu Rev Nutr, 2005.

195. Selhub, J., *Homocysteine metabolism.* Annu Rev Nutr, 1999. **19**: p. 217-46.

196. Delgado-Reyes, C.V., M.A. Wallig, and T.A. Garrow, *Immunohistochemical detection of betaine-homocysteine S-methyltransferase in human, pig, and rat liver and kidney.* Arch Biochem Biophys, 2001. **393**(1): p. 184-6.

197. Grossman, E.B. and S.C. Herbert, *Renal inner medullary choline dehydrogenase activity; characterization and modulation.* Am. J. Physiol., 1989. **256**: p. F107-F112.

198. Wagner, C., W.T. Briggs, and R.J. Cook, *Inhibition of glycine N-methyltransferase activity by folate derivatives: implications for regulation of methyl group metabolism.* Biochem Biophys Res Commun, 1985. **127**(3): p. 746-52.

199. Ridgway, N.D. and D.E. Vance, *Kinetic mechanism of phosphatidylethanolamine N-methyltransferase.* J. Biol. Chem., 1988. **263**(32): p. 16864-71.

200. Ridgway, N.D. and D.E. Vance, *Specificity of rat hepatic phosphatidylethanolamine N-methyltransferase for molecular species of diacyl phosphatidylethanolamine.* J. Biol. Chem., 1988. **263**(32): p. 16856-63.

201. Bradford, M.M., *A rapid and sensitive method for the quantitation of microgram quantities of protein utilizing the principle of protein-dye binding.* Anal. Biochem., 1976. **72**: p. 248-254.

202. Koc, H., et al., *Quantitation of choline and its metabolites in tissues and foods by liquid chromatography/electrospray ionization-isotope dilution mass spectrometry.* Anal Chem, 2002. **74**(18): p. 4734-40.

203. Shivapurkar, N. and L.A. Poirier, *Tissue levels of S-adenosylmethionine and S-adenosylhomocysteine in rats fed methyl-deficient, amino acid-defined diets for one to five weeks.* Carcinogenesis, 1983. **4**(8): p. 1051-7.

204. Molloy, A.M., et al., *A new high performance liquid chromatographic method for the simultaneous measurement of S-adenosylmethionine and S-adenosylhomocysteine.* Biomedical Chromatography, 1990. **4**(6): p. 257-260.

205. Ubbink, J.B., W.J. Hayward Vermaak, and S. Bissbort, *Rapid high-performance liquid chromatographic assay for total homocysteine levels in human serum.* J Chromatogr, 1991. **565**(1-2): p. 441-6.

206. Stabler, S.P., et al., *Alpha-lipoic acid induces elevated S-adenosylhomocysteine and depletes S-adenosylmethionine.* Free Radic Biol Med, 2009. **47**(8): p. 1147-53.

207. Horne, D.W. and D. Patterson, *Lactobacillus casei microbiological assay of folic acid derivatives in 96-well microtiter plates.* Clin Chem, 1988. **34**(11): p. 2357-9.

208. Bligh, E.G. and W.J. Dyer, *A rapid method of total lipid extraction and purification.* Can. J. Biochem. Physiol., 1959. **37**: p. 911-917.

209. Watkins, S.M., et al., *Unique phospholipid metabolism in mouse heart in response to dietary docosahexaenoic or alpha-linolenic acids.* Lipids, 2001. **36**(3): p. 247-54.

210. Svanborg, A. and L. Svennerholm, *Plasma total lipids, cholesterol, triglycerides, phospholipids and free fatty acids in a healthy Scandanavian population.* Acta Med. Scand., 1961. **169**: p. 43-49.

211. Folch, J., M. Lees, and G.H. Sloane Stanley, *A simple method for the isolation and purification of total lipides from animal tissues.* J Biol Chem, 1957. **226**(1): p. 497-509.

212. Lillie, R., *Histopathologic Technic and Practical Histochemistry, 3rd Edition*. 1965: McGraw-Hill Book Co., New York.

213. Lowry, O.H., et al., *Protein measurement with the Folin phenol reagent.* J. Biol. Chem., 1951. **193**: p. 265-275.

214. Zhou, L., J. Liu, and F. Luo, *Serum tumor markers for detection of hepatocellular carcinoma.* World J Gastroenterol, 2006. **12**(8): p. 1175-81.

215. Johnson, A.R., et al., *Deletion of murine choline dehydrogenase results in diminished sperm motility.* Faseb J, 2010. **24**(8): p. 2752-61.

216. Blumenstein, J. and G.R. Williams, *Glycine methyltransferase.* Can J Biochem Physiol, 1963. **41**: p. 201-10.

217. Finkelstein, J.D., *Methionine metabolism in mammals.* J Nutr Biochem, 1990. **1**(5): p. 228-37.

218. Schwahn, B.C., et al., *Homocysteine-betaine interactions in a murine model of 5,10-methylenetetrahydrofolate reductase deficiency.* FASEB J, 2003. **17**(3): p. 512-4.

219. Kim, S.K., K.H. Choi, and Y.C. Kim, *Effect of acute betaine administration on hepatic metabolism of S-amino acids in rats and mice.* Biochem Pharmacol, 2003. **65**(9): p. 1565-74.

220. Prudova, A., et al., *S-adenosylmethionine stabilizes cystathionine beta-synthase and modulates redox capacity.* Proc Natl Acad Sci U S A, 2006. **103**(17): p. 6489-94.

221. Noga, A.A., Y. Zhao, and D.E. Vance, *An unexpected requirement for phosphatidylethanolamine N-methyltransferase in the secretion of very low density lipoproteins.* J Biol Chem, 2002. **277**(44): p. 42358-65.

222. Fischer, L.M., et al., *Sex and menopausal status influence human dietary requirements for the nutrient choline.* Am J Clin Nutr, 2007. **85**(5): p. 1275-85.

223. da Costa, K.A., et al., *Accumulation of 1,2-sn-diradylglycerol with increased membrane-associated protein kinase C may be the mechanism for spontaneous hepatocarcinogenesis in choline-deficient rats.* J Biol Chem, 1993. **268**(3): p. 2100-5.

224. Feo, F., et al., *Hepatocellular carcinoma as a complex polygenic disease. Interpretive analysis of recent developments on genetic predisposition.* Biochim Biophys Acta, 2006. **1765**(2): p. 126-47.

225. Newell, P., et al., *Experimental models of hepatocellular carcinoma.* J Hepatol, 2008. **48**(5): p. 858-79.

226. Teng, Y.W., et al., *Deletion of murine betaine-homocysteine S-methyltransferase in mice perturbs choline and 1-carbon metabolism, resulting in fatty liver and hepatocellular carcinoma.* J Biol Chem.

227. Passonneau, J.V. and V.R. Lauderdale, *A comparison of three methods of glycogen measurement in tissues.* Anal Biochem, 1974. **60**(2): p. 405-12.

228. Boudonck, K.J., et al., *Discovery of metabolomics biomarkers for early detection of nephrotoxicity.* Toxicol Pathol, 2009. **37**(3): p. 280-92.

229. Evans, A.M., et al., *Integrated, nontargeted ultrahigh performance liquid chromatography/electrospray ionization tandem mass spectrometry platform for the identification and relative quantification of the small-molecule complement of biological systems.* Anal Chem, 2009. **81**(16): p. 6656-67.

230. Lawton, K.A., et al., *Analysis of the adult human plasma metabolome.* Pharmacogenomics, 2008. **9**(4): p. 383-97.

231. Barrett, T., Dehaven, C.D., Alexander, D.C., *System, method, and computer program product using a database in a computing system to compile and compare metabolomic data obtained from a plurality of samples.* U.S. Patent, 2008. **7**(433,787).

232. Manfredi, G., et al., *Measurements of ATP in mammalian cells.* Methods, 2002. **26**(4): p. 317-26.

233. Jaworski, K., et al., *AdPLA ablation increases lipolysis and prevents obesity induced by high-fat feeding or leptin deficiency.* Nat Med, 2009. **15**(2): p. 159-68.

234. Warne, J.P., et al., *Gene deletion reveals roles for annexin A1 in the regulation of lipolysis and IL-6 release in epididymal adipose tissue.* Am J Physiol Endocrinol Metab, 2006. **291**(6): p. E1264-73.

235. Viswanadha, S. and C. Londos, *Optimized conditions for measuring lipolysis in murine primary adipocytes.* J Lipid Res, 2006. **47**(8): p. 1859-64.

236. Bligh, E.G. and W.J. Dyer, *A rapid method of total lipid extraction and purification.* Can J Biochem Physiol, 1959. **37**(8): p. 911-7.

237. Loncar, D., *Convertible adipose tissue in mice.* Cell Tissue Res, 1991. **266**(1): p. 149-61.

238. Ortega, F.J., et al., *Subcutaneous fat shows higher thyroid hormone receptor-alpha1 gene expression than omental fat.* Obesity (Silver Spring), 2009. **17**(12): p. 2134-41.

239. Rossmeisl, M., et al., *Expression of the uncoupling protein 1 from the aP2 gene promoter stimulates mitochondrial biogenesis in unilocular adipocytes in vivo.* Eur J Biochem, 2002. **269**(1): p. 19-28.

240. Kopecky, J., et al., *Expression of the mitochondrial uncoupling protein gene from the aP2 gene promoter prevents genetic obesity.* J Clin Invest, 1995. **96**(6): p. 2914-23.

241. Lefebvre, A.M., et al., *Depot-specific differences in adipose tissue gene expression in lean and obese subjects.* Diabetes, 1998. **47**(1): p. 98-103.

242. Sewter, C.P., et al., *Regional differences in the response of human pre-adipocytes to PPARgamma and RXRalpha agonists.* Diabetes, 2002. **51**(3): p. 718-23.

243. Adams, M., et al., *Activators of peroxisome proliferator-activated receptor gamma have depot-specific effects on human preadipocyte differentiation.* J Clin Invest, 1997. **100**(12): p. 3149-53.

244. Tran, T.T., et al., *Beneficial effects of subcutaneous fat transplantation on metabolism.* Cell Metab, 2008. **7**(5): p. 410-20.

245. Flachs, P., et al., *Impaired noradrenaline-induced lipolysis in white fat of aP2-Ucp1 transgenic mice is associated with changes in G-protein levels.* Biochem J, 2002. **364**(Pt 2): p. 369-76.

246. Watanabe, M., et al., *Mice deficient in cystathionine beta-synthase: animal models for mild and severe homocyst(e)inemia.* Proc Natl Acad Sci U S A, 1995. **92**(5): p. 1585-9.

247. Chen, Z., et al., *Mice deficient in methylenetetrahydrofolate reductase exhibit hyperhomocysteinemia and decreased methylation capacity, with neuropathology and aortic lipid deposition.* Hum Mol Genet, 2001. **10**(5): p. 433-43.

248. Swanson, D.A., et al., *Targeted disruption of the methionine synthase gene in mice.* Mol Cell Biol, 2001. **21**(4): p. 1058-65.

249. Dayal, S., et al., *Endothelial dysfunction and elevation of S-adenosylhomocysteine in cystathionine beta-synthase-deficient mice.* Circ Res, 2001. **88**(11): p. 1203-9.

250. Dayal, S., et al., *Cerebral vascular dysfunction in methionine synthase-deficient mice.* Circulation, 2005. **112**(5): p. 737-44.

251. Devlin, A.M., et al., *Effect of Mthfr genotype on diet-induced hyperhomocysteinemia and vascular function in mice.* Blood, 2004. **103**(7): p. 2624-9.

252. Johnson, A.R., et al., *Deletion of murine choline dehydrogenase results in diminished sperm motility.* FASEB J. **24**(8): p. 2752-61.

253. Lever, M. and S. Slow, *The clinical significance of betaine, an osmolyte with a key role in methyl group metabolism.* Clin Biochem. **43**(9): p. 732-44.

254. Garcia-Perez, A. and M.B. Burg, *Renal medullary organic osmolytes.* Physiol Rev, 1991. **71**(4): p. 1081-115.

255. Avila, M.A., et al., *Reduced mRNA abundance of the main enzymes involved in methionine metabolism in human liver cirrhosis and hepatocellular carcinoma.* J Hepatol, 2000. **33**(6): p. 907-14.

256. Wijekoon, E.P., et al., *Homocysteine metabolism in ZDF (type 2) diabetic rats.* Diabetes, 2005. **54**(11): p. 3245-51.

257. Nieman, K.M., et al., *Modulation of methyl group metabolism by streptozotocin-induced diabetes and all-trans-retinoic acid.* J Biol Chem, 2004. **279**(44): p. 45708-12.

258. Patrick, L., *Nonalcoholic fatty liver disease: relationship to insulin sensitivity and oxidative stress. Treatment approaches using vitamin E, magnesium, and betaine.* Altern Med Rev, 2002. **7**(4): p. 276-91.

259. Matteoni, C.A., et al., *Nonalcoholic fatty liver disease: a spectrum of clinical and pathological severity.* Gastroenterology, 1999. **116**(6): p. 1413-9.

260. *Centers for Disease Control and Prevention.* www.cdc.gov/obesity/data/trends.html.